Deteção Remota Microondas

Aplicações InSAR

João Catalão Fernandes, FCUL

Tópicos

- Medição da deformação intra-ilha no arquipélago dos Açores
- Medição da subsidência em Lisboa
- Monitorização dos movimentos verticais em Singapura – relação com subida do mar

- Estimativa da batimetria intertidal com imagens SAR
- Monitorização de infraestruturas com imagens SAR de alta resolução (TSX)
- Monitorização da barragem do Tua e região envolvente
- Classificação da ocupação do solo com imagem SAR
- Deteção de corte de árvores

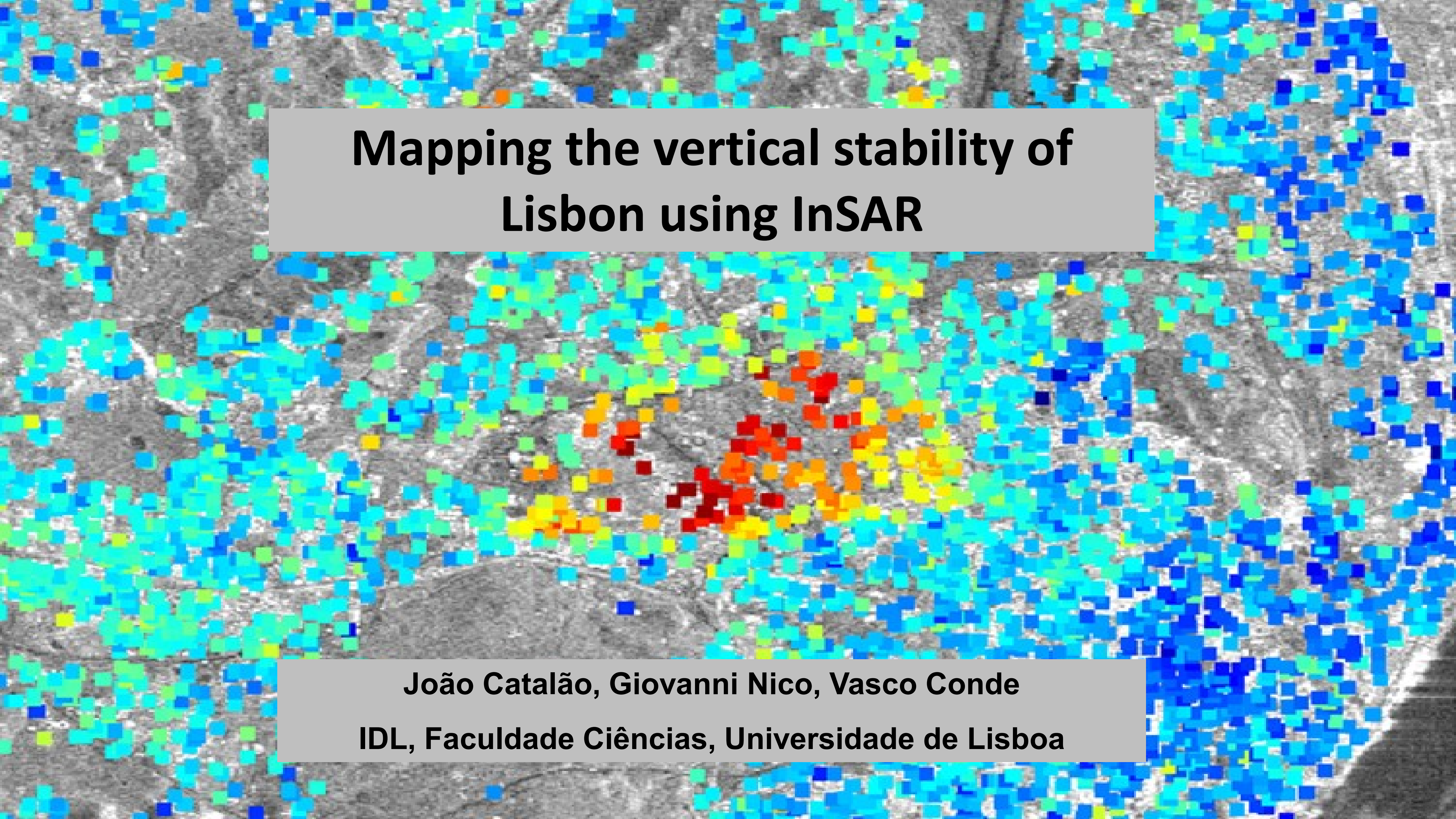

Mapping the vertical stability of Lisbon using InSAR

João Catalão, Giovanni Nico, Vasco Conde

IDL, Faculdade Ciências, Universidade de Lisboa

Deformation ERS 1995-2000

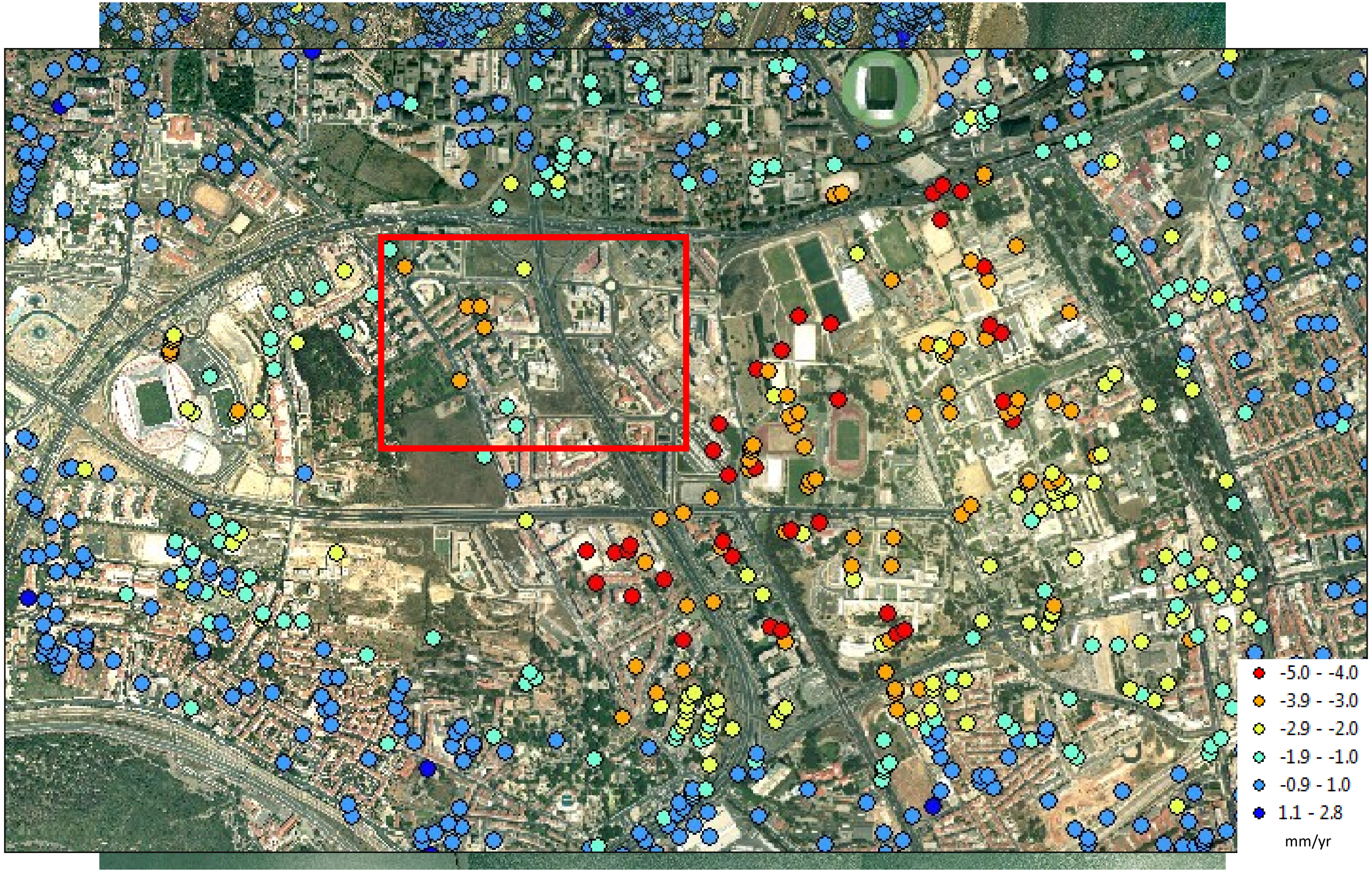

Deformation ERS 2000-2005

Deformation Envisat 2003-2005

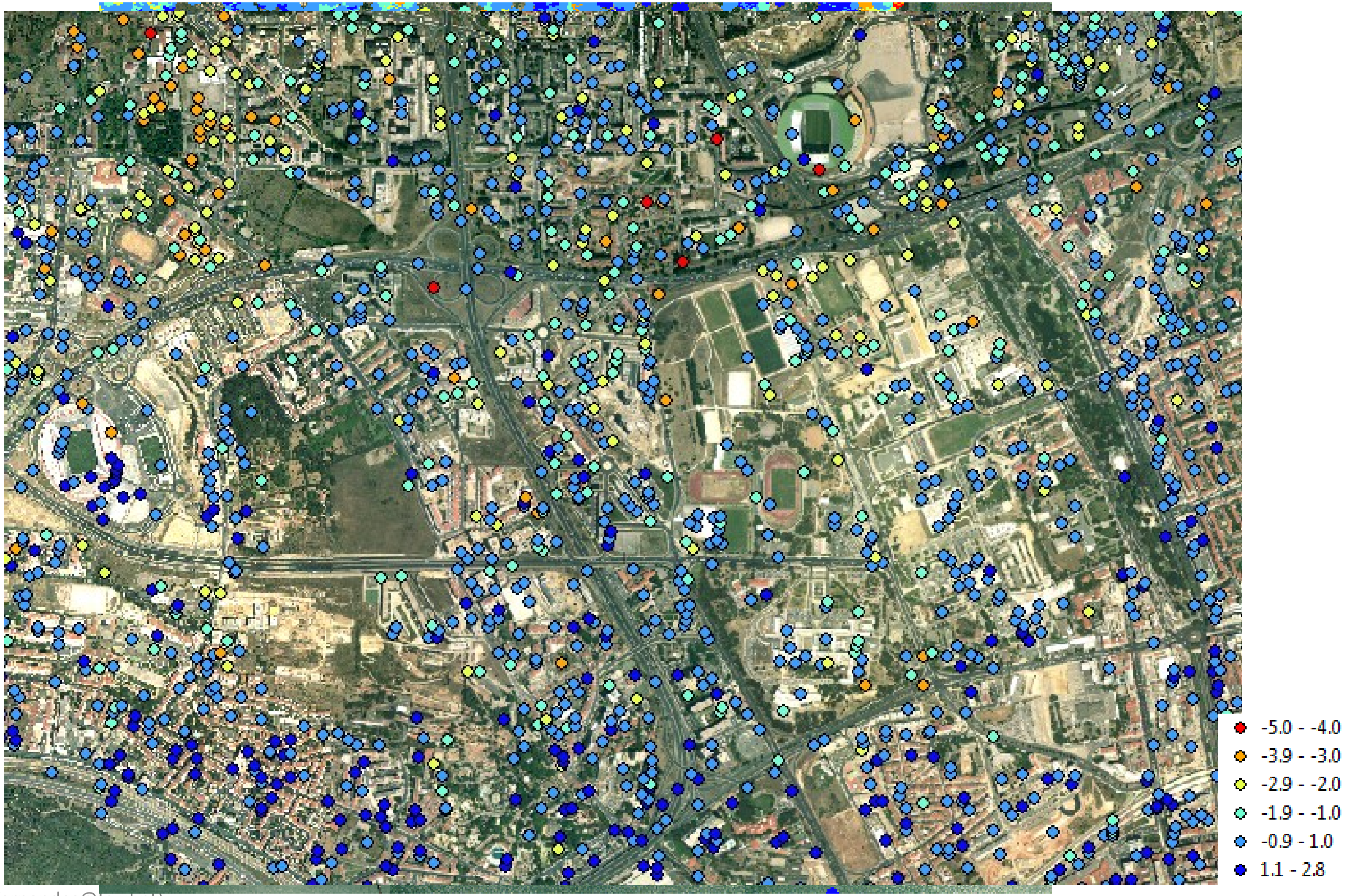

Deformation ENVISAT 2008-2010

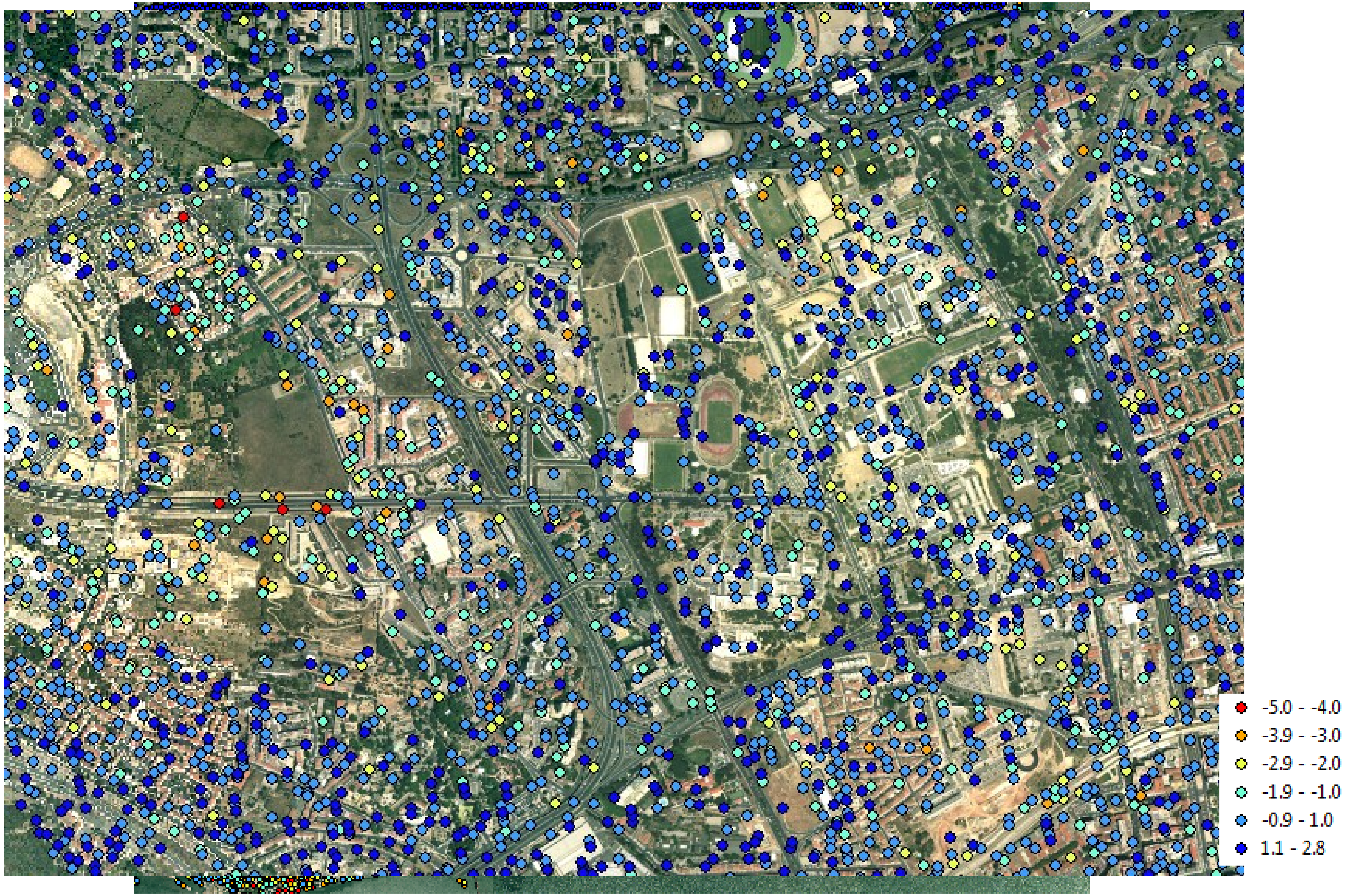

Deformation 2010-2011- TRX

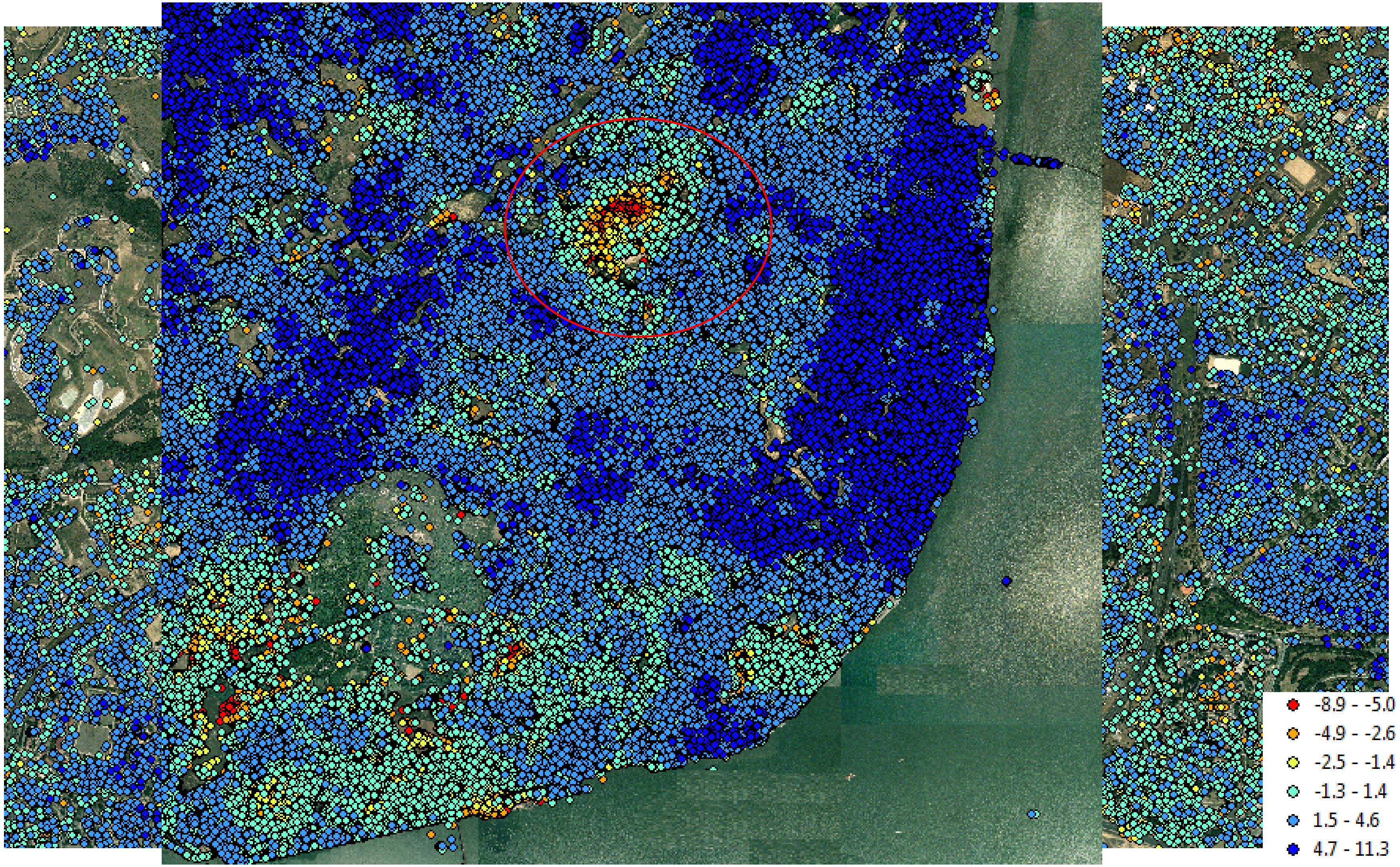

Deformation 2010-2011- TRX

Temporal evolution

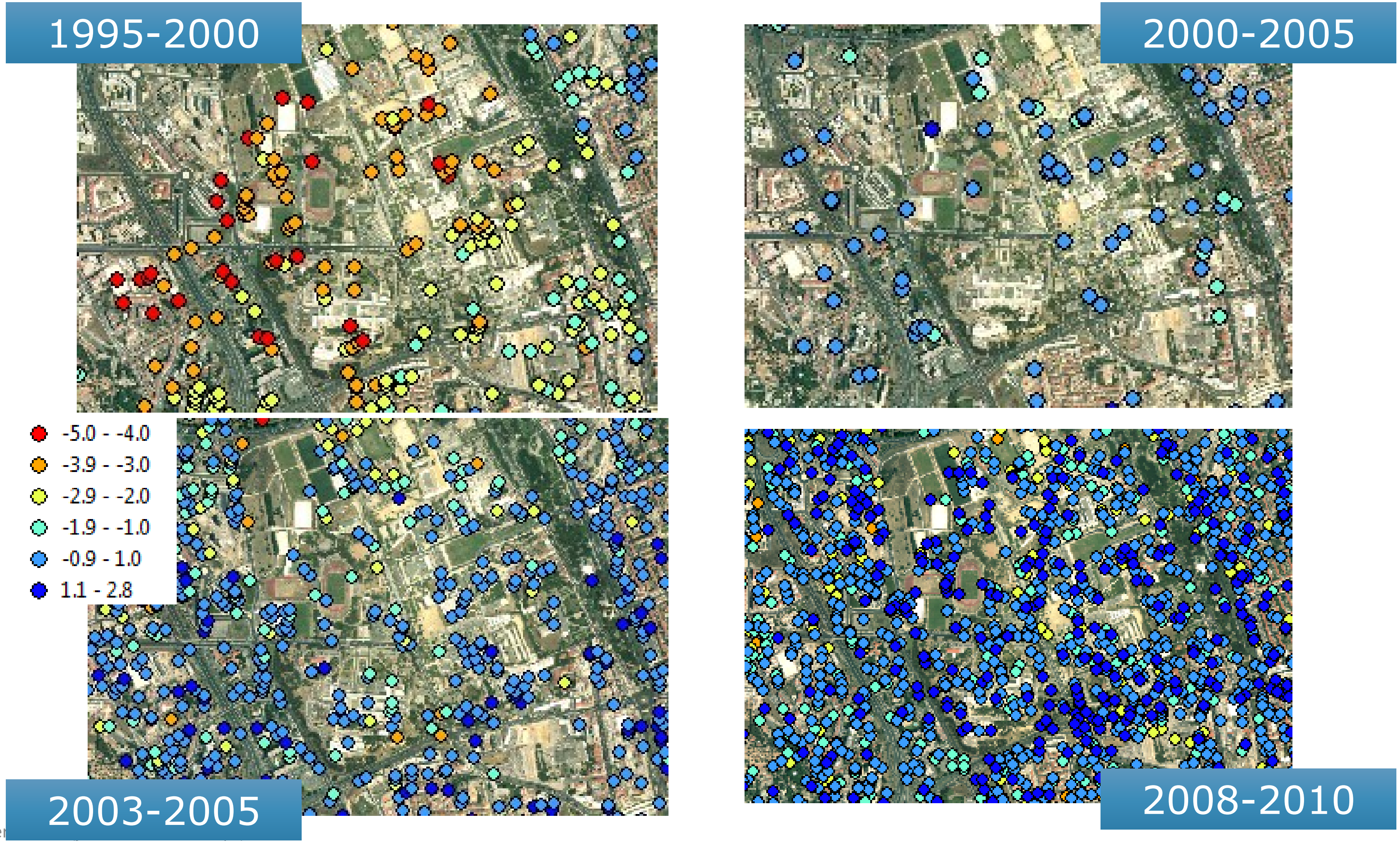

Levelling measurements

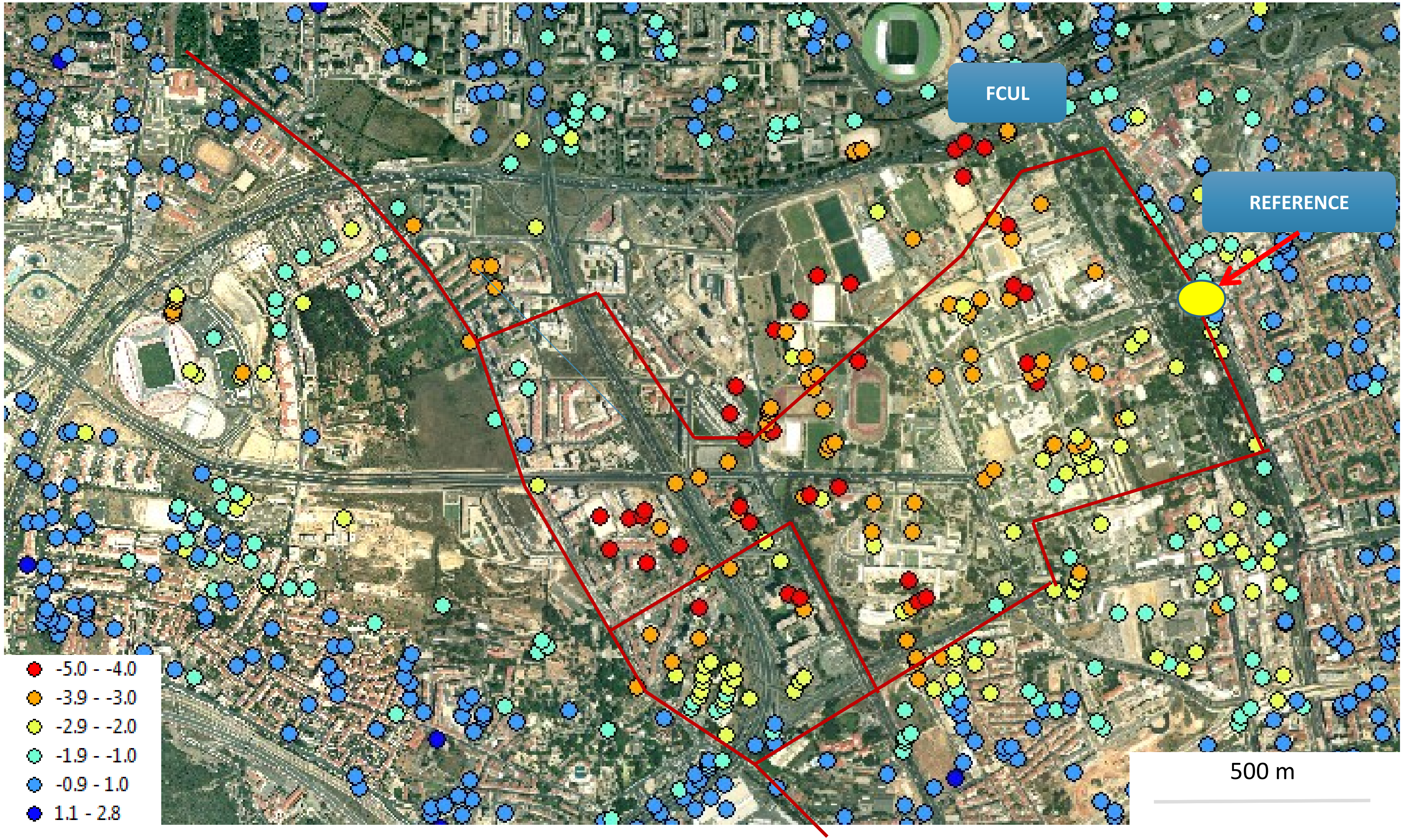

Ciências ULisboa

Levelling measurements

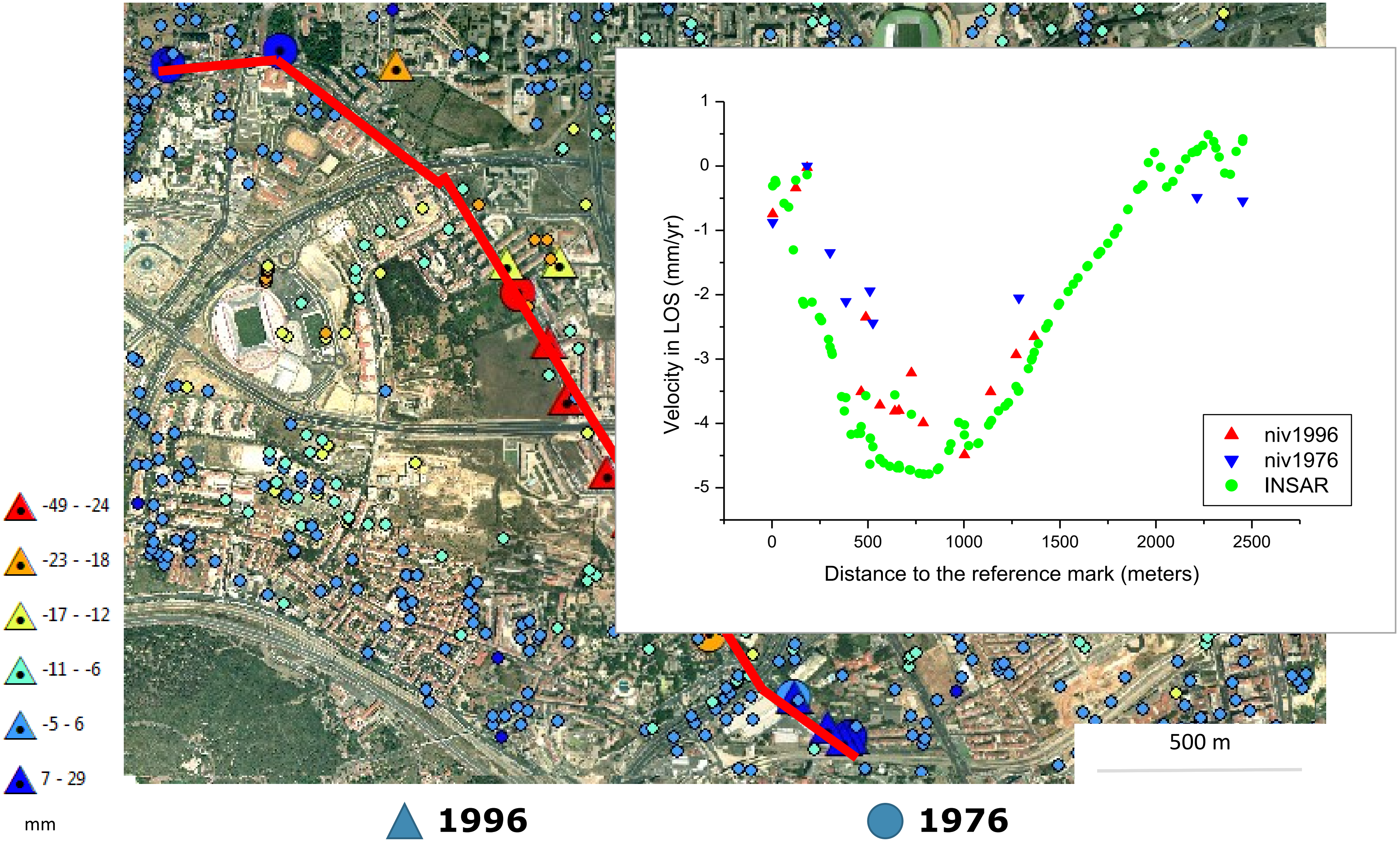

Ciências ULisboa

Anthropogenic intervention

Anthropogenic intervention

Ciências
ULisboa

Série temporal do deslocamento vertical

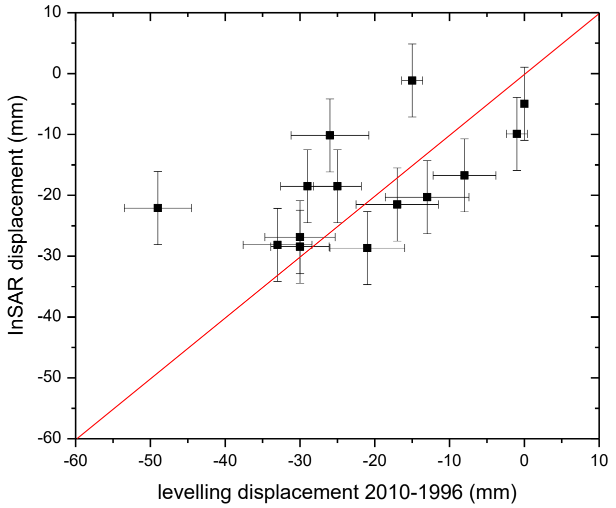

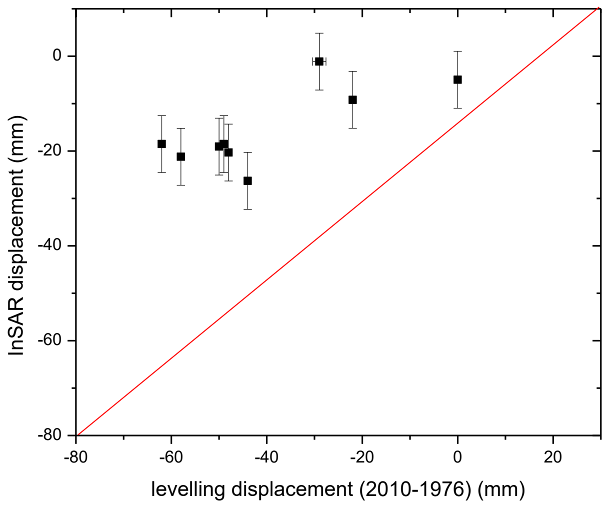

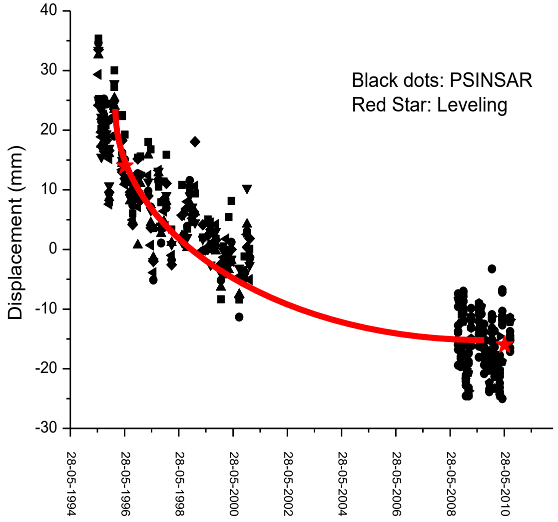

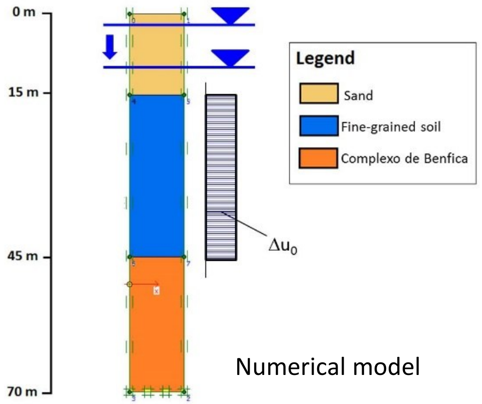

Numerical model

Modelação numérica

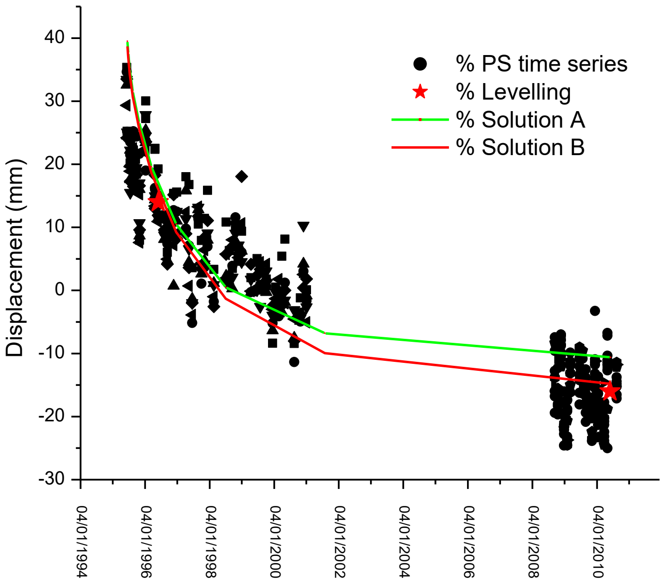

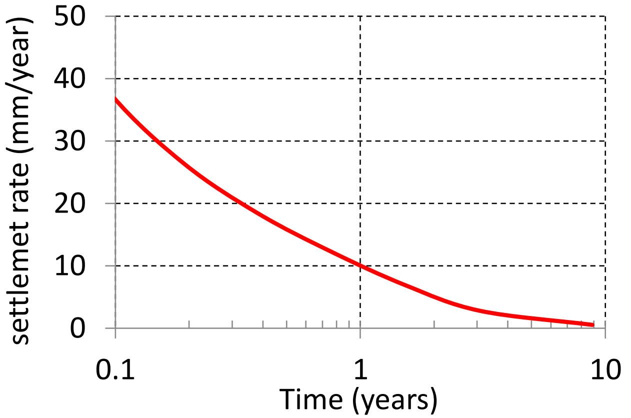

Catalão et al., 2015

LandMov is a two year Project under a contract research agreement between National University of Singapore (NUS) and the Instituto D.Luiz, University of Lisbon (IDL-UL).

LandMov is part of Building and Construction Authority (BCA) Project “Coastal Inundation Risk Map Study for Singapore”, a contract between the BCA and NUS, aimed at creation of the risk maps that can be applied to Singapore coasts subject to coastal inundation, inland flood, and soil subsidence. The BCA project aims to address the concerns surrounding coastal protection in the light of climate change and sea-level rise over the next 100 years.

Background and Motivation

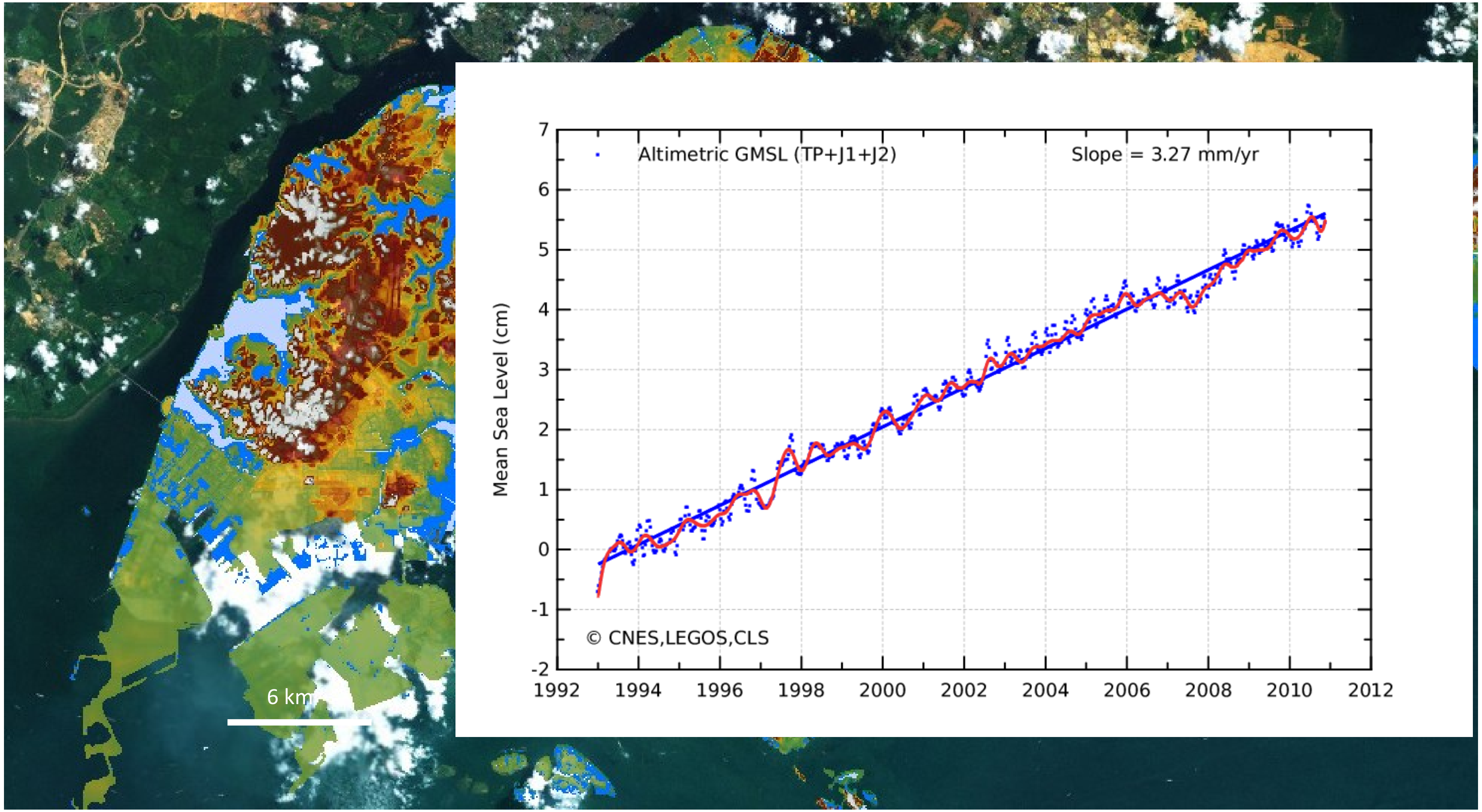

Main objective

To map the spatial variation in vertical land motion (VLM) along the coast of Singapore over the past two decades.

Archived ERS1 and ERS2 images from 1995 to 2000

New acquisitions from TerraSAR-X (Oct 2010 – 2014)

SAR images (ERS)

Perpendicular baseline / scene acquisition time

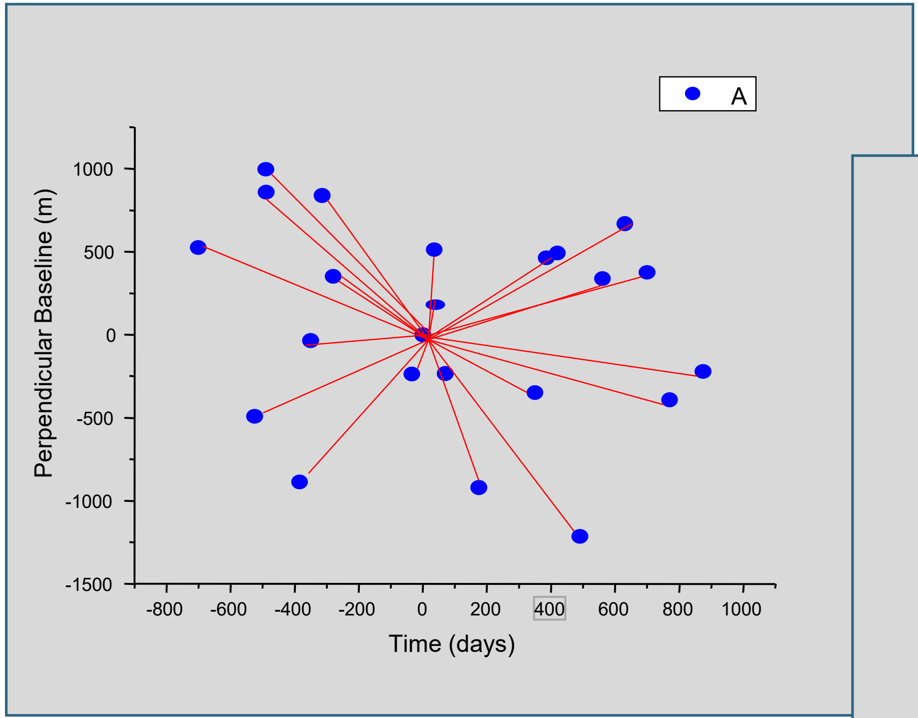

Ascending Pass

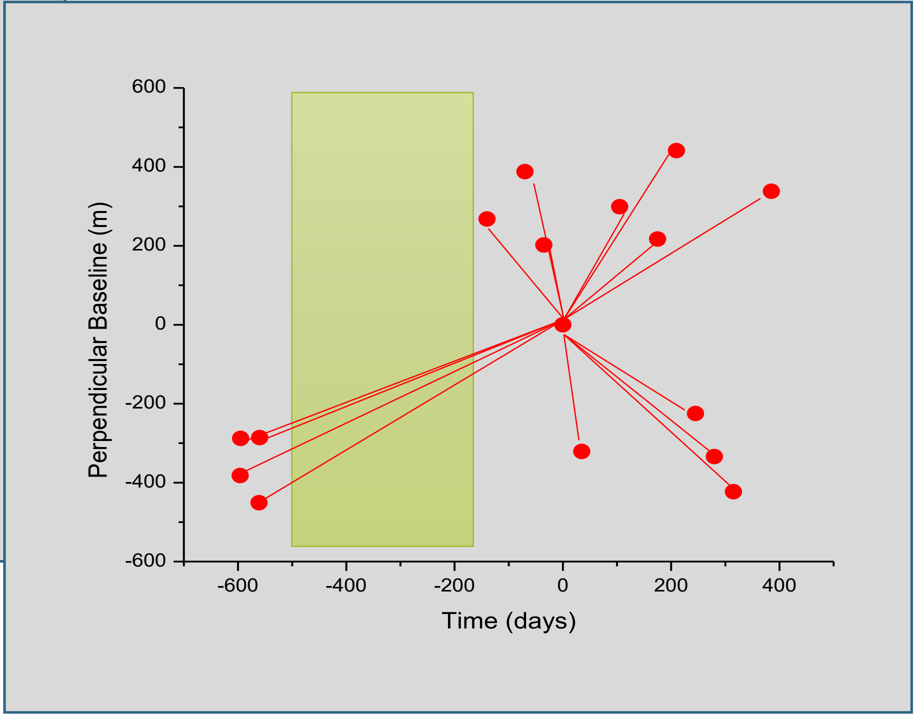

Descending Pass

TRX: Interferogram (amplitude)

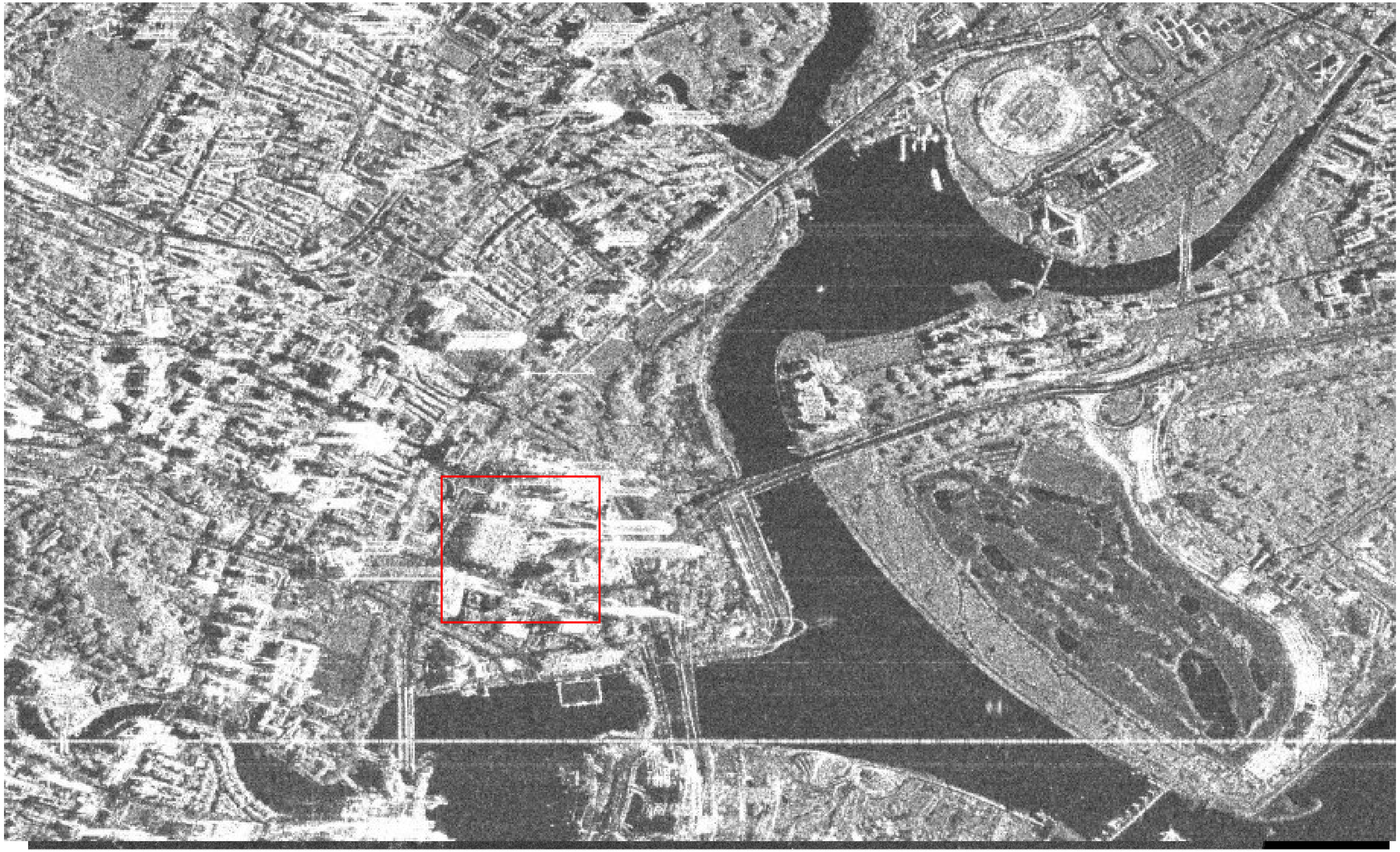

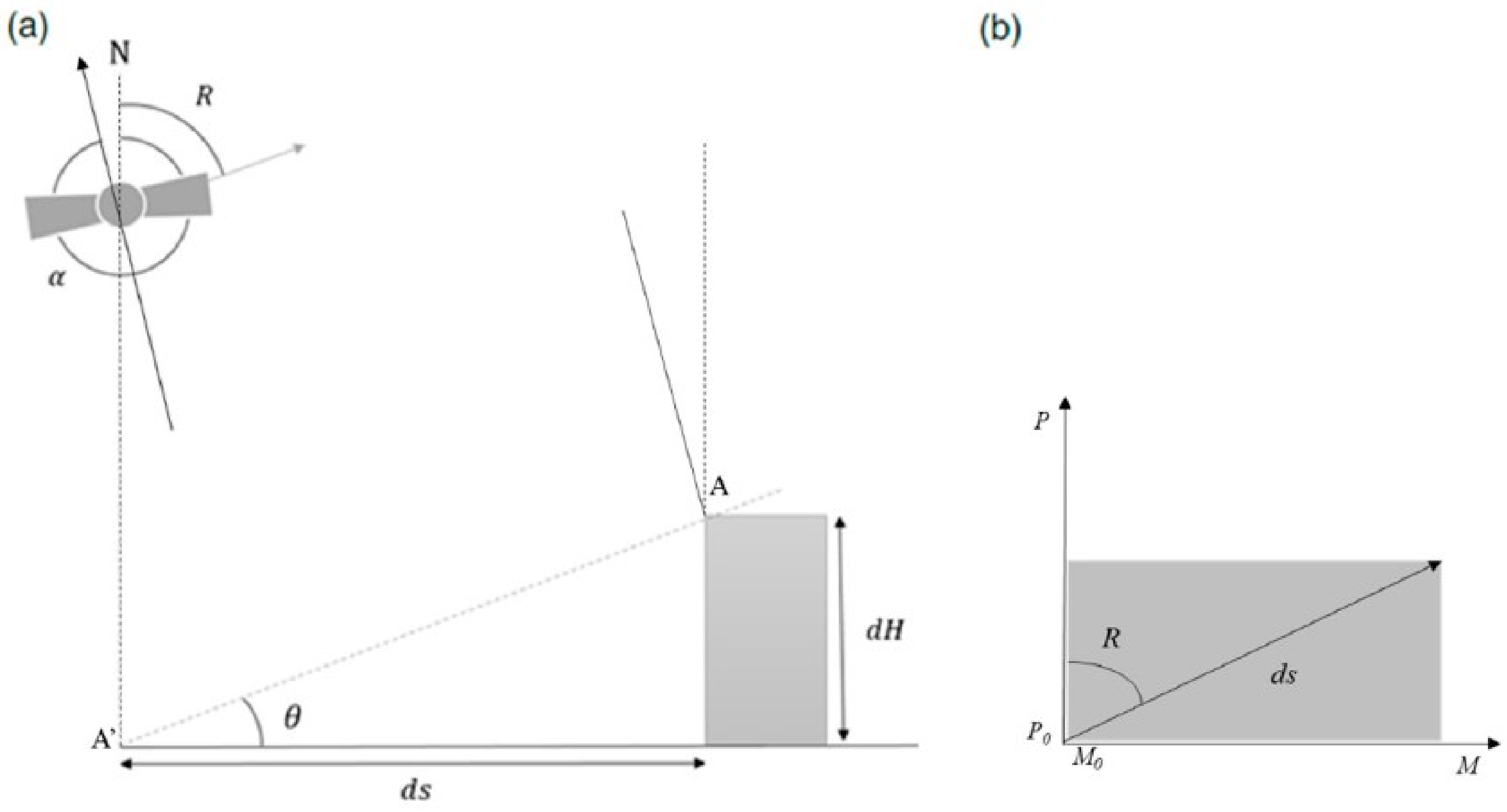

$$ds = \frac{dH}{\sin\theta}$$

$$\begin{cases} M = M_0 + ds \times \sin R \\ P = P_0 + ds \times \cos R \end{cases}$$

Figure 3. (**a**) SAR acquisition geometry of a building and (**b**) planimetric view of the geolocation error.

(a) (b)

Figure 4. Geolocation of the Persistent Scatterers: (**a**) original position, (**b**) corrected position. Displacement rates in mm·yr^{-1}.

TRX: Interferogram (phase)

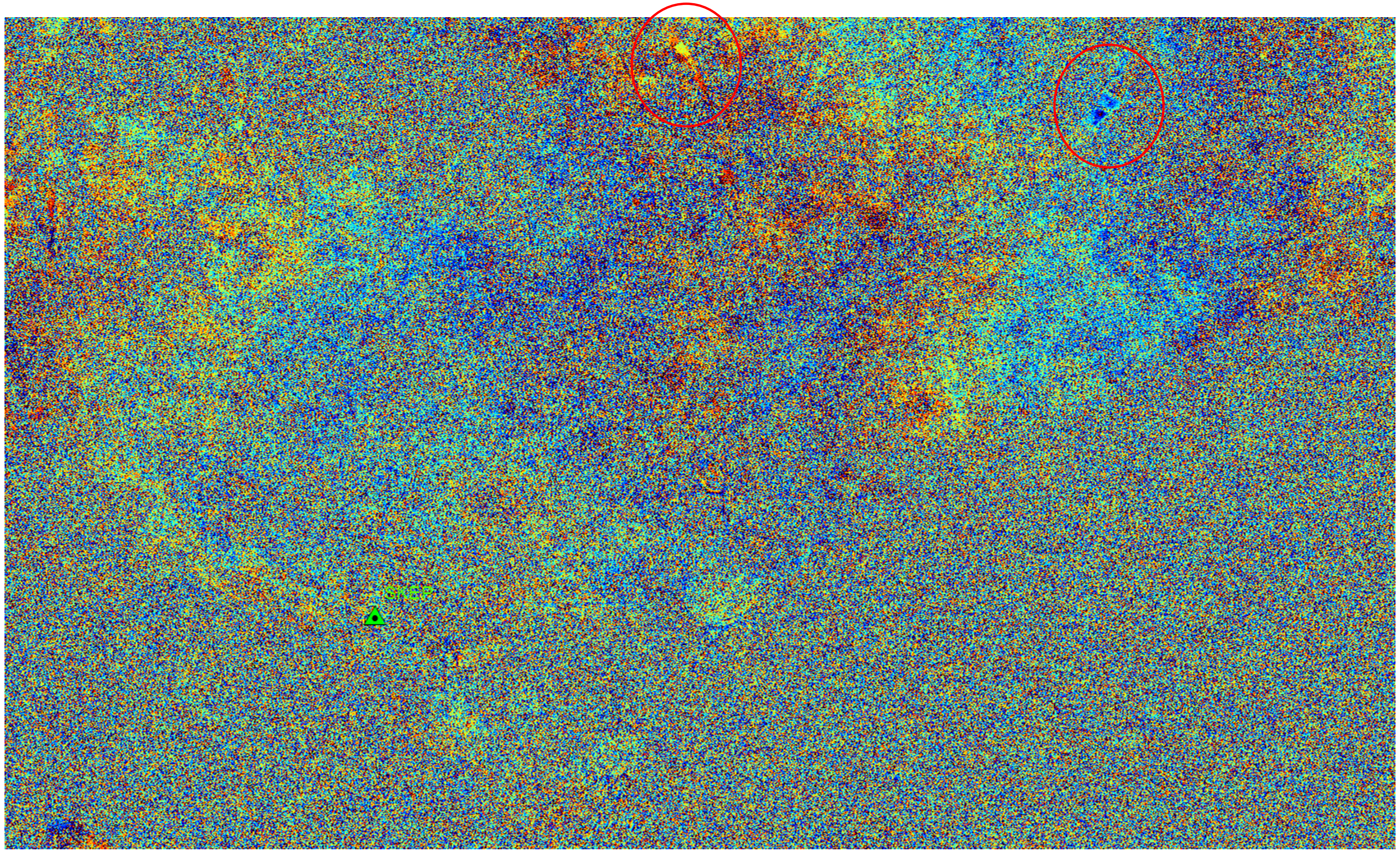

remote sensing

Article

Insar Maps of Land Subsidence and Sea Level Scenarios to Quantify the Flood Inundation Risk in Coastal Cities: The Case of Singapore

Joao Catalao [1,*], Durairaju Raju [2] and Giovanni Nico [3,4]

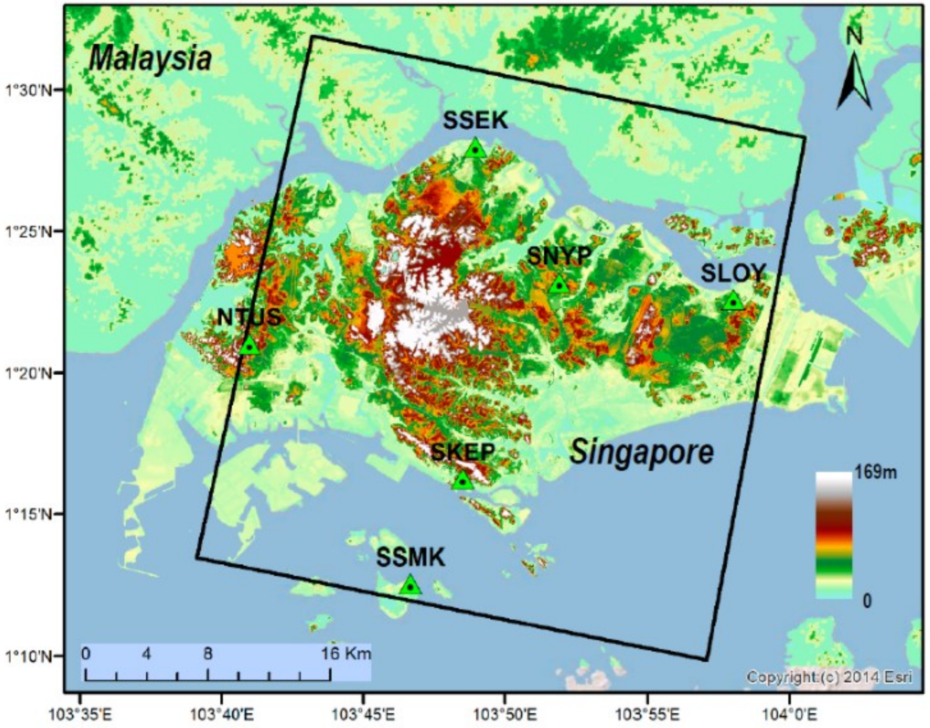

TRX: Persistent Scatterers

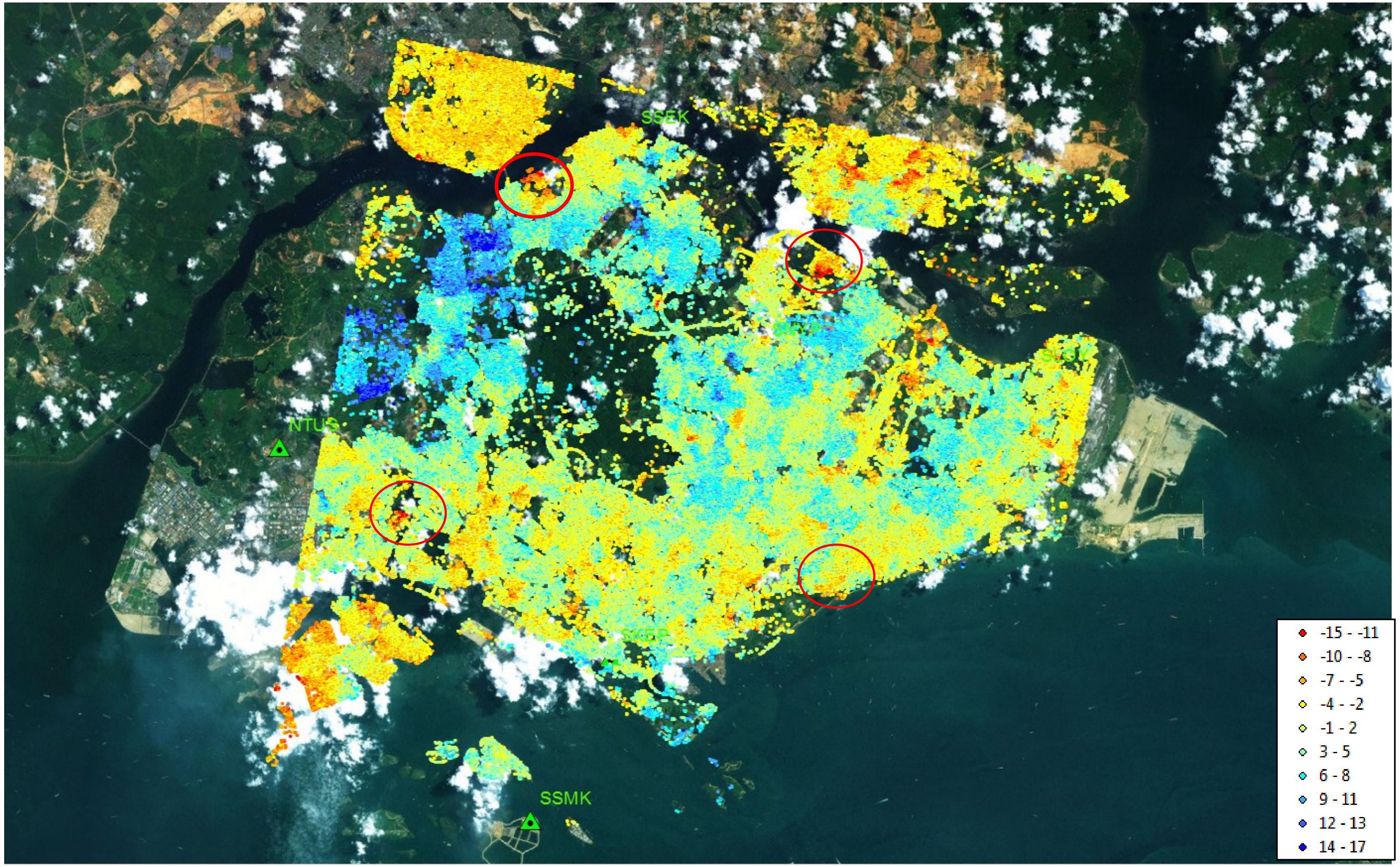

mm/yr

Sand Deposits

Road compaction

Marin

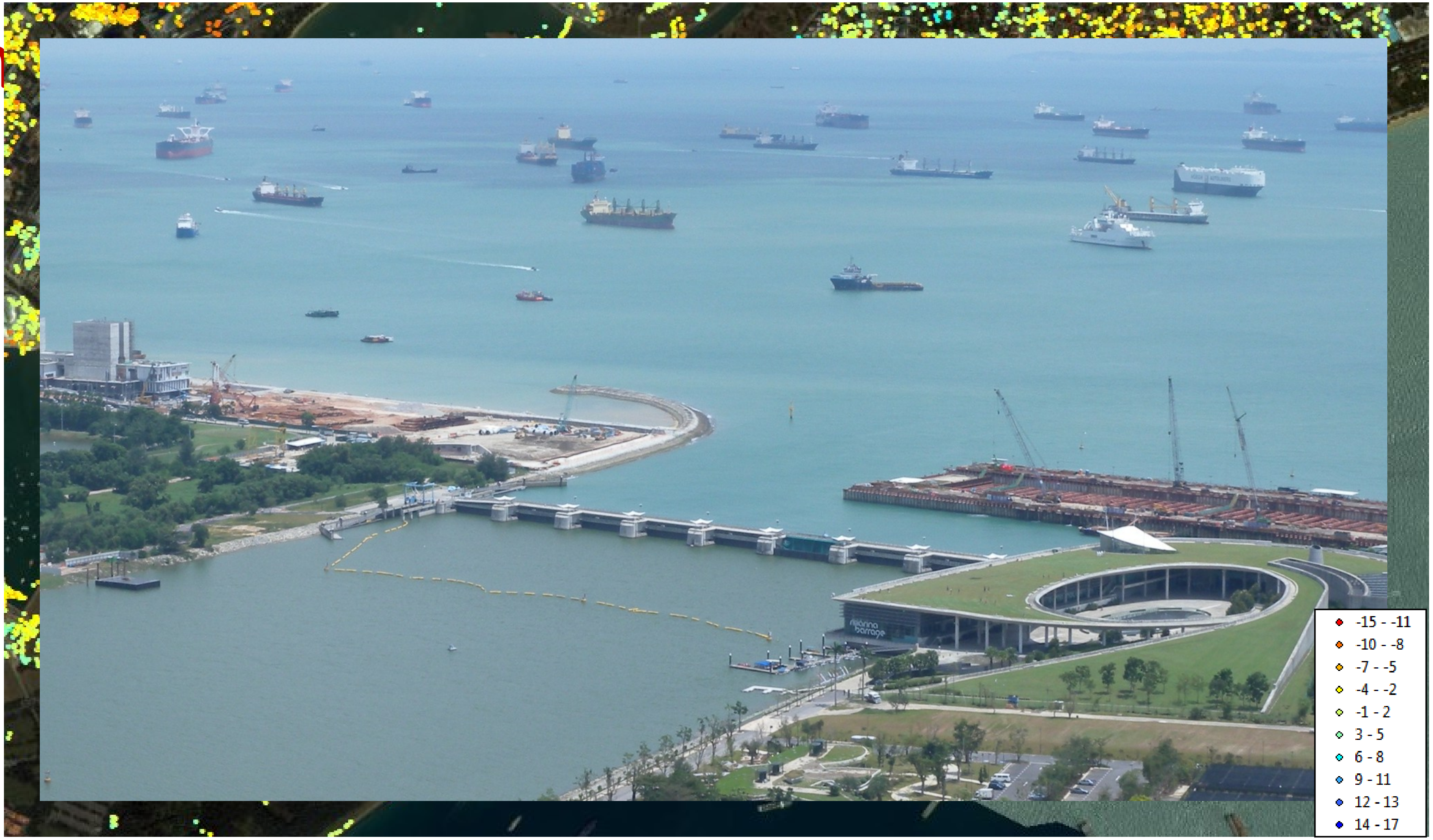

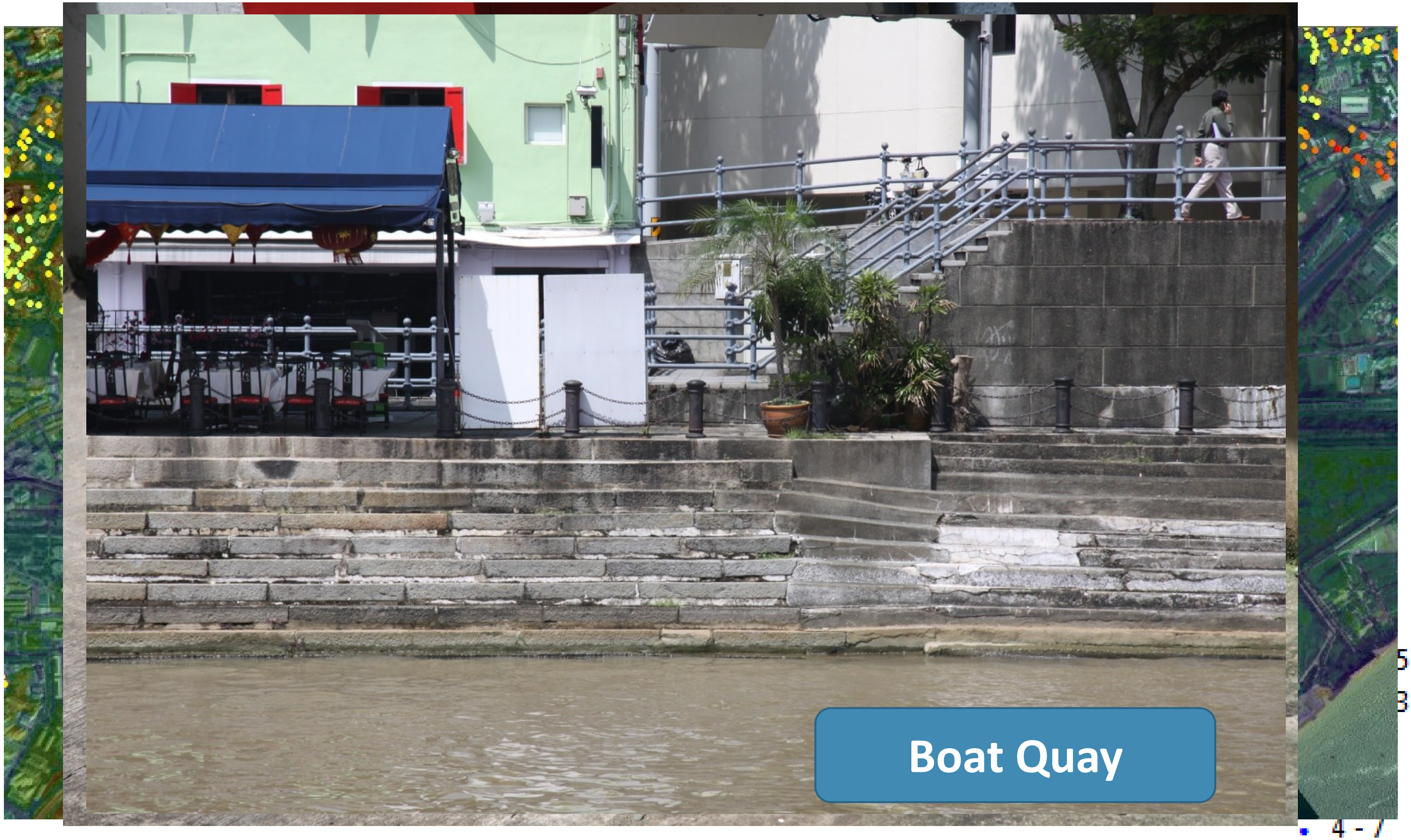
Boat Quay

Field evidences

3D visualization in GoogleEarth

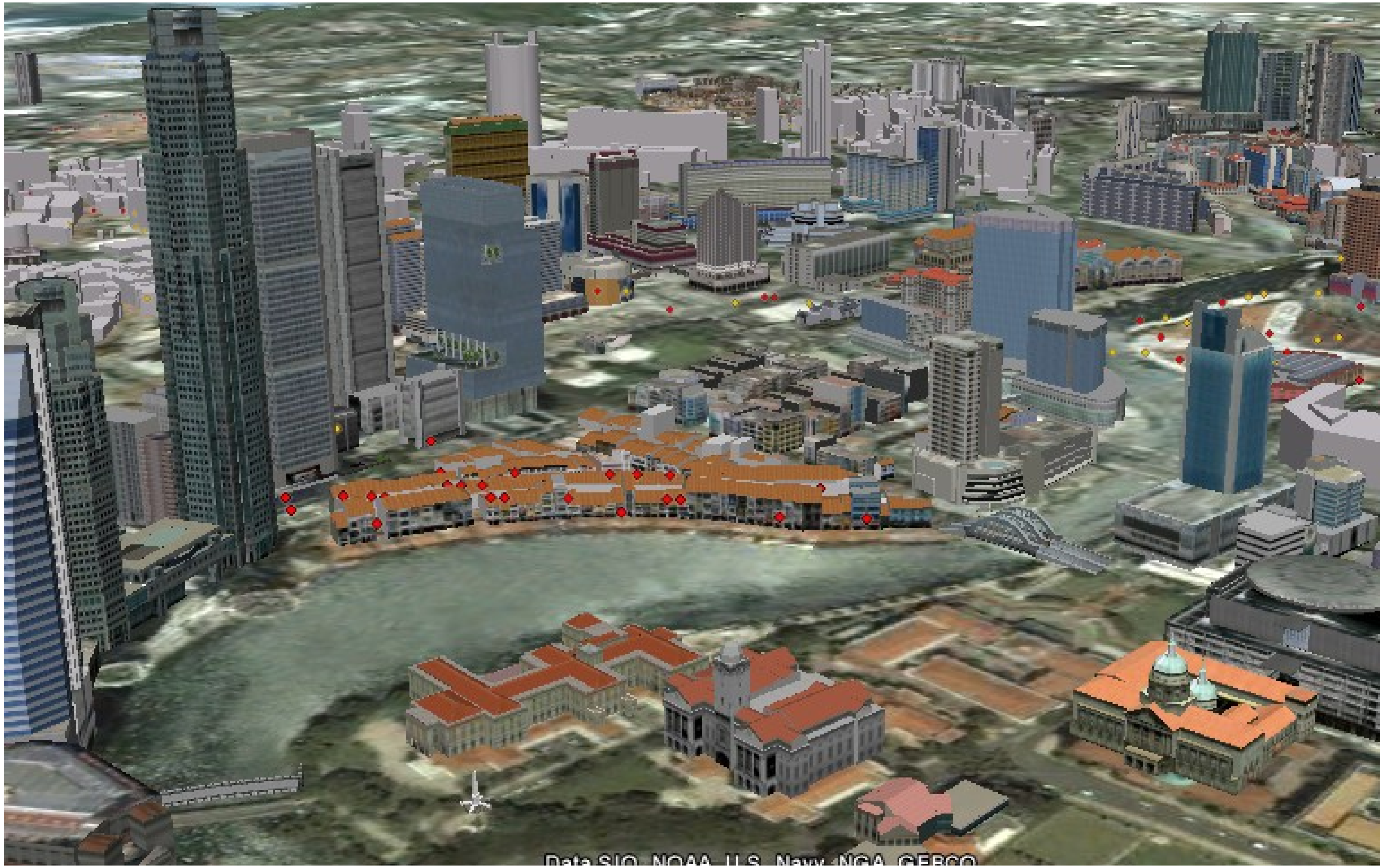

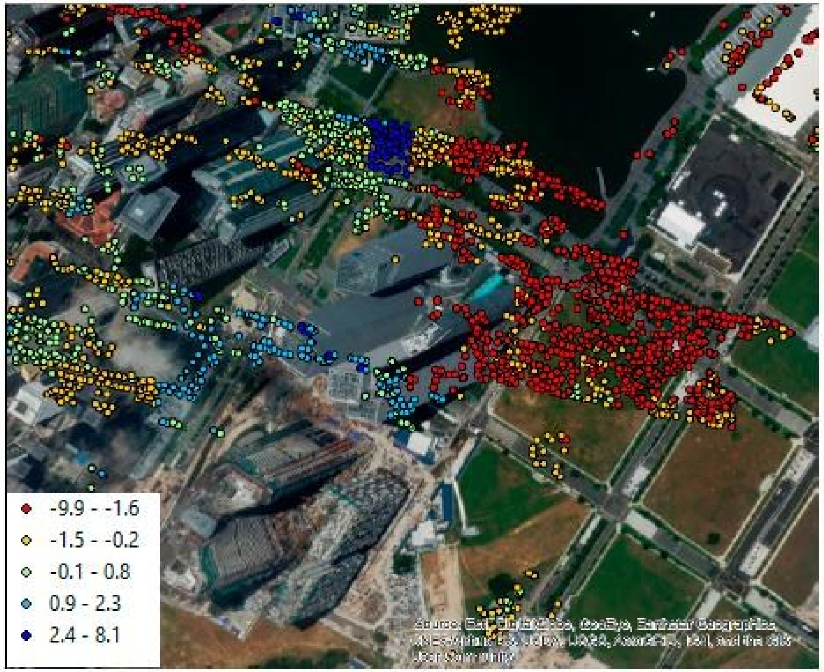

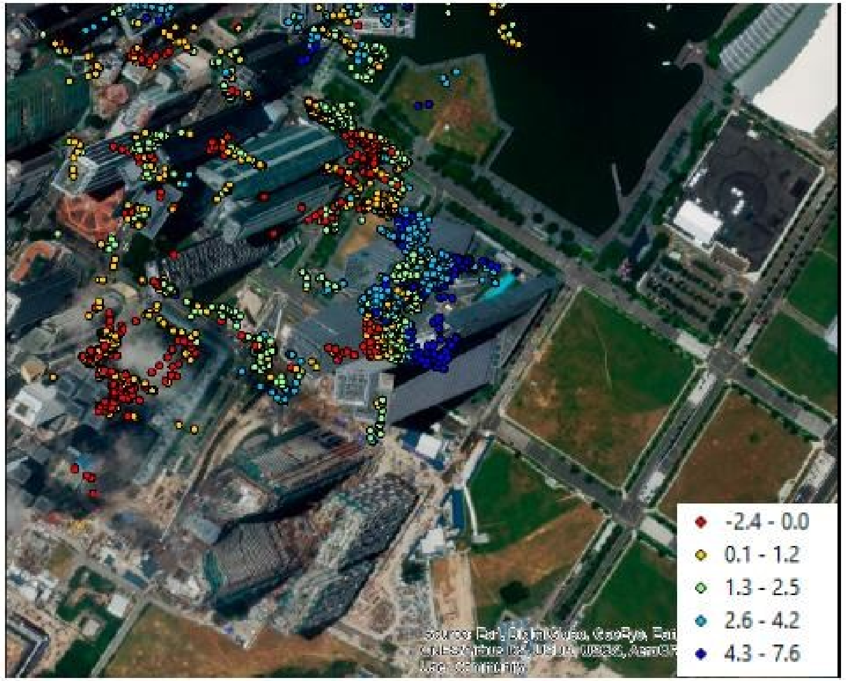

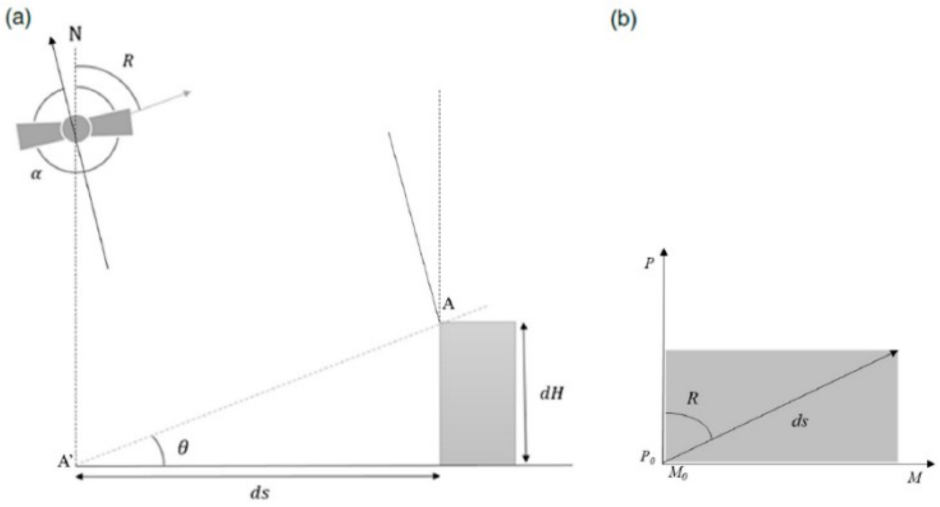

Figure 3. (**a**) SAR acquisition geometry of a building and (**b**) planimetric view of the geolocation error.

Deformation vs Height

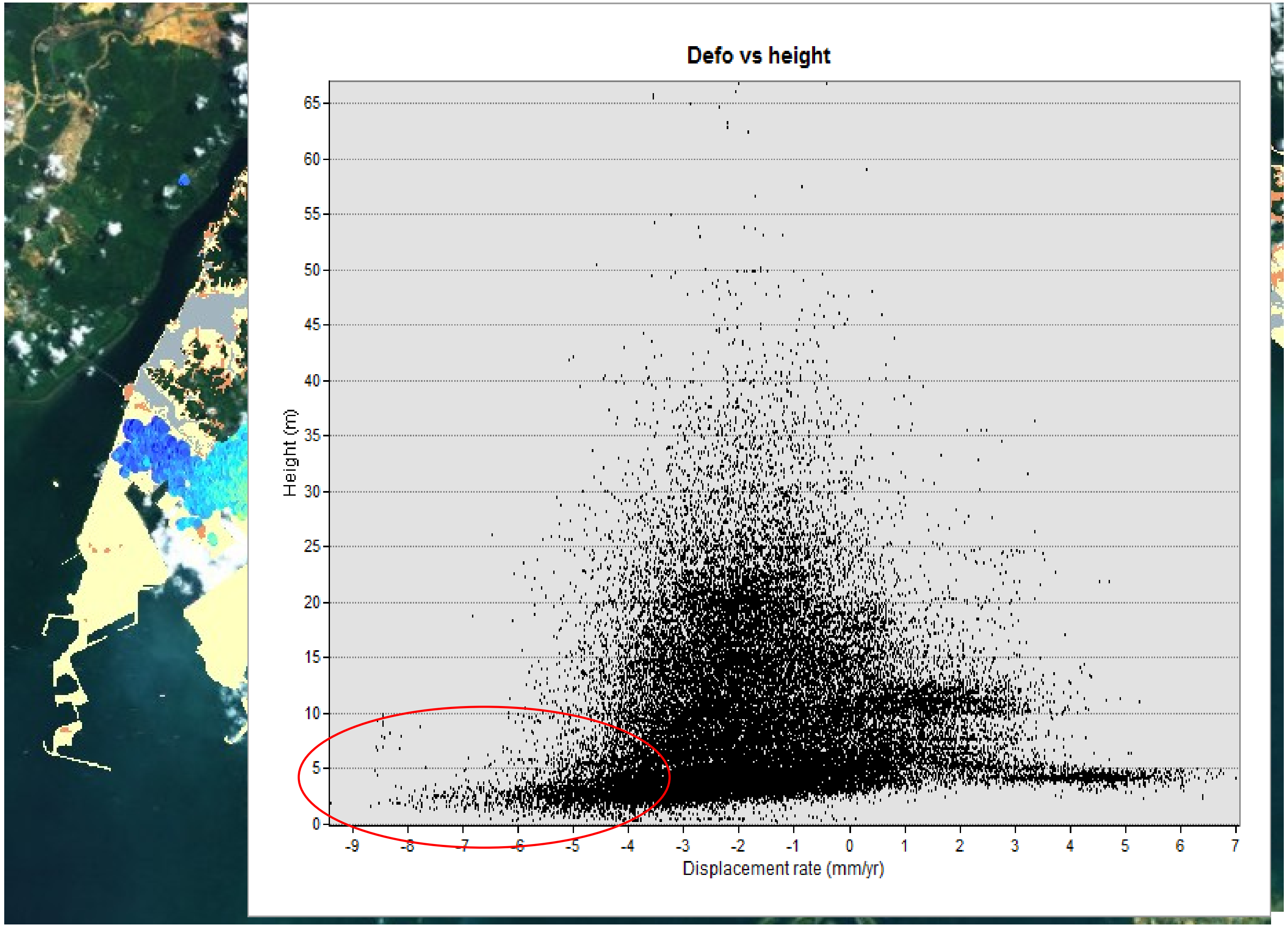

- < 0 m
- 0 – 2 m
- 2 – 5 m
- 5 – 10 m
- > 10 m

João Catalão Fernandes (jcfernandes@fc.ul.pt)

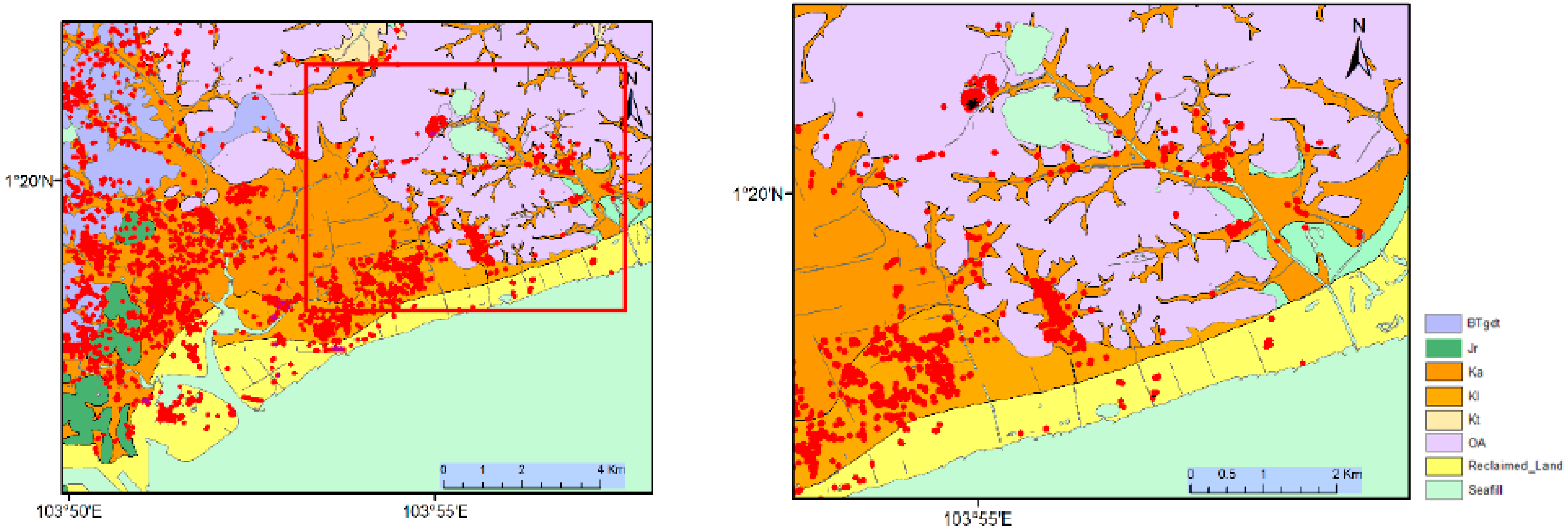

Figure 8. (left panel) Stratigraphy of marine Parade overlaid with persistent scatterers. Orange: Kallang formation (Ka); Purple: Old Alluvium (OA); yellow: reclaimed; Green: Juron Formation (Jt), Dark purple: Granite (BTgdt). Red dots are persistent scatterers with deformation rate between 2 and 5 mm/yr. Details of the area within the red rectangle are shown in right panel.

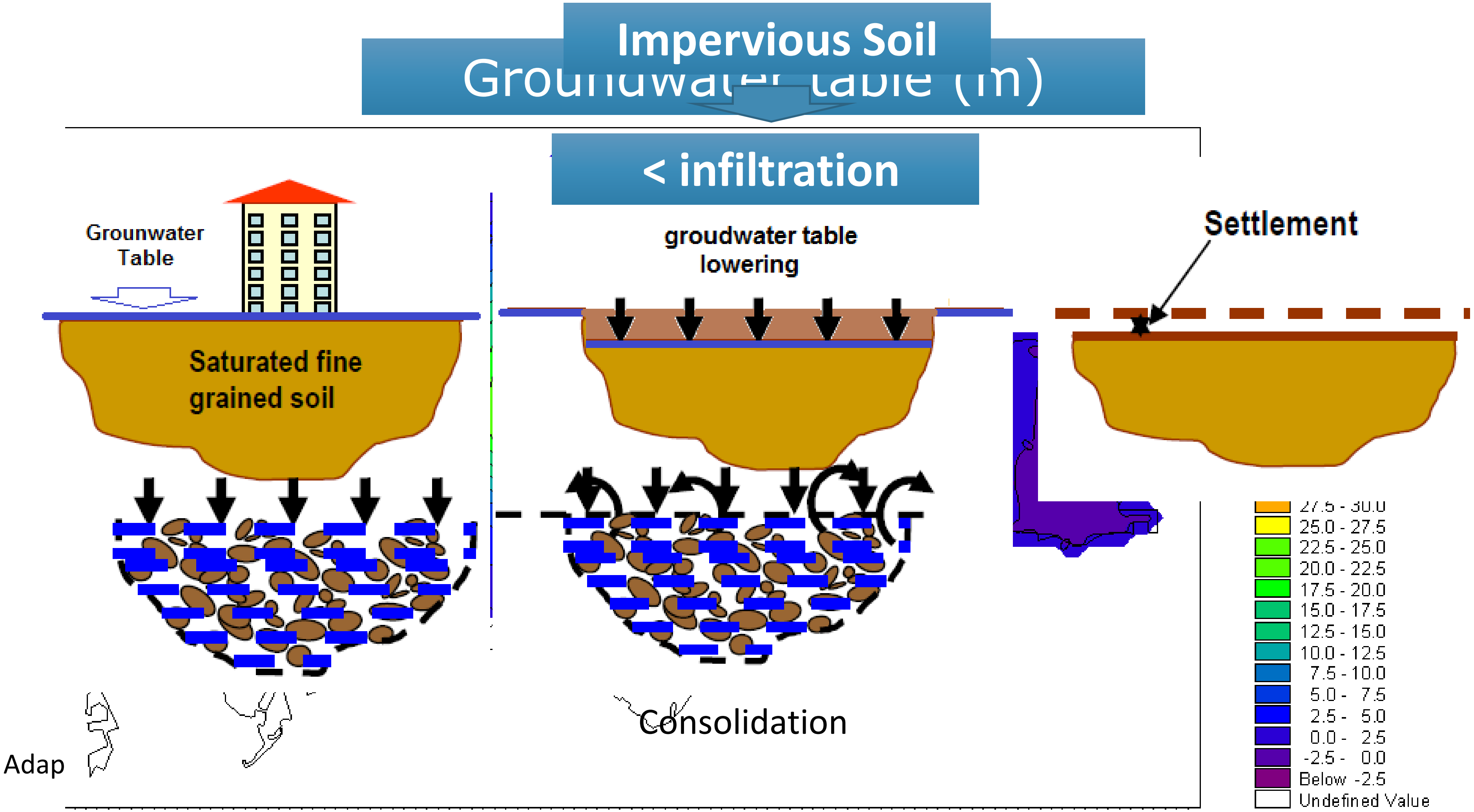

Impervious Soil
Groundwater table (m)
< infiltration
Grounwater Table
Saturated fine grained soil
groudwater table lowering
Settlement
Consolidation
Adap
27.5 - 30.0
25.0 - 27.5
22.5 - 25.0
20.0 - 22.5
17.5 - 20.0
15.0 - 17.5
12.5 - 15.0
10.0 - 12.5
7.5 - 10.0
5.0 - 7.5
2.5 - 5.0
0.0 - 2.5
-2.5 - 0.0
Below -2.5
Undefined Value

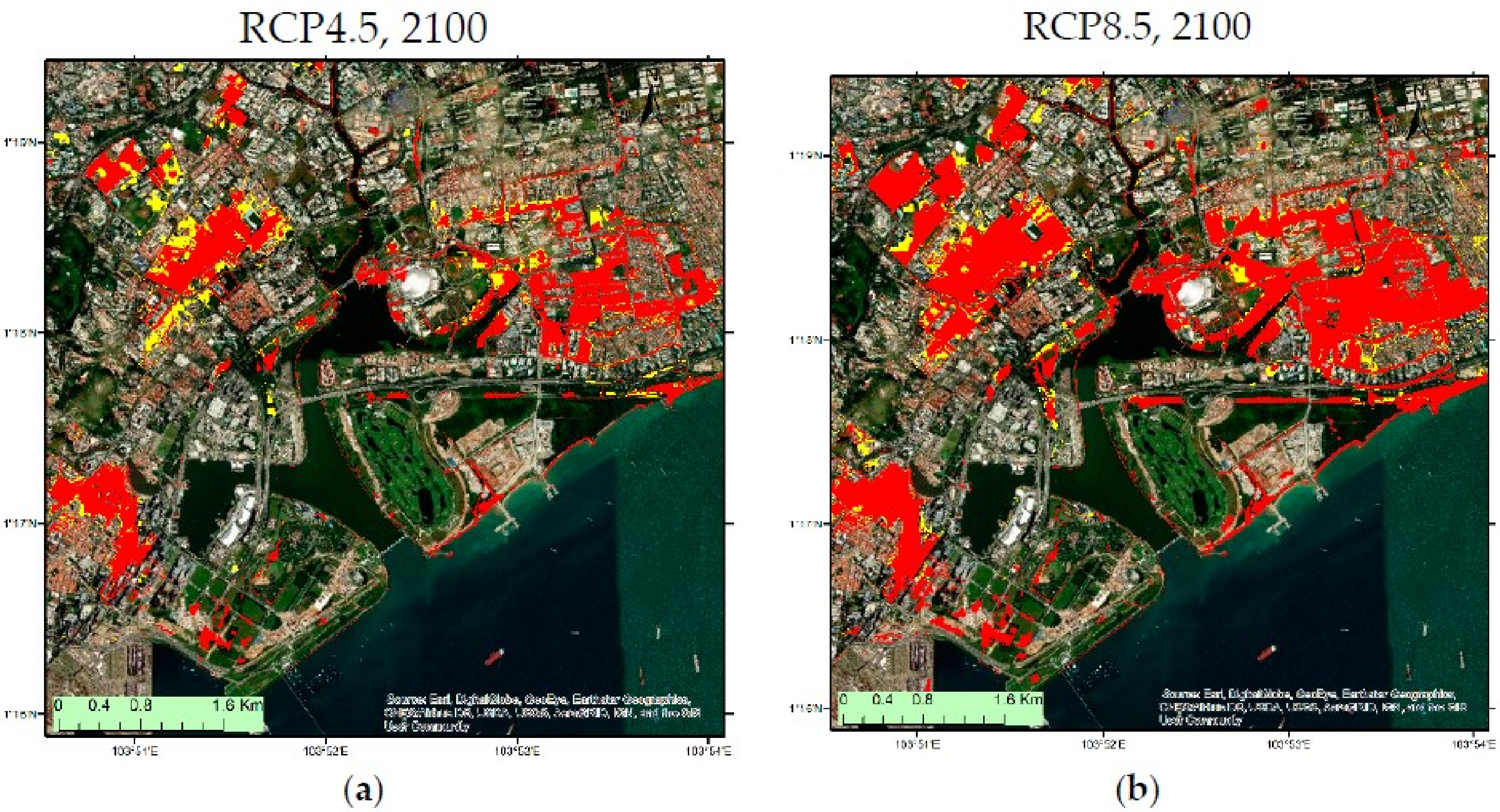

Figure 9. Inundation maps for Singapore downtown under two RCPs scenarios and local land subsidence estimated by SAR interferometry. The effect of sea level rise is shown in red and the combined effect of sea level rise and local land subsidence is shown in yellow. (a) Inundated area under RCP4.5 projection and (b) inundation area under RCP8.5 projection.

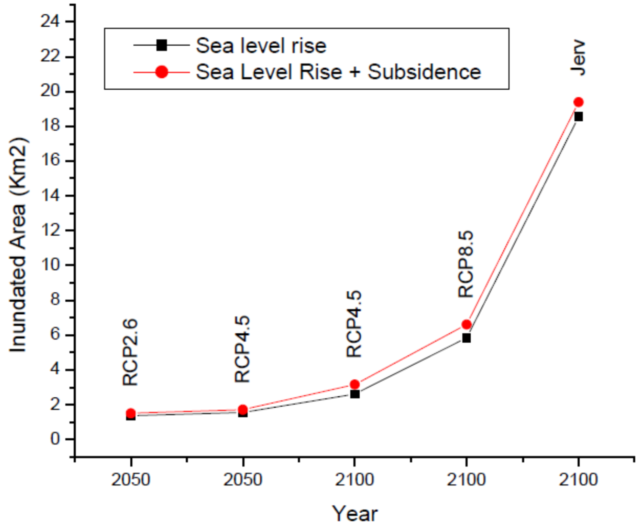

Figure 10. Projected inundated area under different RCP scenarios.

Catalao, J.; Raju, D.; Nico, G. Insar Maps of Land Subsidence and Sea Level Scenarios to Quantify the Flood Inundation Risk in Coastal Cities: The Case of Singapore. *Remote Sens.* **2020**, *12*, 296. https://doi.org/10.3390/rs12020296

Conclusions

Singapore mainland has experienced a subsidence phenomena with a mean subsidence rate of 1.5 mm/yr.

On some localized areas, a significant subsidence with subsiding rates of 7 mm/yr, was detected

Highest subsiding rates are near the shore on low flat land, above 5m, associated with reclaimed areas or built areas in the past years.

There are evidences of an anthropogenic cause, associated with compaction of built areas or reclaimed areas, rather than a natural cause.

Monitorização de Infraestruras e envolventes

Casos Subsidência: Cais do Sodré

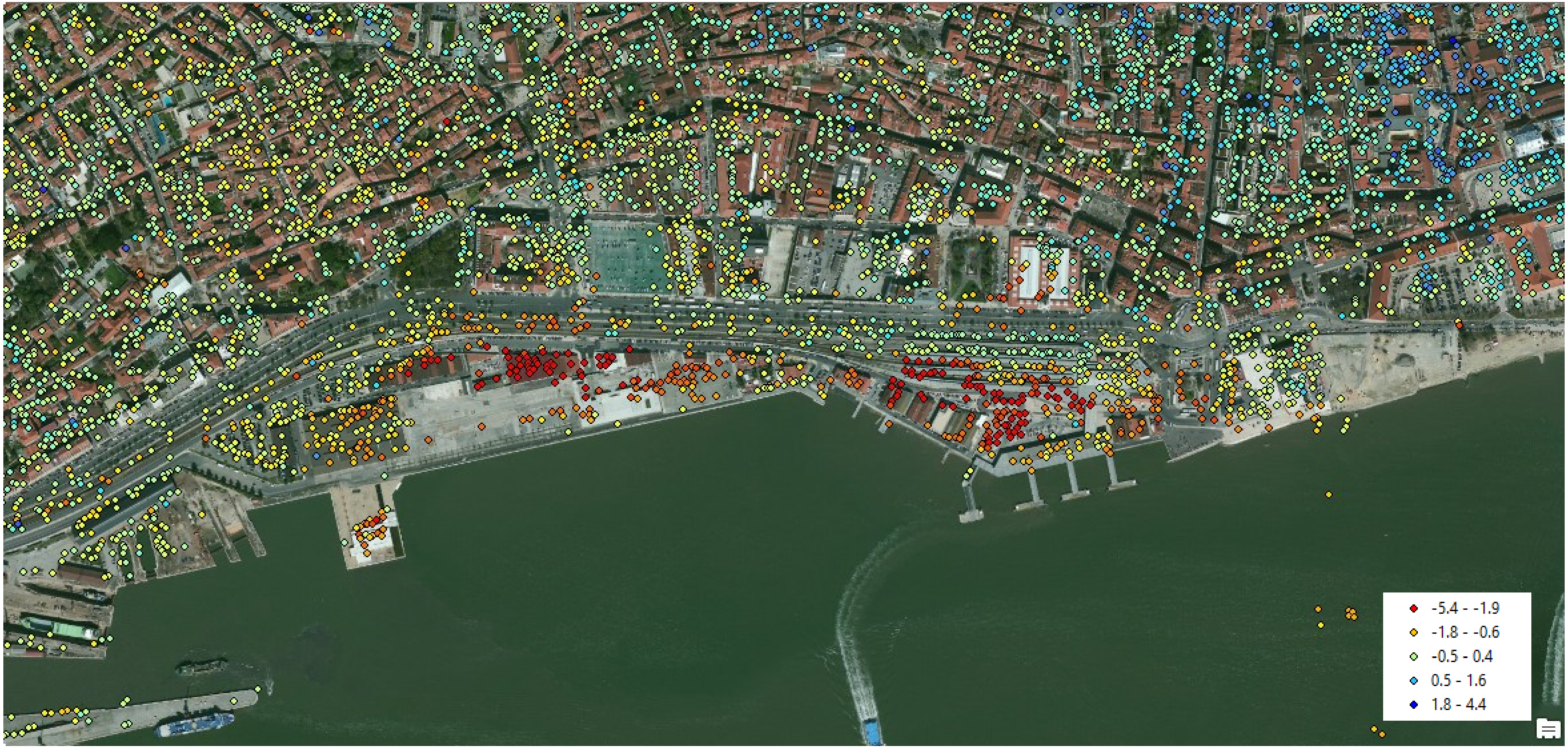

Casos Subsidência: A30 (St Iria Azoia)

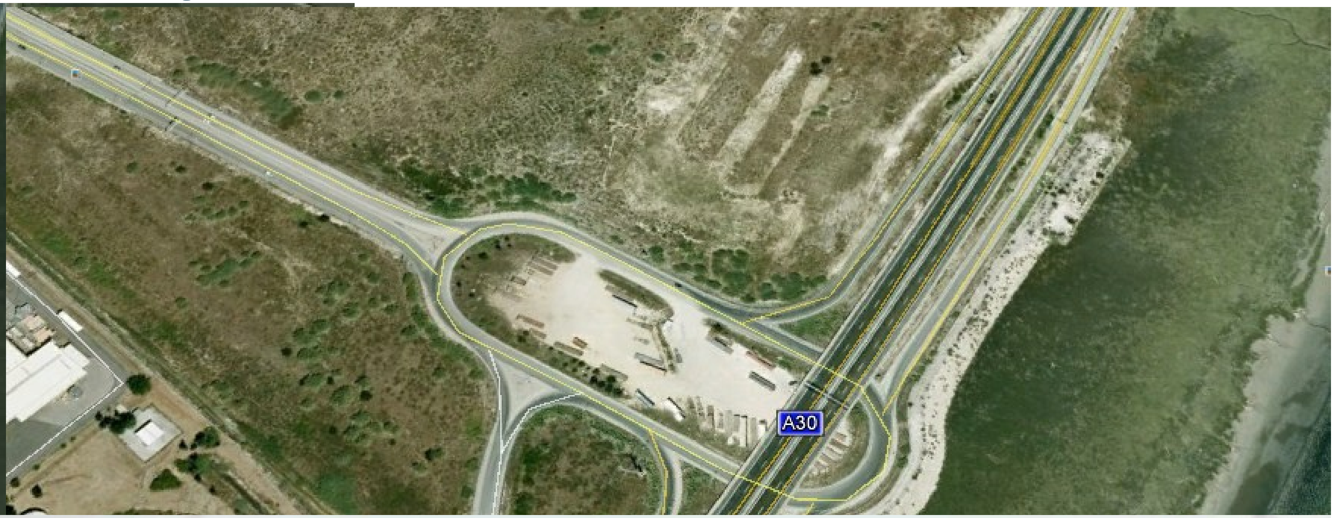

Estudo de viabilidade da monitorização de infraestruturas rodoviárias com interferometria SAR - Caso de estudo a A9

RELATÓRIO DE EXECUÇÃO

JOÃO CATALÃO

Ciências ULisboa

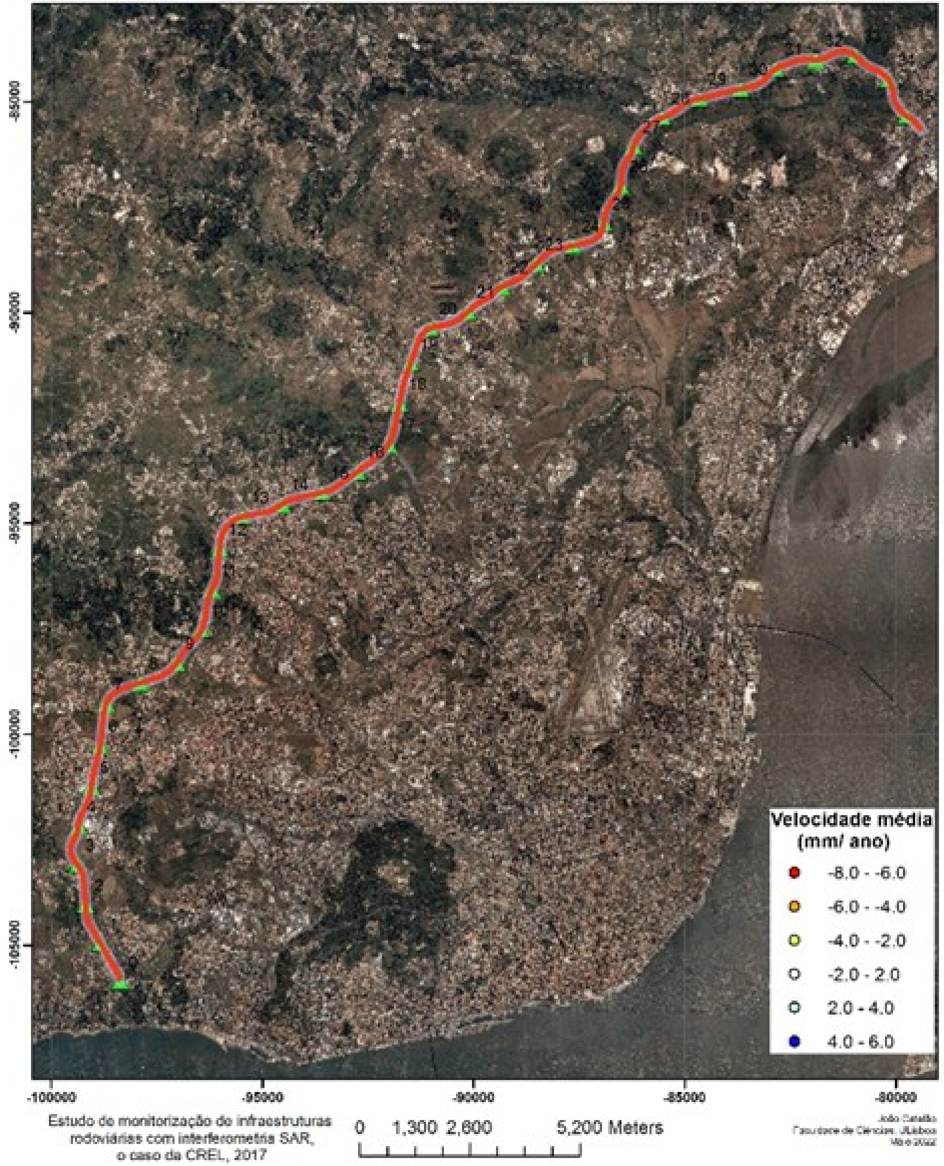

CREL - 2017

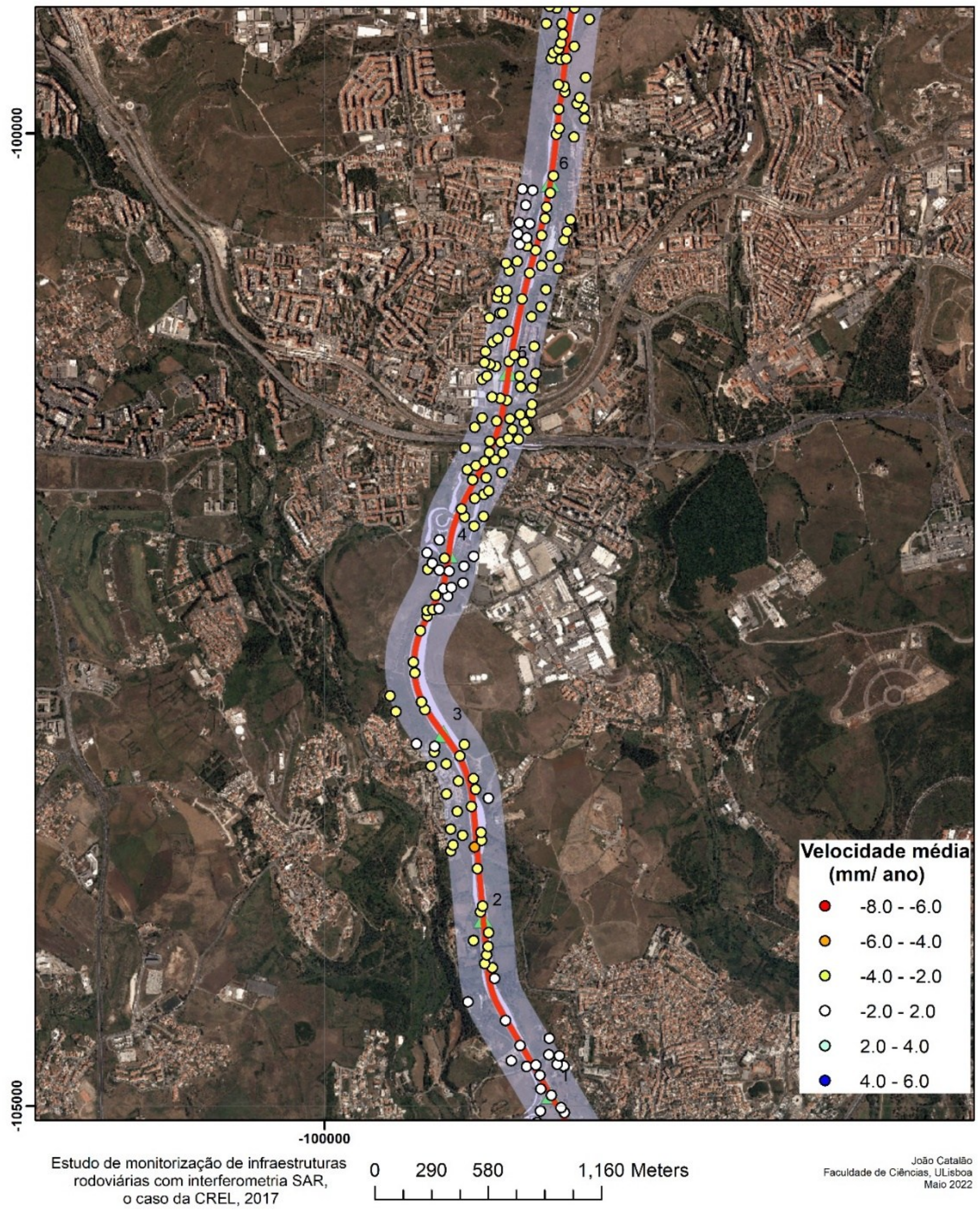

CREL - 2017

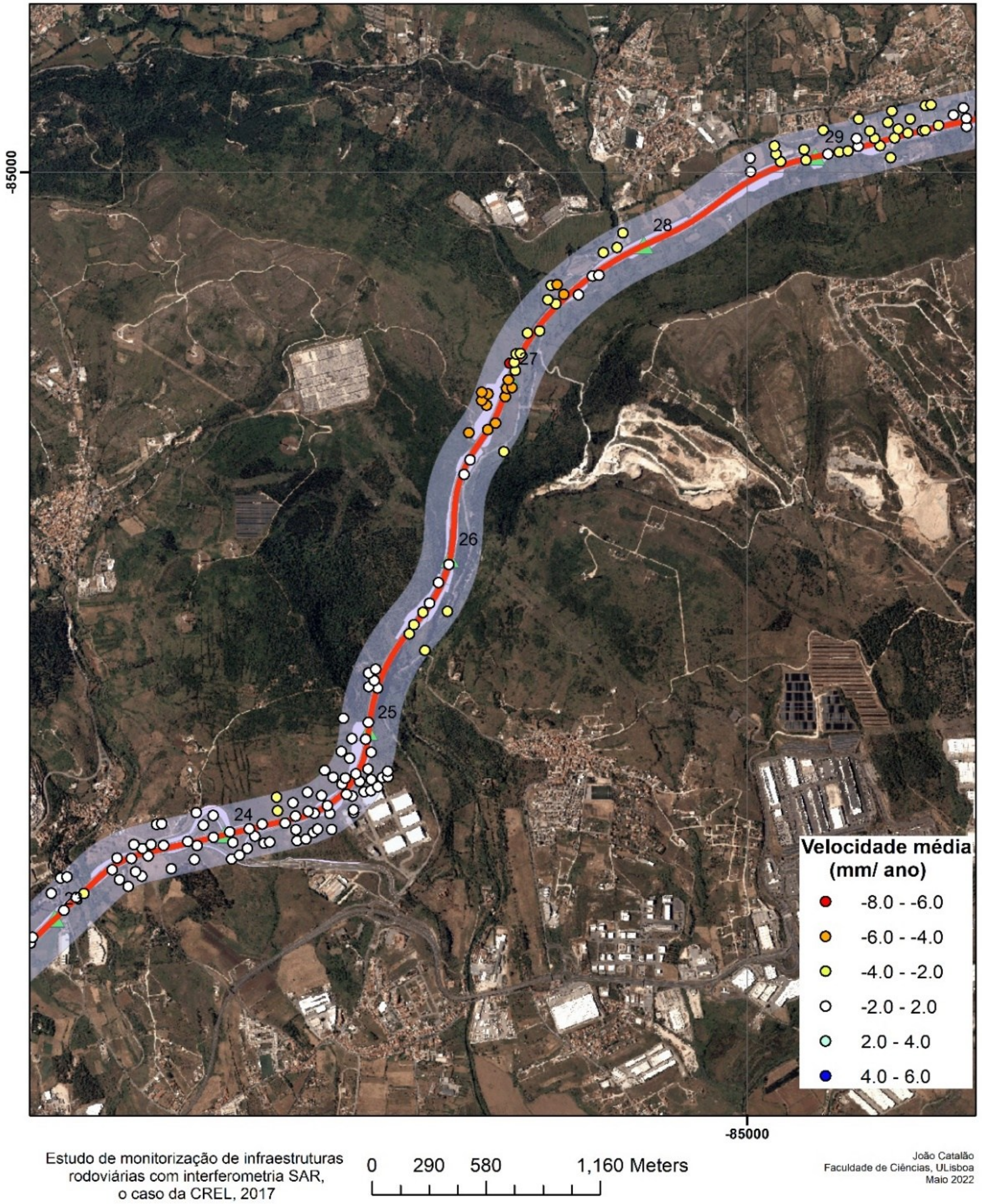

Estudo de viabilidade da monitorização de infraestruturas rodoviárias com interferometria SAR de elevada resolução espacial – Portagem de Odivelas da A40.

RELATÓRIO DE EXECUÇÃO

JOÃO CATALÃO

Ciências ULisboa

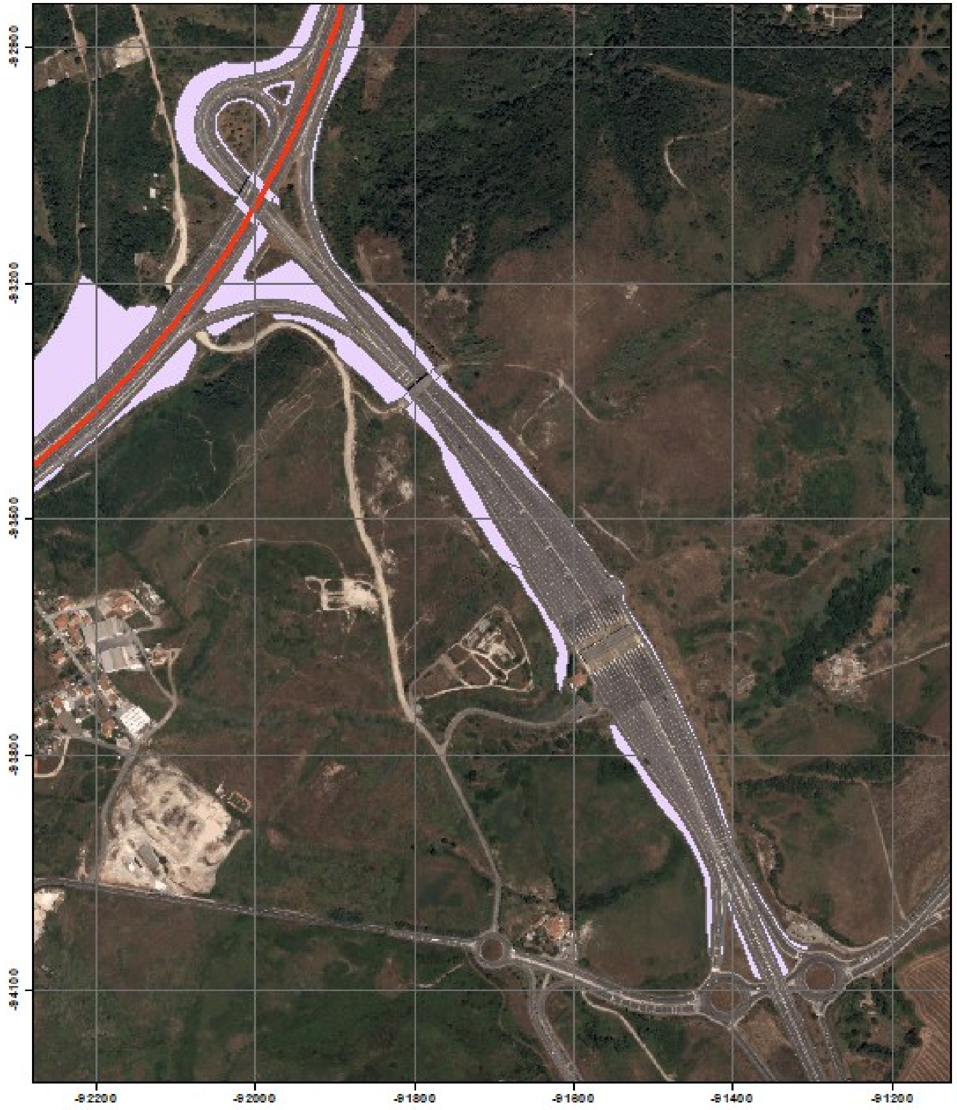

A40: Nó de Odivelas

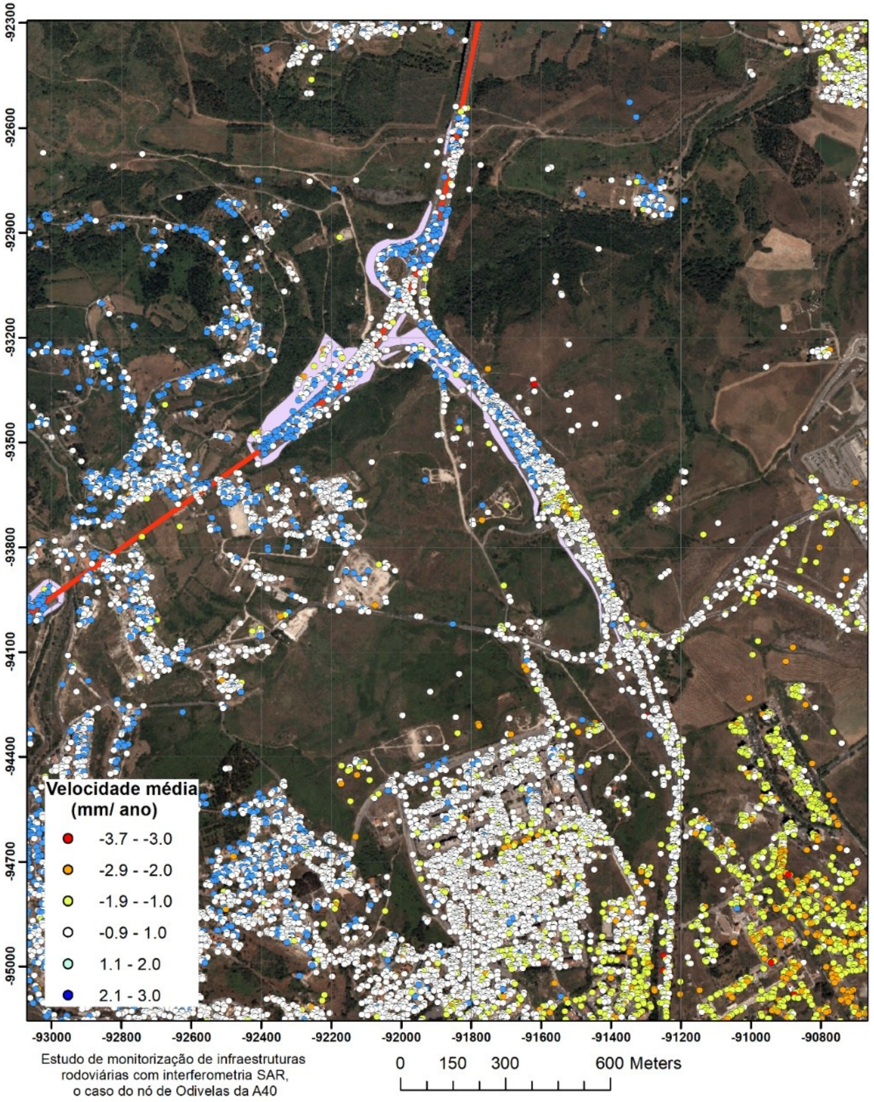

A40: Nó de Odivelas

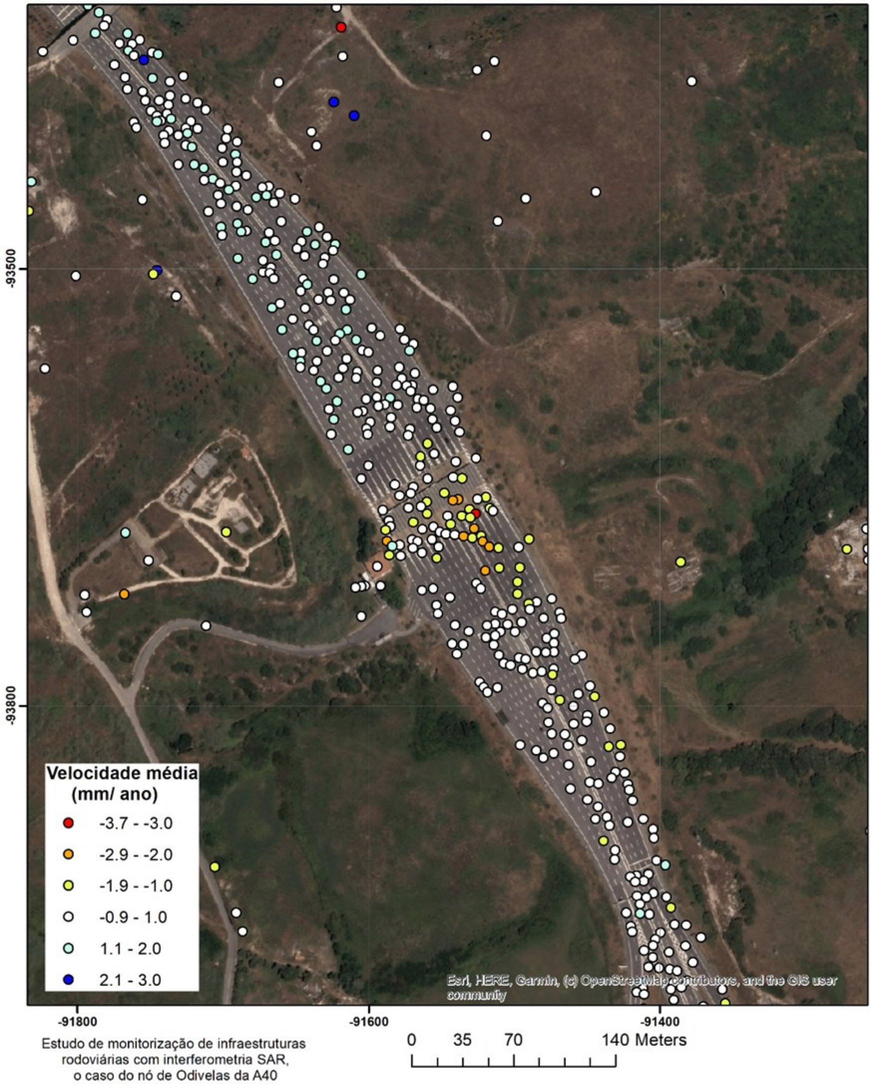

Casos Subsidência: CREL, Caneças

Implementação de um sistema de monitorização baseado na técnica PS-INSAR na envolvente à albufeira da barragem do Aproveitamento Hidroelétrico de Foz Tua

Data	Data da master	Inicio da série	Fim da série	Mínimo da $B_{\perp}$ (m)	Máxima da $B_{\perp}$ (m)	Num. Interf.
2016 Desc	20160519	20151215	20170126	-69.2	99.59	31
2016 Asc	20160724	20151209	20170120	-71.3	103.0	34
2017 Desc	20170619	20161209	20180121	-80.6	97.7	31
2017 Asc	20170625	20161215	20180127	-106.6	105.9	31
2018 Desc	20180509	20171216	20190128	-107.9	103.4	33
2018 Asc	20180620	20171210	20190122	-63.1	133.9	33
2019 Desc	20190528	20181211	20200111	-102.2	117.7	34
2019 Asc	20190709	20181205	20200117	-100.9	106.4	34

Parâmetro	Valor	Parâmetro	Valor
Dispersão amplitude	0.4	Dimensão do filtro	50 m
Erro Topográfico máximo	5 m	Janela temporal de desenrolamento da fase	730
Percentagem máxima de PS com fase aleatória	20	Grelha de desenrolamento da fase	200 m

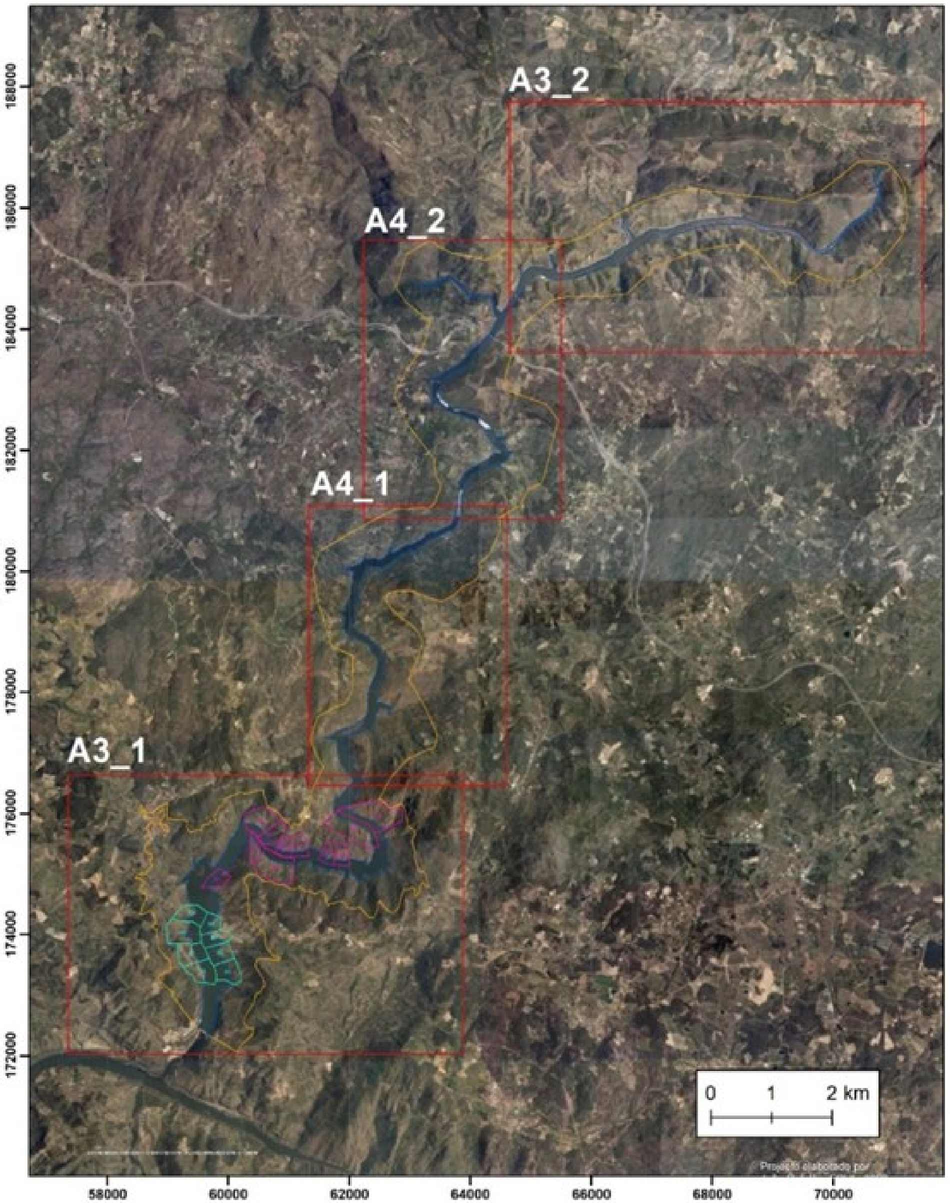
A3_2
A4_2
A4_1
A3_1
0 1 2 km
Projeto elaborado por

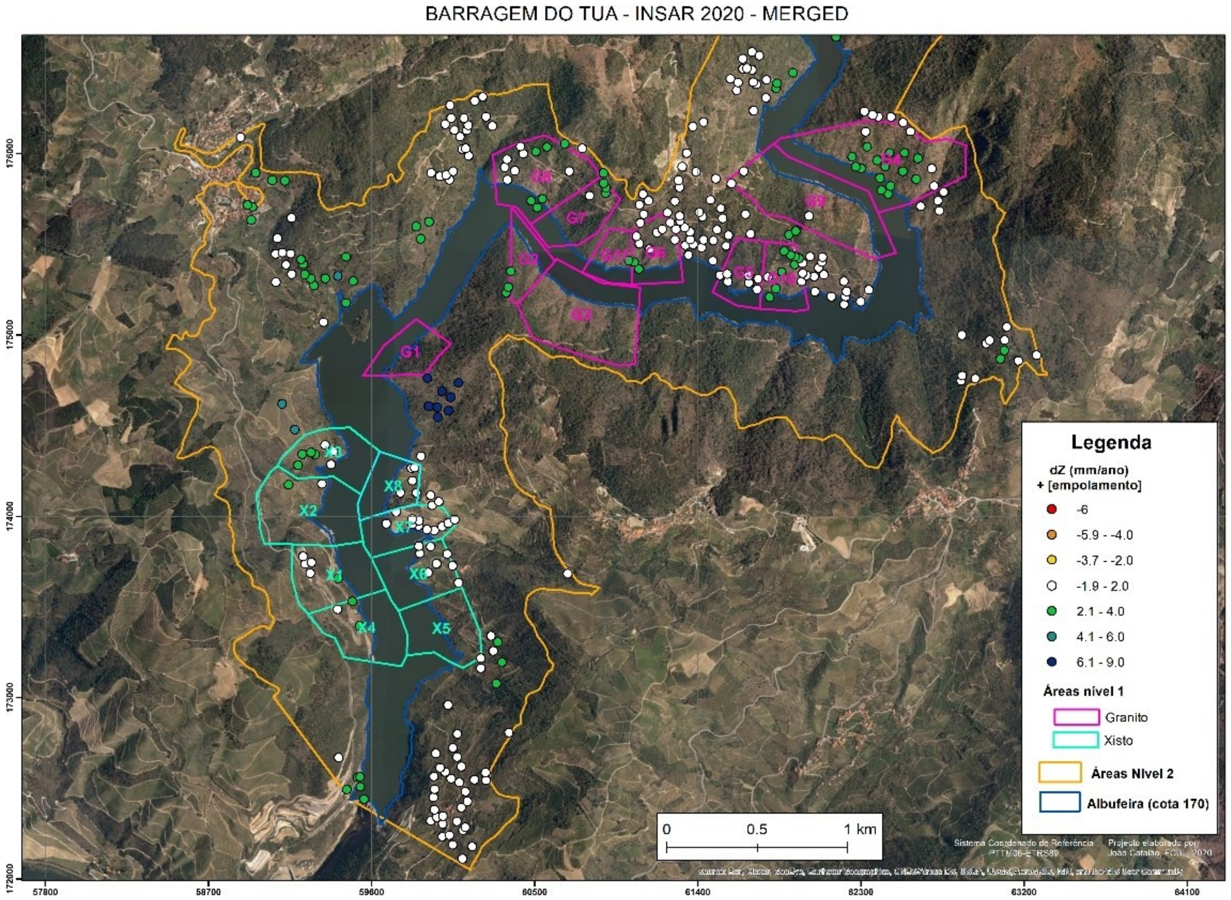
BARRAGEM DO TUA - INSAR 2020 - MERGED
Legenda
dZ (mm/ano)
+ [empolamento]
-6
-5.9 - -4.0
-3.7 - -2.0
-1.9 - 2.0
2.1 - 4.0
4.1 - 6.0
6.1 - 9.0
Áreas nível 1
Granito
Xisto
Áreas Nível 2
Albufeira (cota 170)
0 0.5 1 km
X1
X2
X3
X4
X5
X6
G1

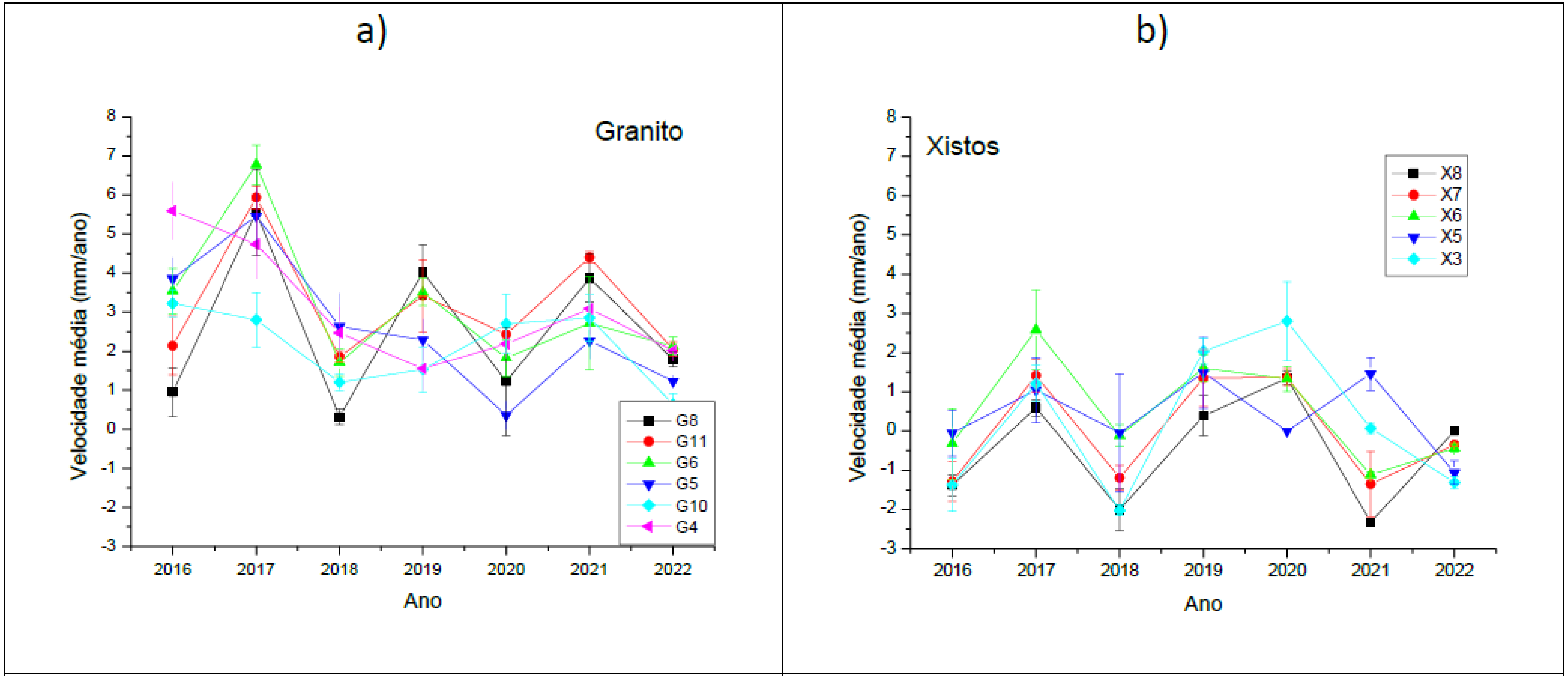

Figura 1.5. Evolução temporal da deformação nos polígonos de nível-1, a) zona dos granitos, b) zona dos xistos

BARRAGEM DO TUA - INSAR 2020 - MERGED

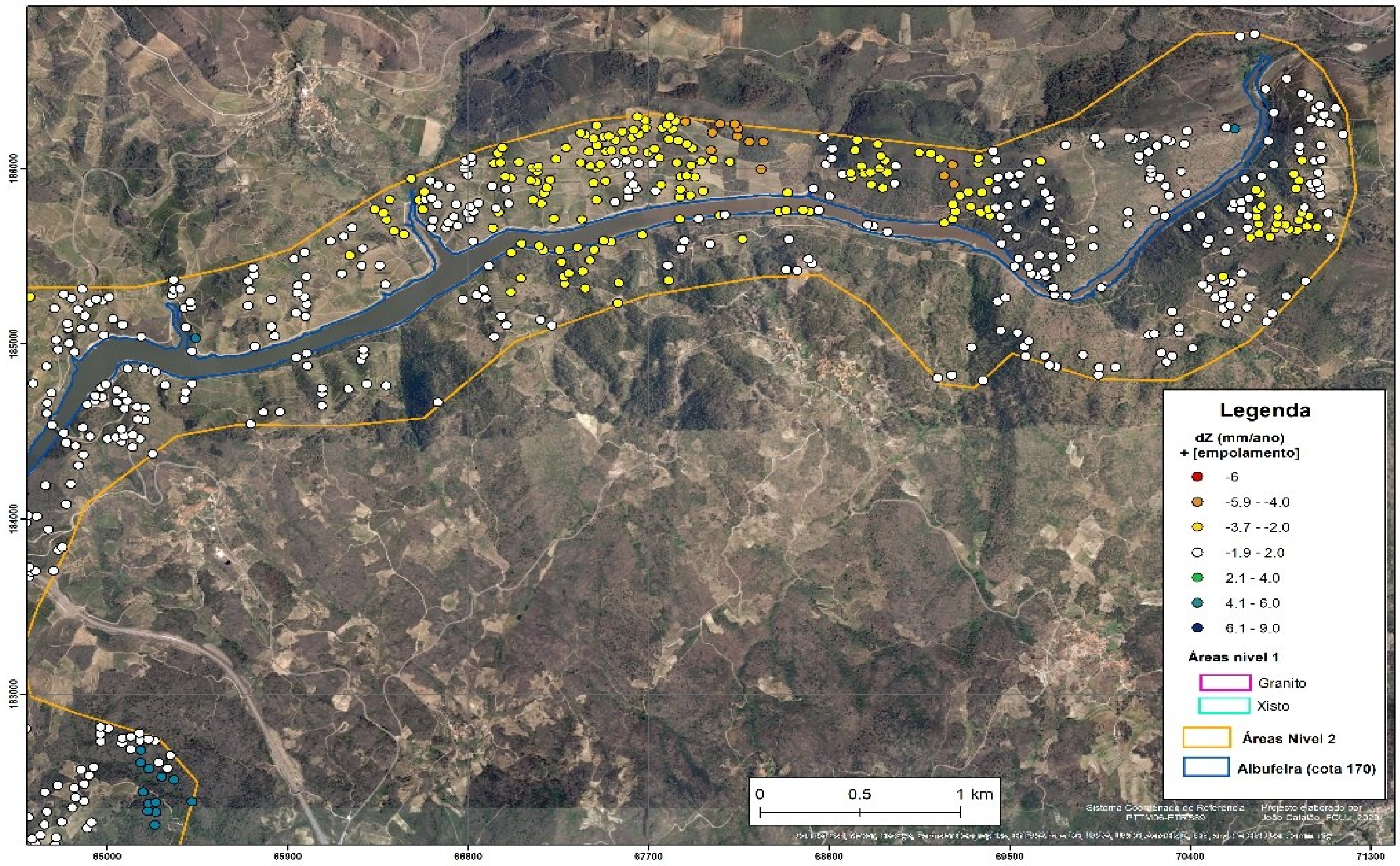

Aplicações
SAR e INSAR

IEEE TRANSACTIONS ON GEOSCIENCE AND REMOTE SENSING (2016)

Multitemporal Backscattering Logistic Analysis for Intertidal Bathymetry

J. Catalão, *Member, IEEE*, and G. Nico, *Senior Member, IEEE*

***Abstract*—A new methodology for the mapping of intertidal terrain morphology is presented. It is based on the use of synthetic aperture radar (SAR) images and the temporal correlation between the SAR backscatter intensity and the water level on the intertidal zone. The proposed methodology does not require manual editing, providing a set of geolocated pixels that can be used to generate a digital elevation model of the intertidal zone. The methodology is validated using TerraSAR-X SAR images acquired over Tagus estuary. This methodology can be useful for the regular updating of intertidal bathymetric models useful for both flood hazard mitigation and morphodynamics modeling.**

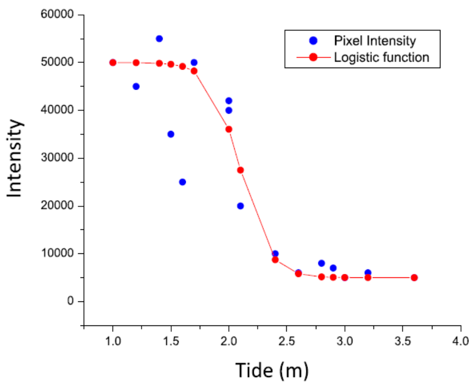

Fig. 2. TV of the intensity versus tide height at a true intertidal pixel wi
the corresponding modeled logistic function.

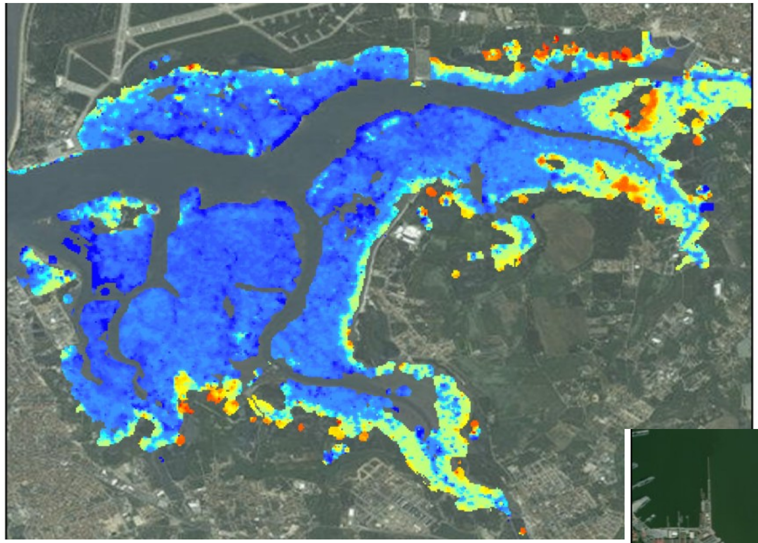

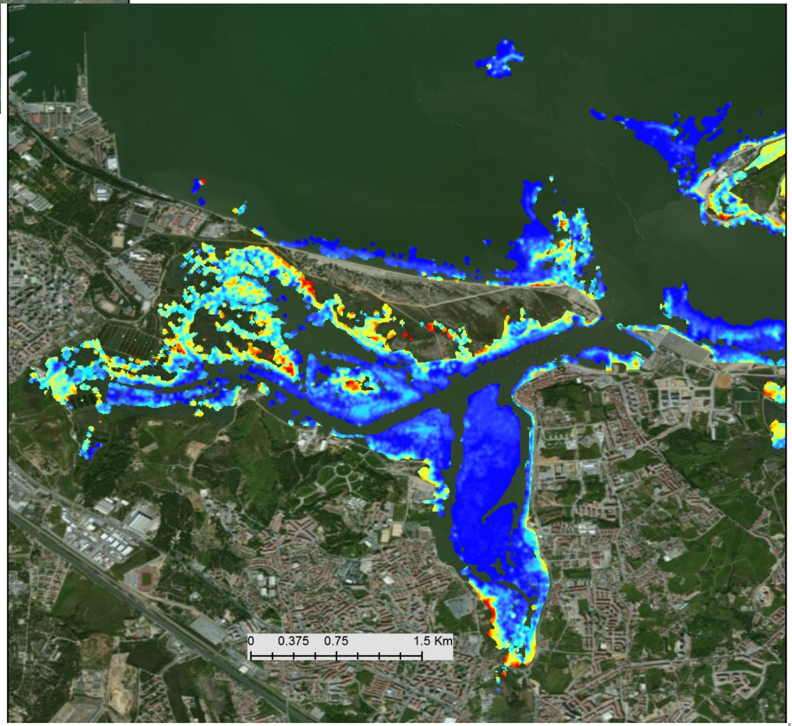

Multitemporal Intensity Logistic Analysis (MILA)

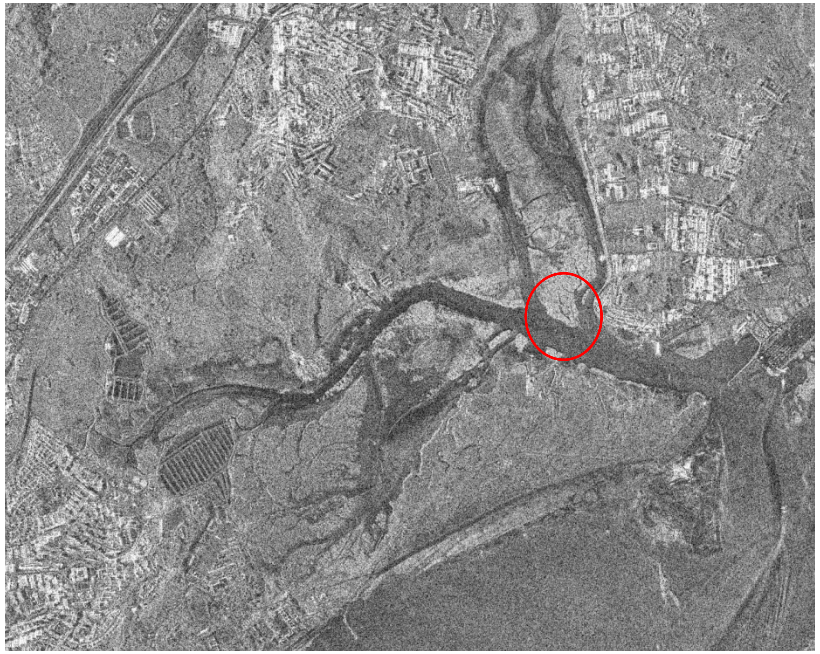

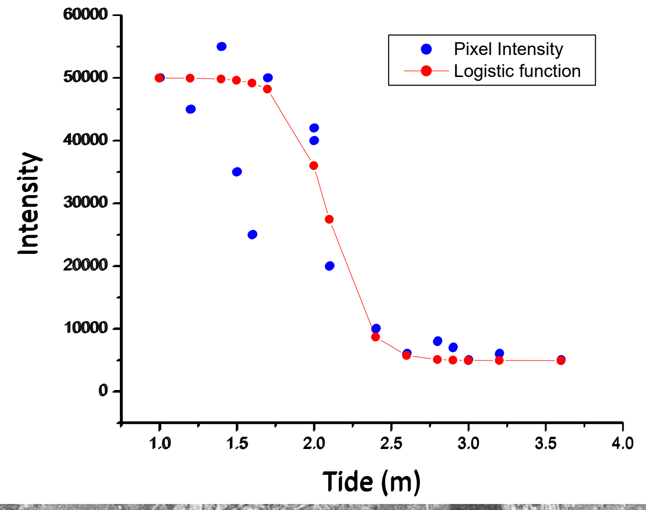

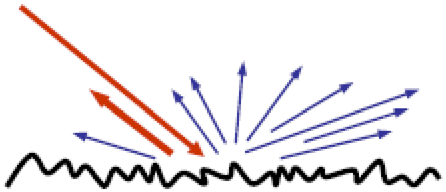

Diffuse to Specular scattering

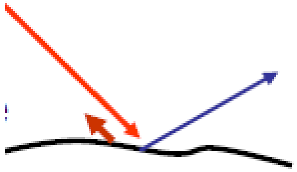

Multitemporal logistic analysis

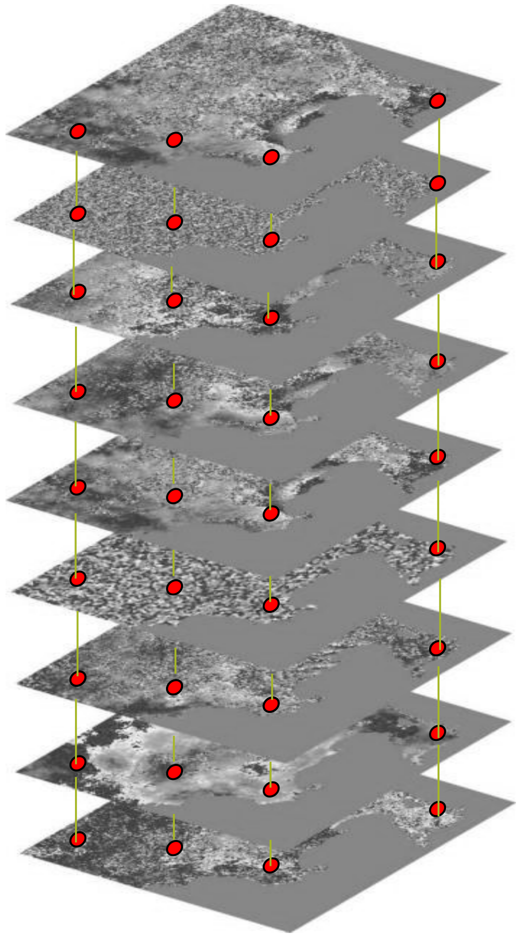

> M intensity images

> Coregister

> Multitemporal Filter
(to reduce the speckle)

$$J_k(x,y) = \frac{\mu_k}{M}\sum_{i=1}^{M}\frac{I_i}{\mu_i}$$

I_i is the pixel intensity
μ_k is the n x n average (image k)
μ_i is the n x n average (image i)

João Catalão Fernandes (jcfernandes@fc.ul.pt)

Logistic analysis

The logistic function relates the height of the resolution cell (h) with the pixel intensity (J_i). The function is defined by the parameters (a, k, h) and is given by:

$$J_i = \frac{k}{1 + e^{-a(h_i - h)}} \qquad i = 1, \ldots, M$$

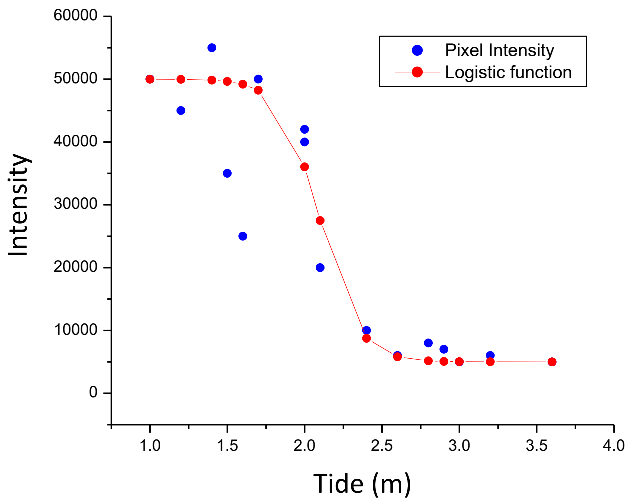

In which **k** is the maximum intensity, **a** is the steepness of the logistic function (a= -8, if negative the function decrease), h is the height of the resolution cell and h_i is the tide height for image i.

$$\min\left\{\sum_{i=1}^{M} h_i - h + \frac{1}{a}\ln\left(\frac{J_i}{k - J_i}\right)\right\}^2$$

We have to search on the solution space for the values (h, k) that minimize the expression.

h and k are the parameters to be estimated

Test Site: Tagus Estuary

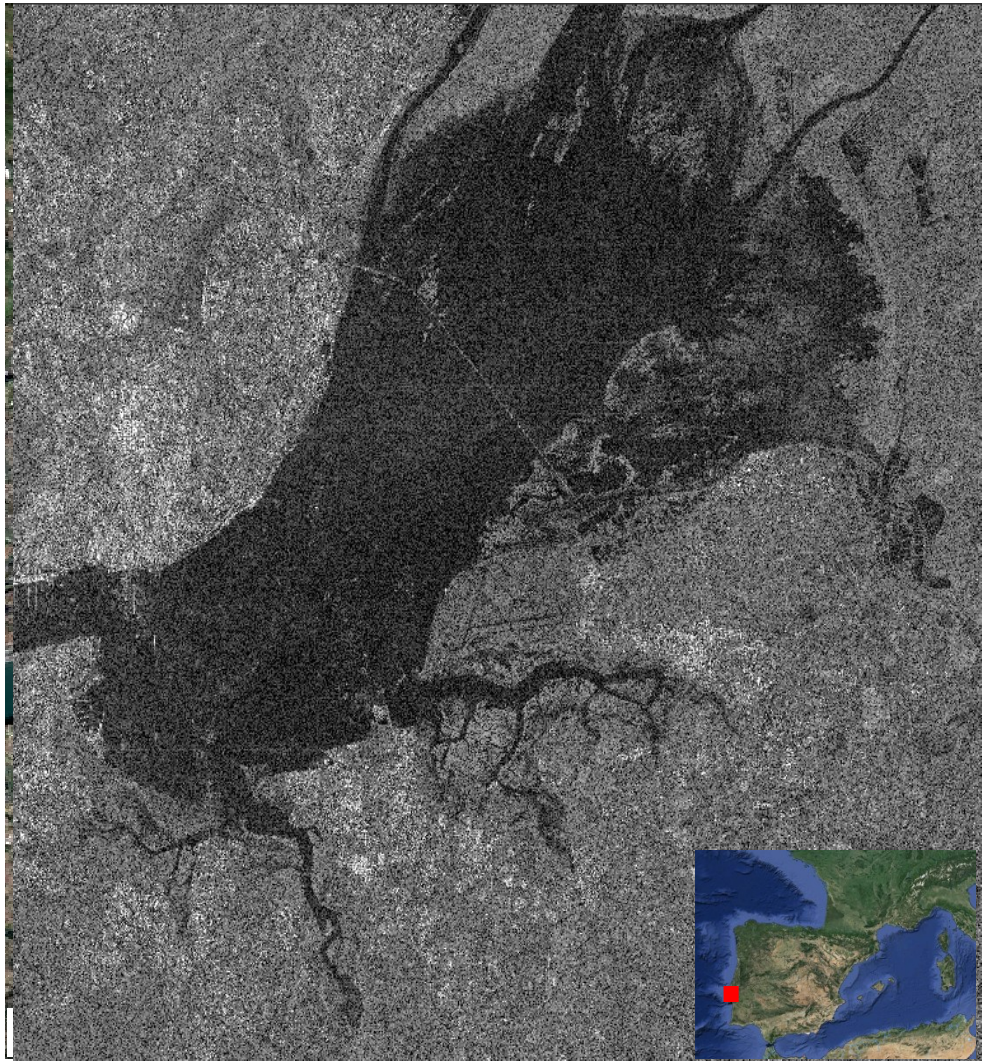

SAR data and Tide height

TerraSAR-X SAR images (19)
From January 2013, January 2014
Ascending, HH polarization, 3 m resolution
Incidence angle: 42.8 degrees
(Project: DLR COA 1840)

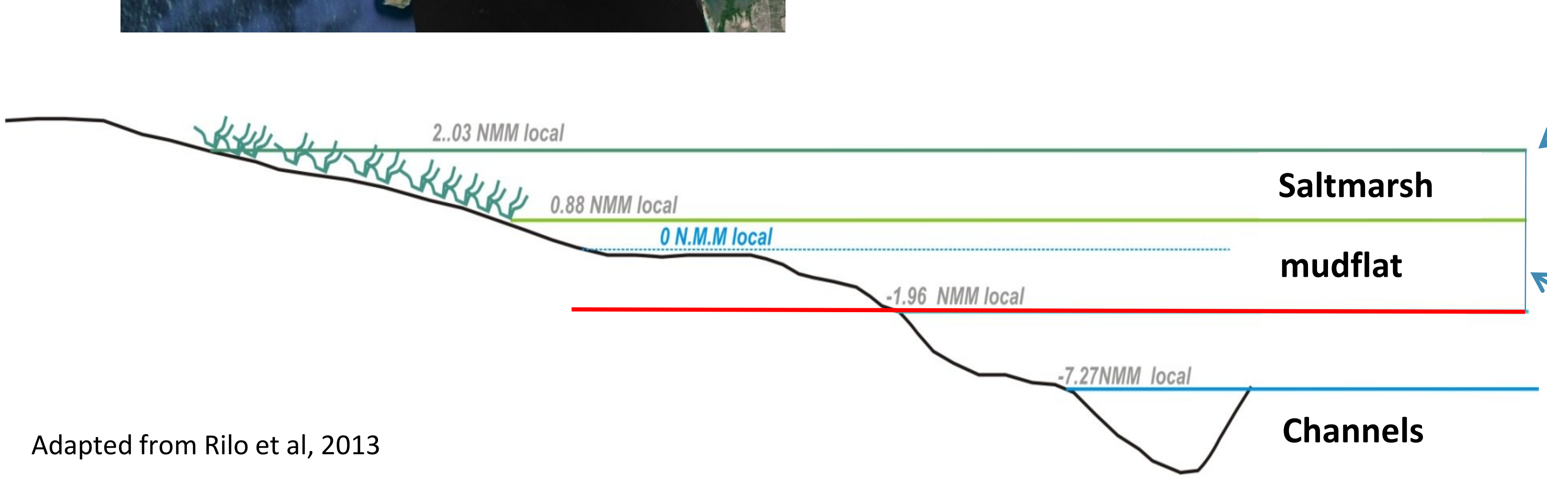

Adapted from Rilo et al, 2013

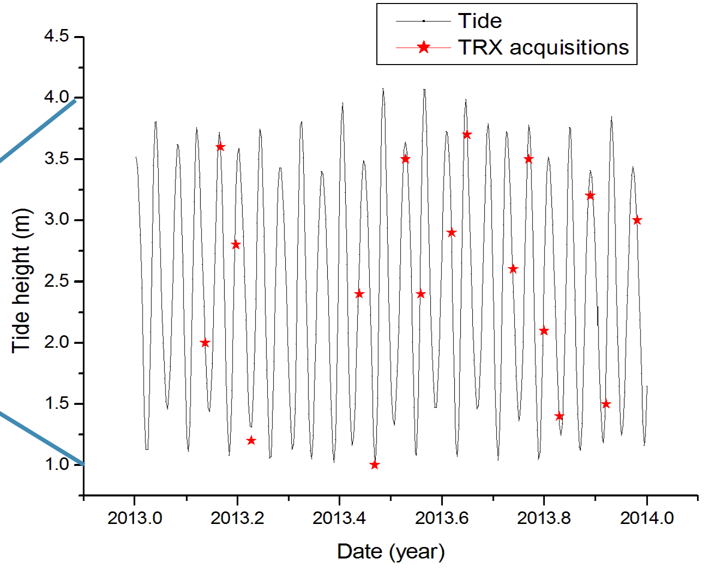

Tagus estuary tide height at 18:30 from 2013, January to 2014, January.

Intertidal elevation model

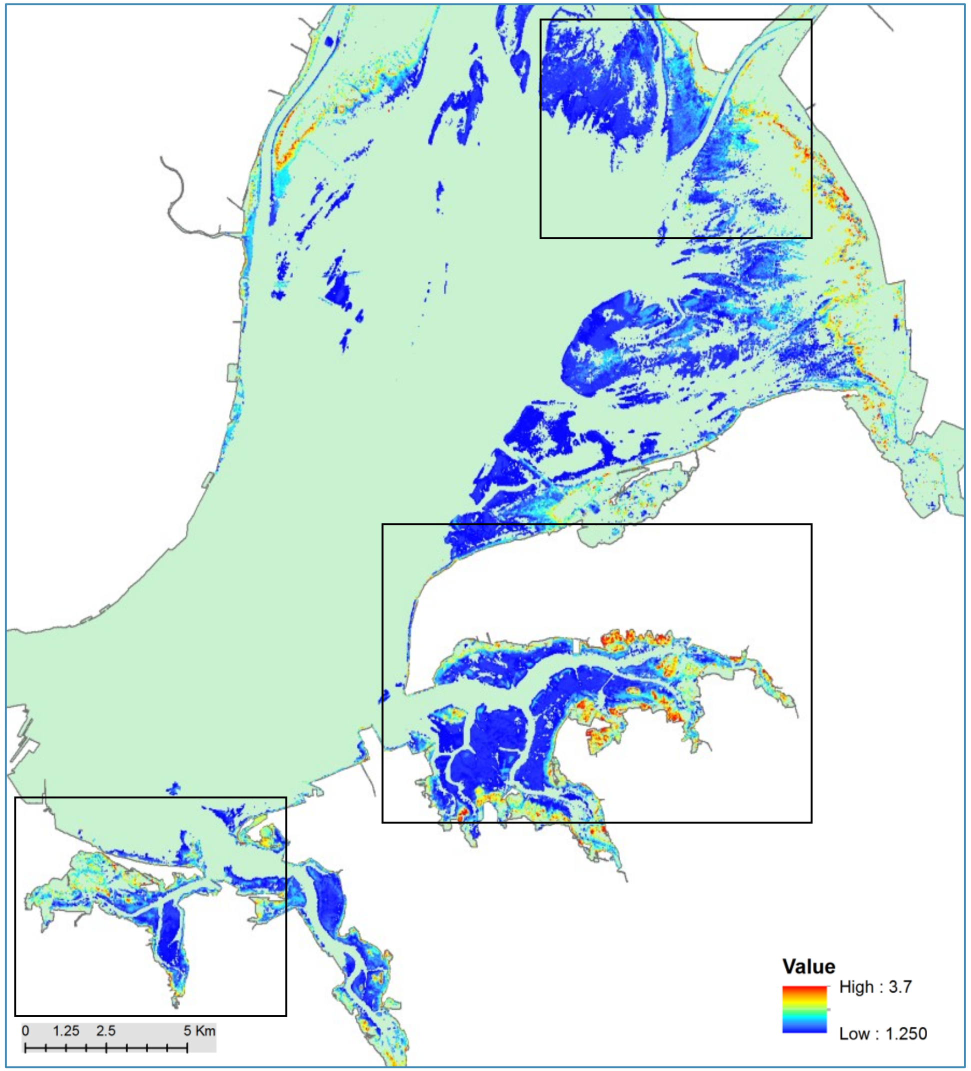

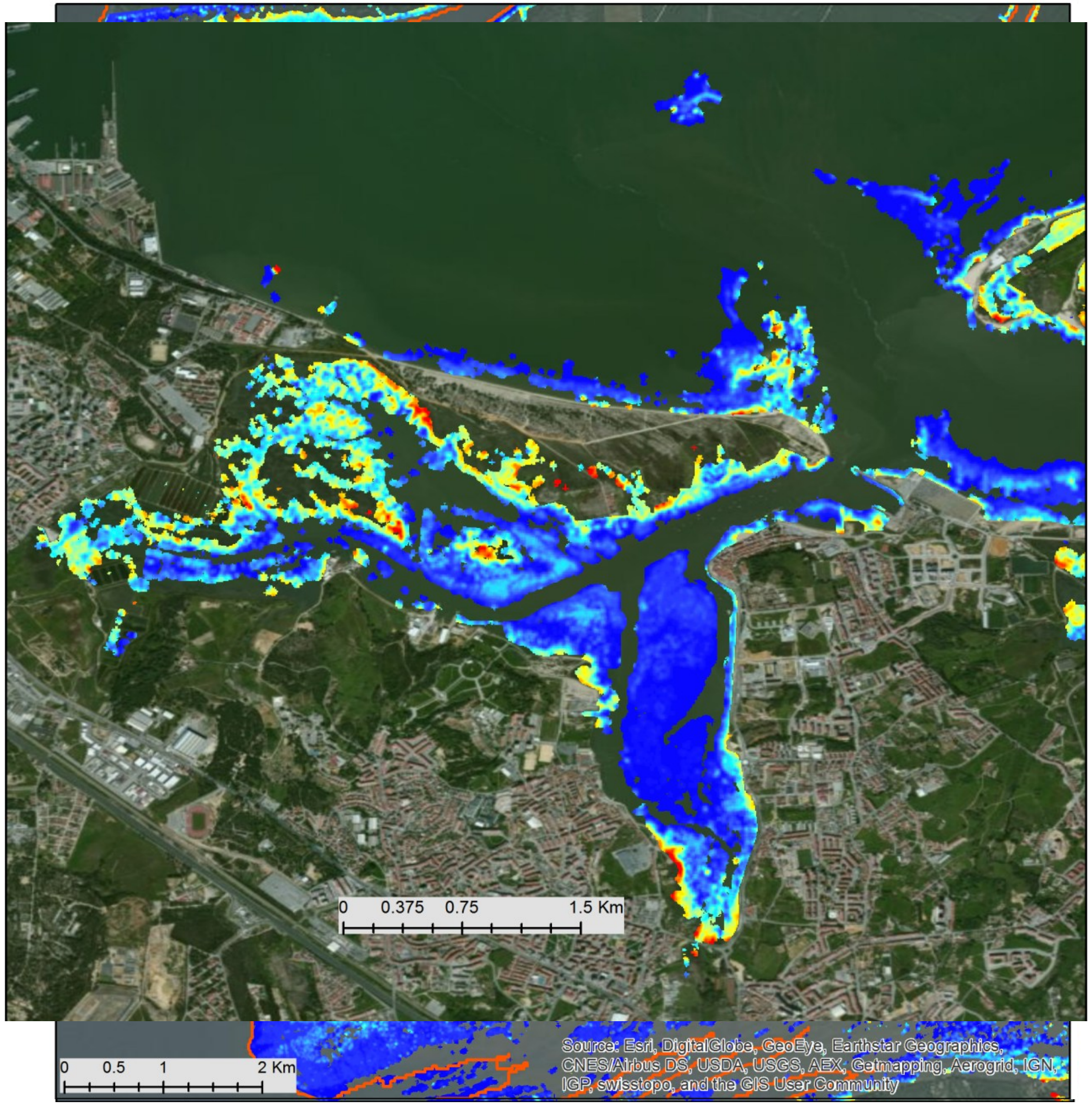

Validation

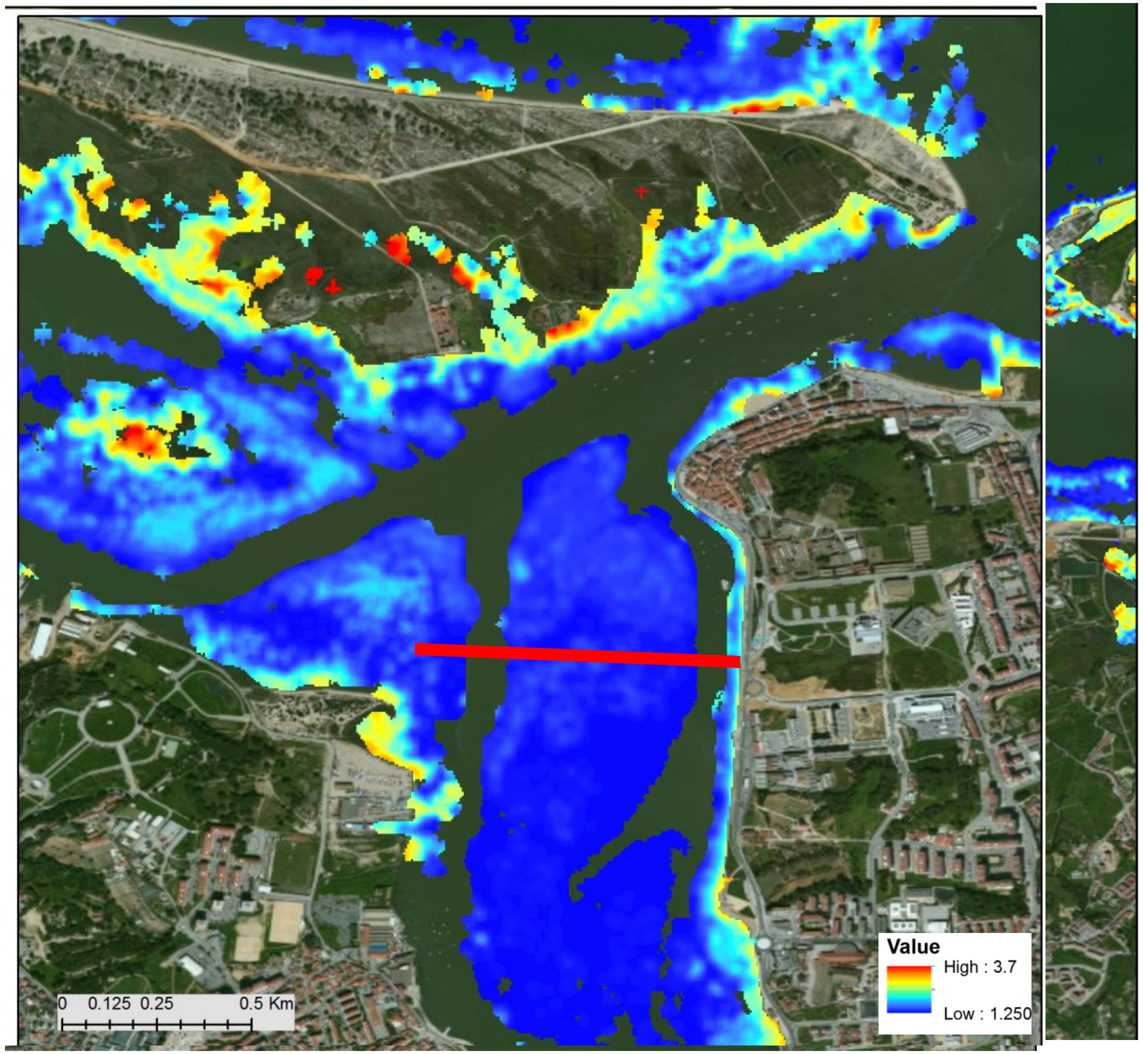

Bathymetric survey with echo sounding
Hydrographic Institute, 2014. Uncertainty= 0.18 m

Comparison between grids:
mean=-0.18 m; std = 0.23 m

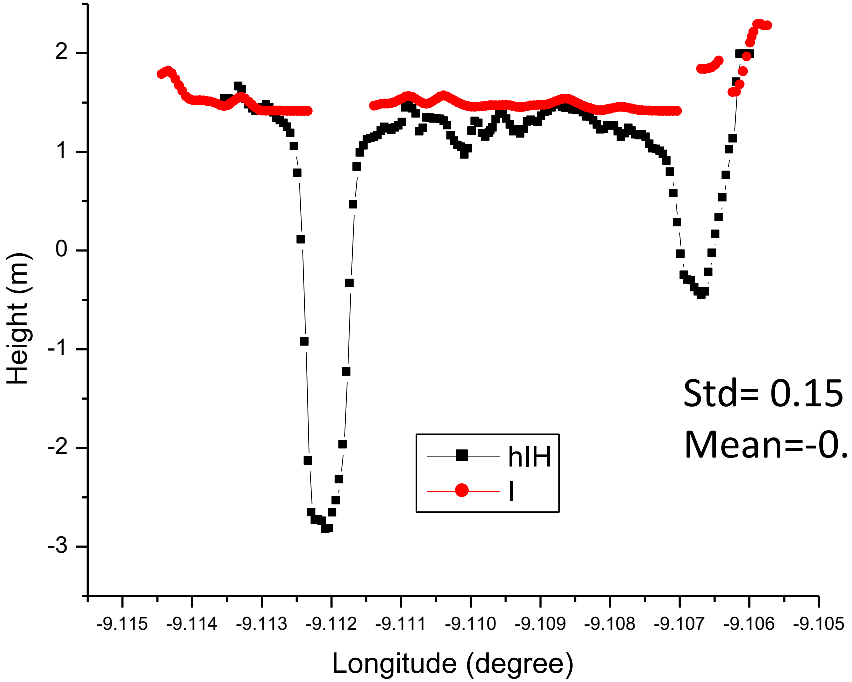

Validation

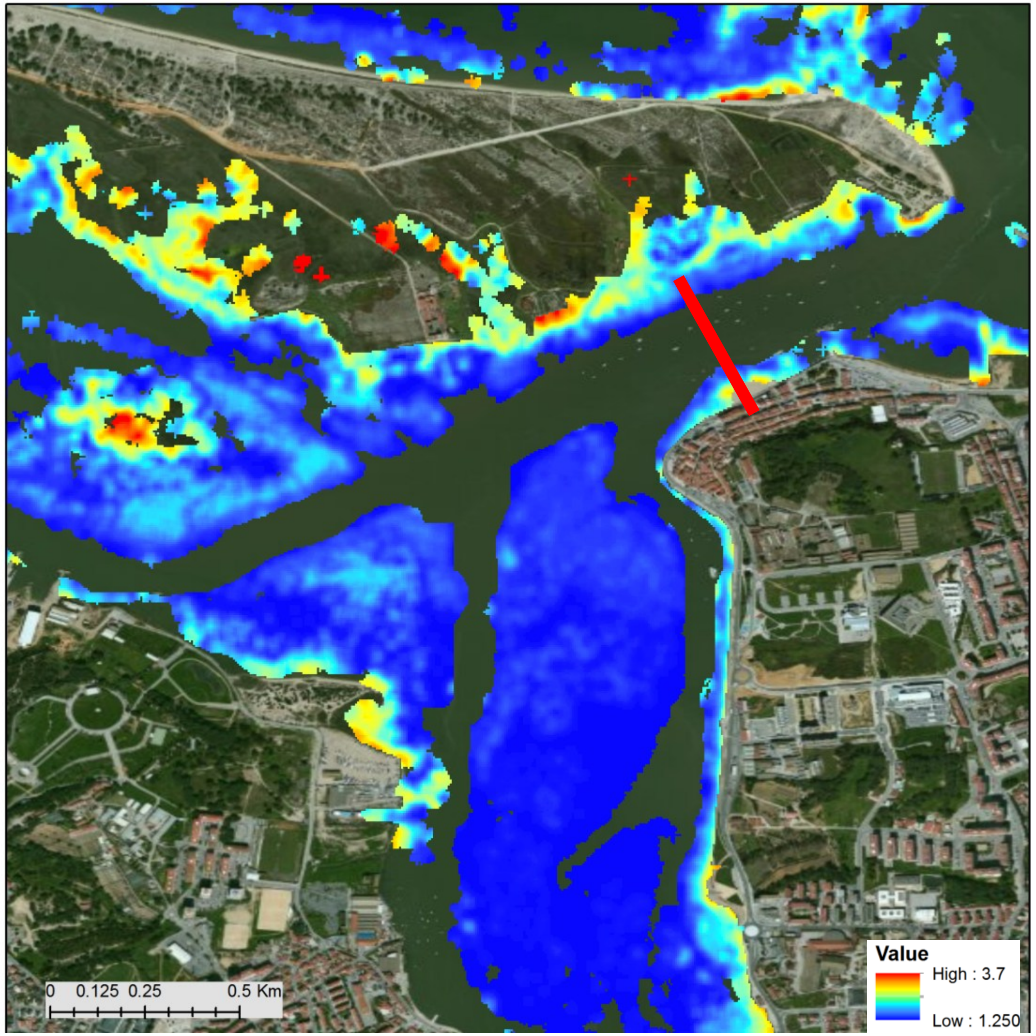

Bathymetric survey with echo sounding
Hydrographic Institute, 2014. Uncertainty= 0.18 m

Comparison between grids:
mean=-0.18 m; std = 0.23 m

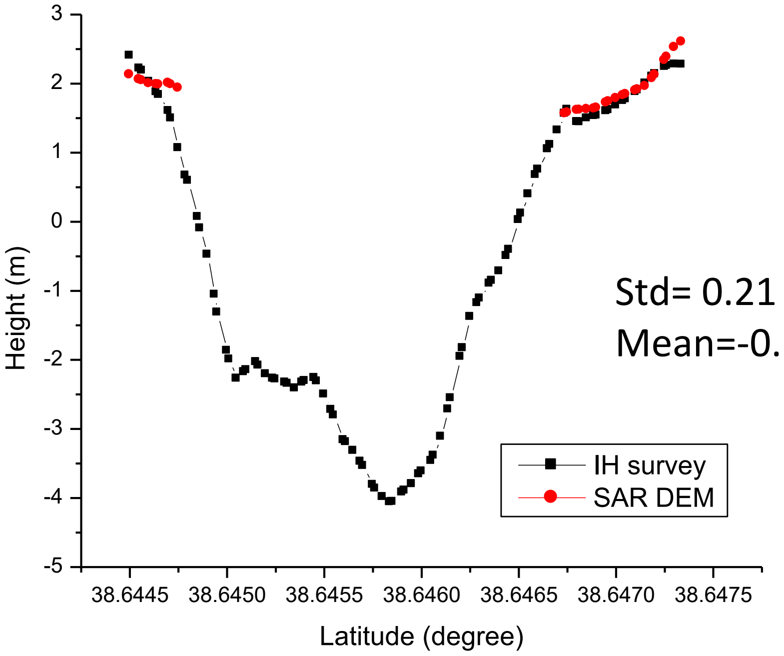

Sentinel-1A SAR data

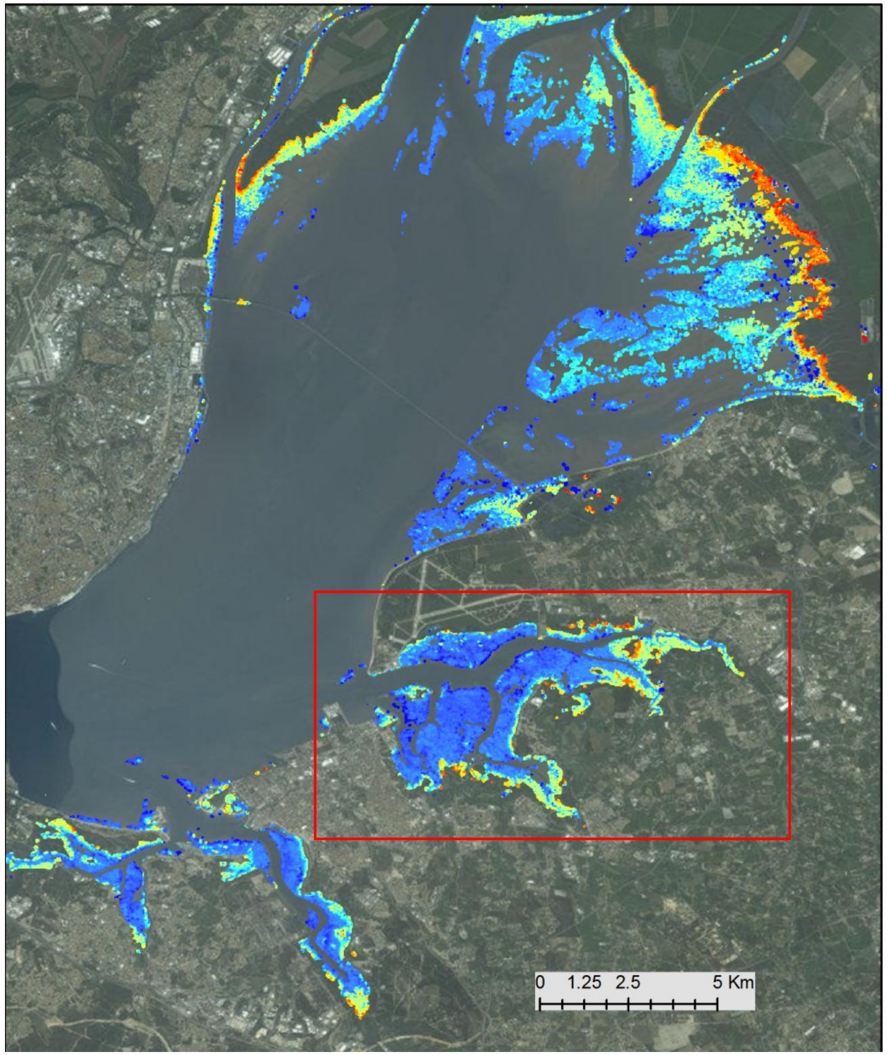

Landsat -7
WaterLine

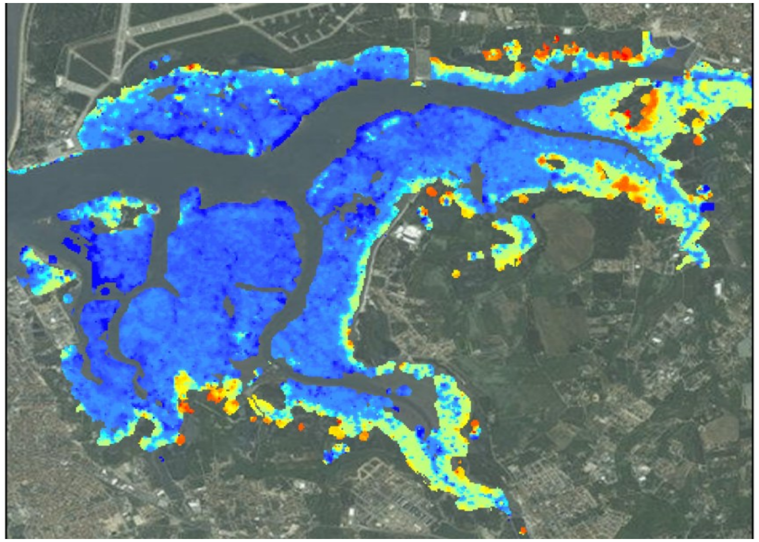

Sentinel-1A, MILA algorithm

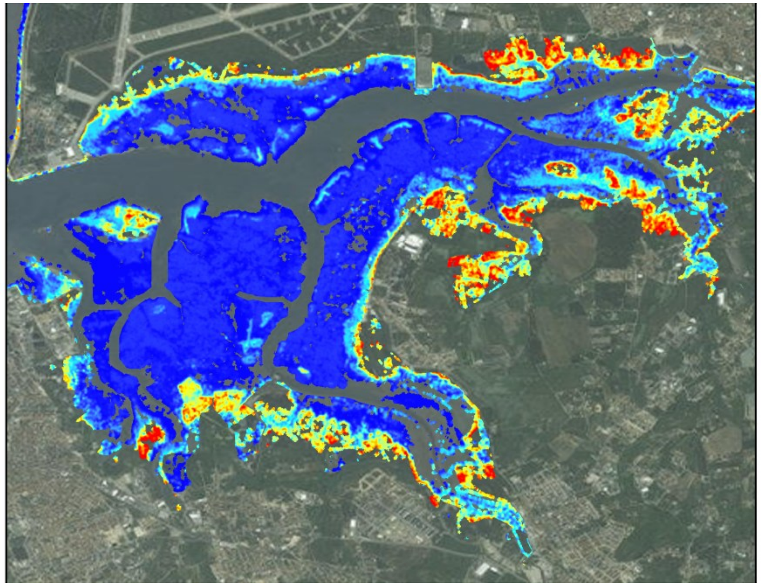

TerraSAR-X, MILA algorithm

remote sensing

MDPI

Article

Intertidal Bathymetry Extraction with Multispectral Images: A Logistic Regression Approach

Isabel Bué [1,2], João Catalão [2,*] and Álvaro Semedo [2,3]

(a)

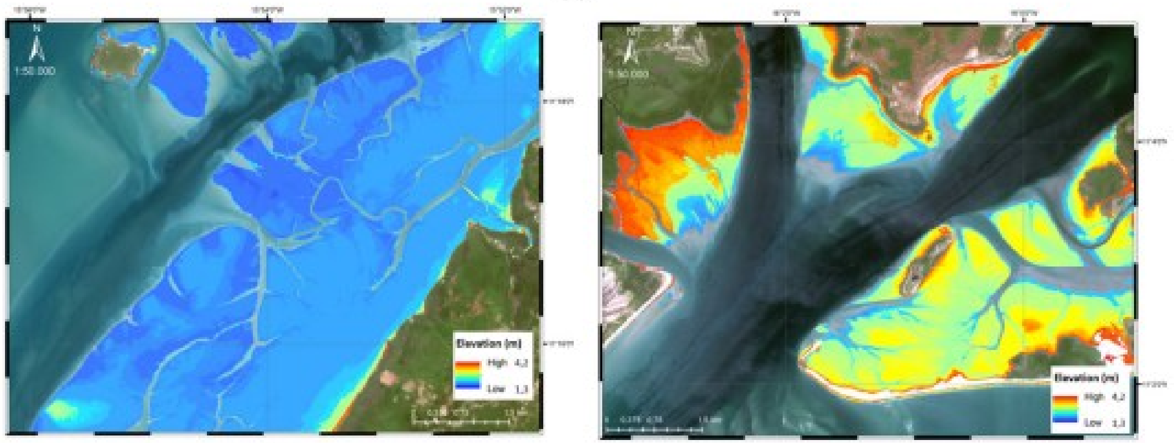

(b) (c)

Figure 2. The Bijagós archipelago in Guinea-Bissau. RGB composite after atmospheric correction of Sentinel-2B imagery on 25 April 2018.

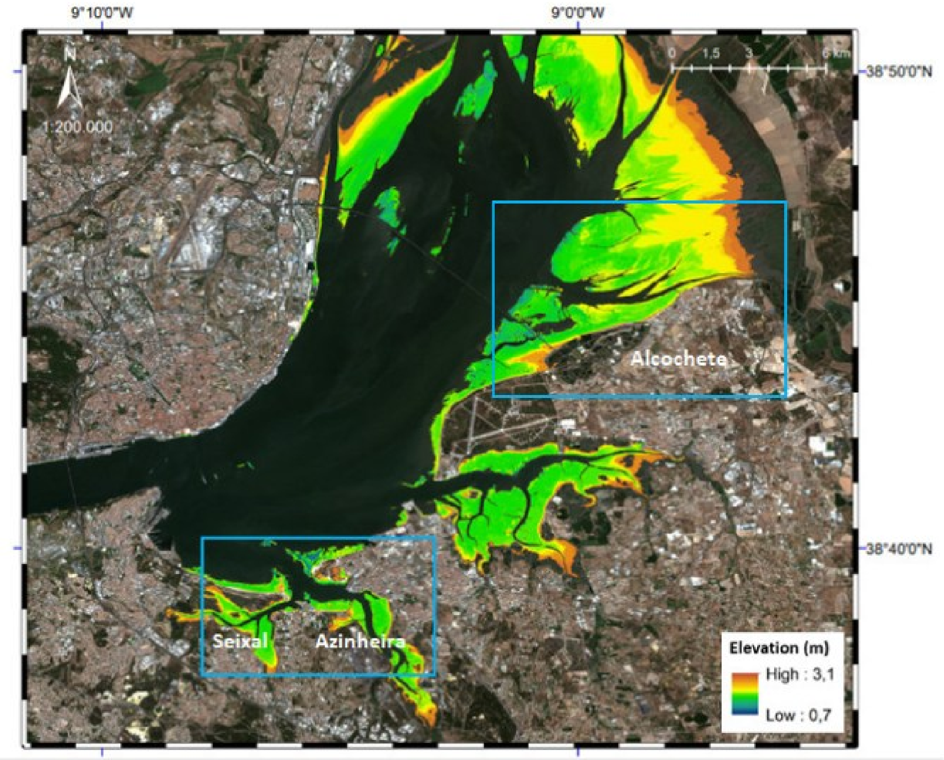

(a)

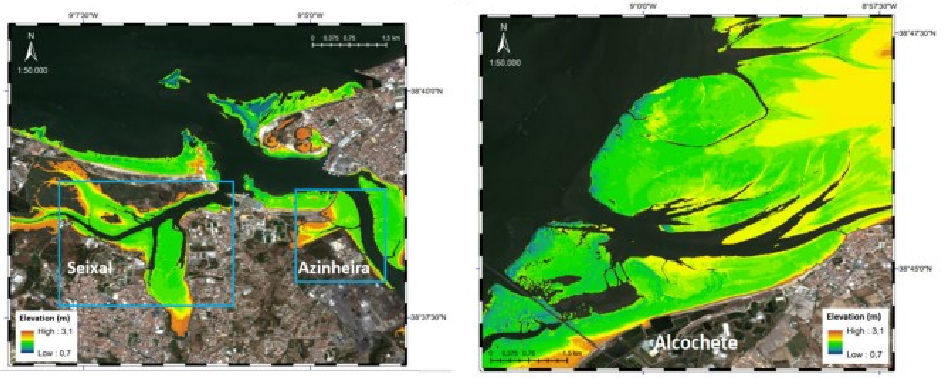

Classificação de culturas agrícolas de Inverno com recurso à plataforma *Google Earth Engine* e imagens dos satélites Sentinel-1 e Sentinel-2

Maria João Gonçalves dos Santos, 2021

Objectivo:Este trabalho de projeto tem dois objetivos:
a) estudar a fusao de imagens *SAR* e imagens multiespectrais (sistemas oticos) para classificacao de culturas de inverno e
b) estudar as potencialidades de processamento na *cloud* atraves da plataforma *Google Earth Engine*.

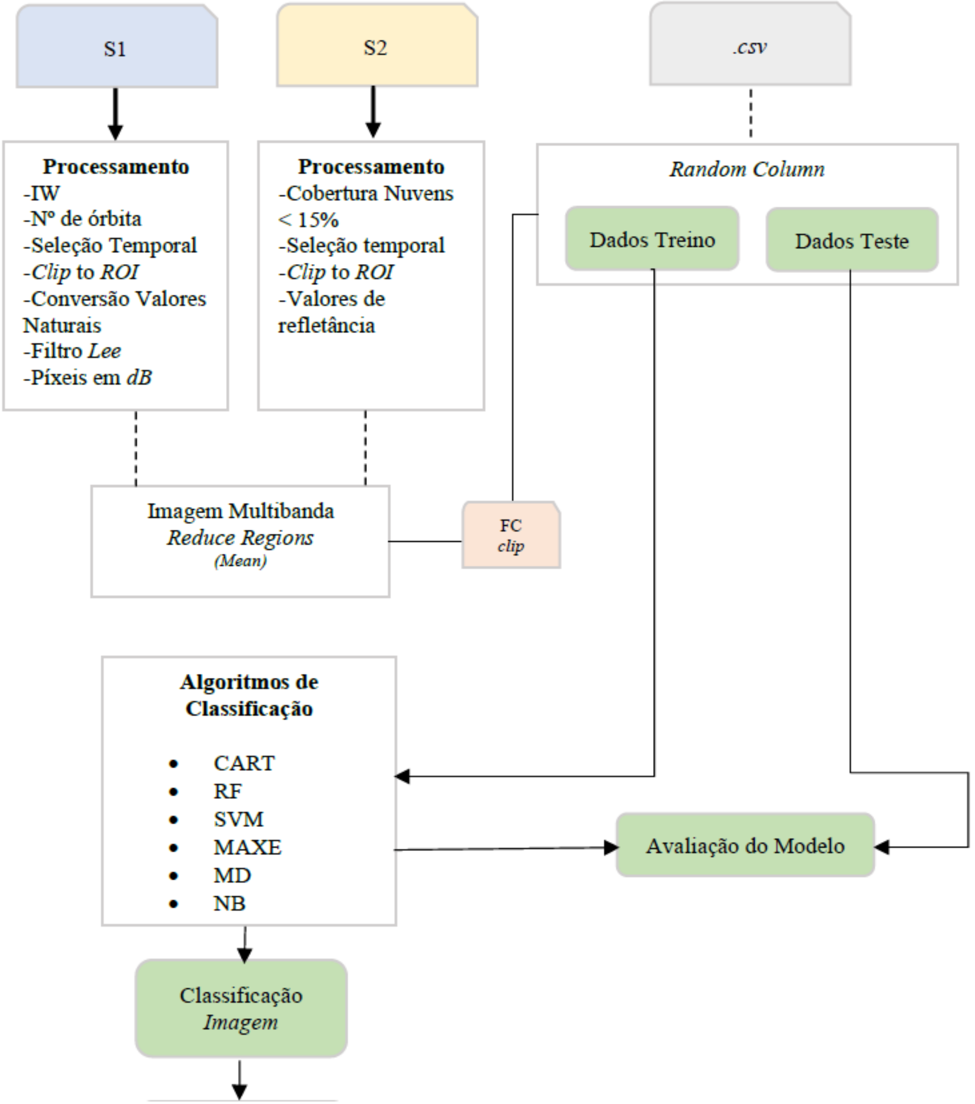

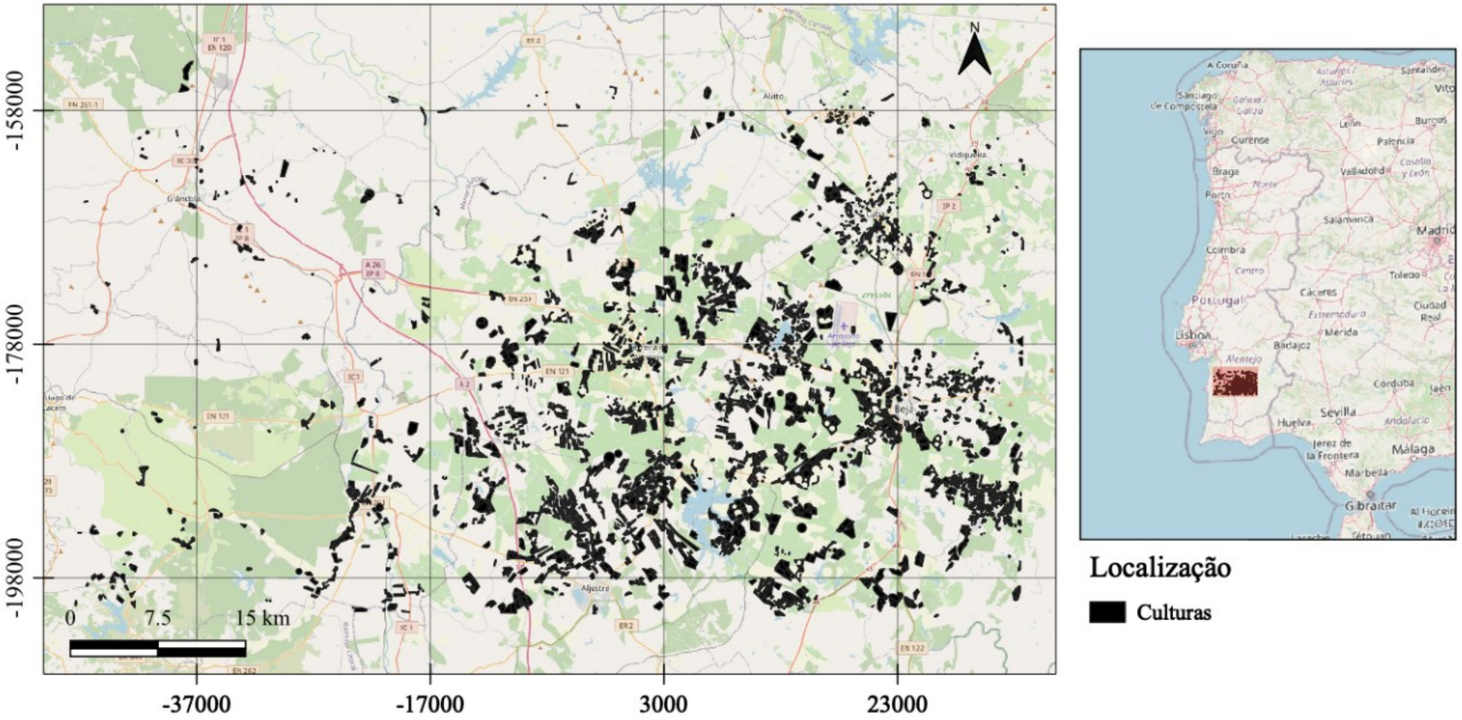

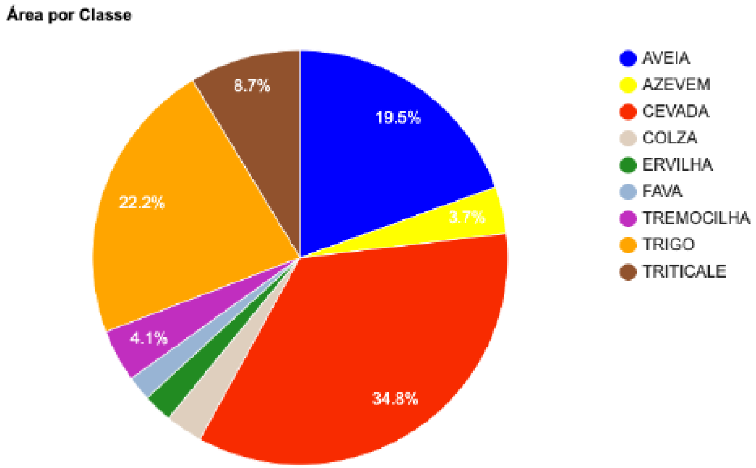

Figura 3.3 Representatividade das classes por área no conjunto de dados

Tabela 4.7 Matriz de confusão obtida para o algoritmo de classificação *RF* na A5

	Dados classificados												
	0	1	2	3	4	5	6	7	8	Total	Fq%	Re%	F1%
0 Aveia	**203**	5	46	1	1	2	1	49	3	311	16.8	65.3	61.9
1 Azevém	23	**39**	7	1	0	1	4	2	2	79	4.26	49.4	60.5
2 Cevada	22	0	**640**	0	3	1	0	9	2	677	36.5	94.5	86.2
3 Colza	0	0	4	**36**	1	0	1	0	0	42	2.26	85.7	88.9
4 Ervilha	5	0	2	0	**41**	0	1	0	0	49	2.64	83.6	78.8
5 Fava	10	0	9	1	4	**31**	2	1	0	58	3.12	53.4	63.9
6 Tremocilha	23	3	2	0	4	3	**39**	2	2	78	6.22	50	61.9
7 Trigo	33	3	55	0	1	0	0	**333**	1	426	22.9	78.2	79.7
8 Triticale	26	0	43	0	0	1	0	14	**51**	135	7.28	37.8	52.1
Total	345	50	808	39	55	39	48	410	61	1855	-	-	-
Precisão	58.8	78	79.2	92.3	74.5	79.5	81.2	81.2	83.6	-	-	-	-

EG: 76.2% **Coeficiente *Kappa*: 68.3%** ***F1- score*: 70.4%**

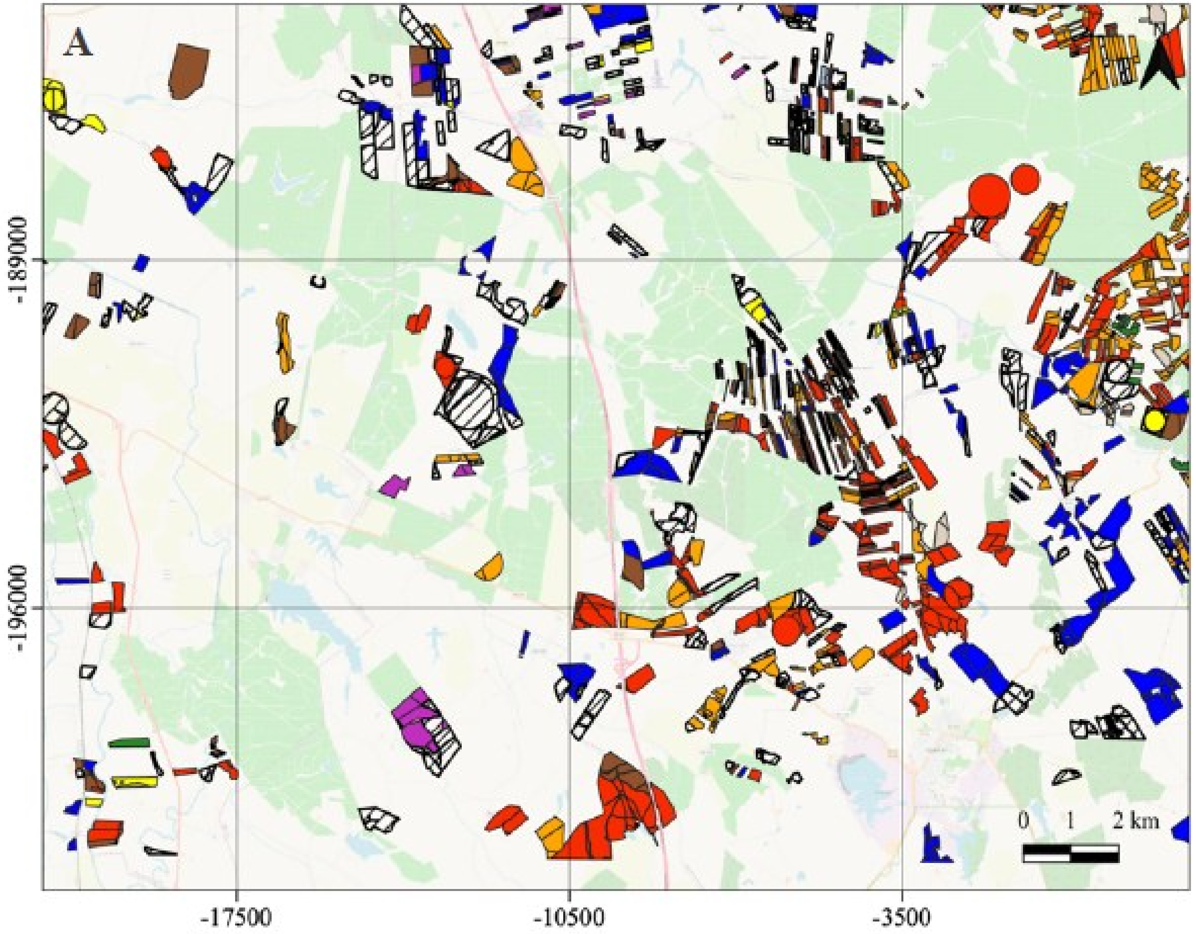

Detecting deforestation using logistic analysis and Sentinel-1 multitemporal backscatter data.

Adrian Dascalu (1), J. Catalão (2), A. Navarro (2)

In this paper, a new approach based on the temporal analysis of the backscattering intensity using the logistic function analysis to detect and delineate clear-cuts in tropical and European-type forests is proposed.

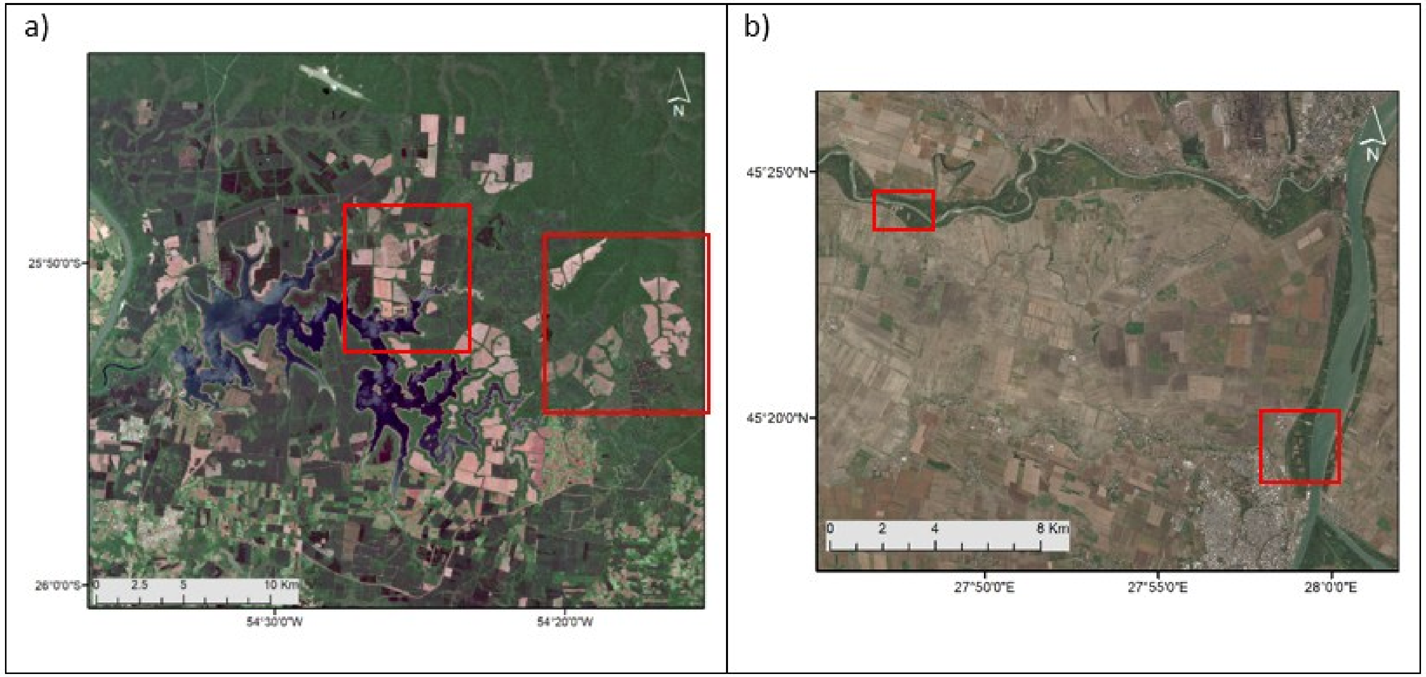

Figure 1. Sentinel-2 images of the test sites: a) Iguazu National Park (Argentina, South America), December 2021 and b) Braila (Romania, Europe) September 2020. Red rectangles are the selected areas used for results presentation and discussion.

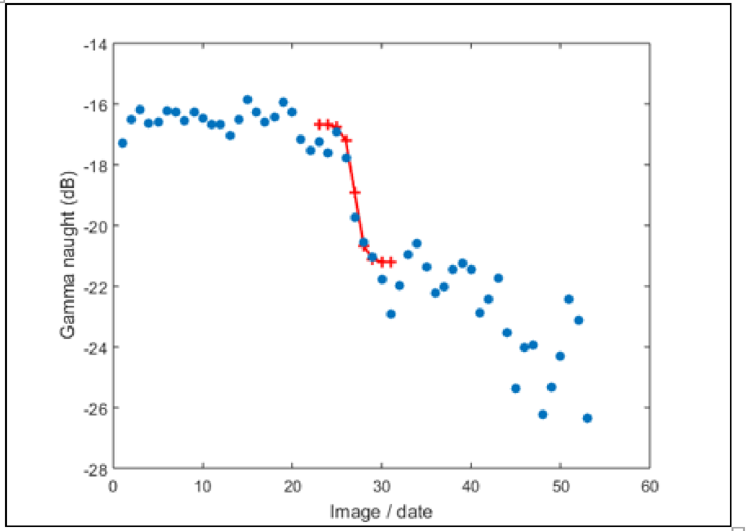

Figure 4. Backscatter intensity (gamma naught) in function of the image /date (blue dots) overlaid with the fitted logistic function (red line).

$$\gamma_i(x,y) = \frac{k}{1+e^{-a(t_i-t_0)}} + \mathrm{LowLim} \qquad i = 1,\dots,M$$

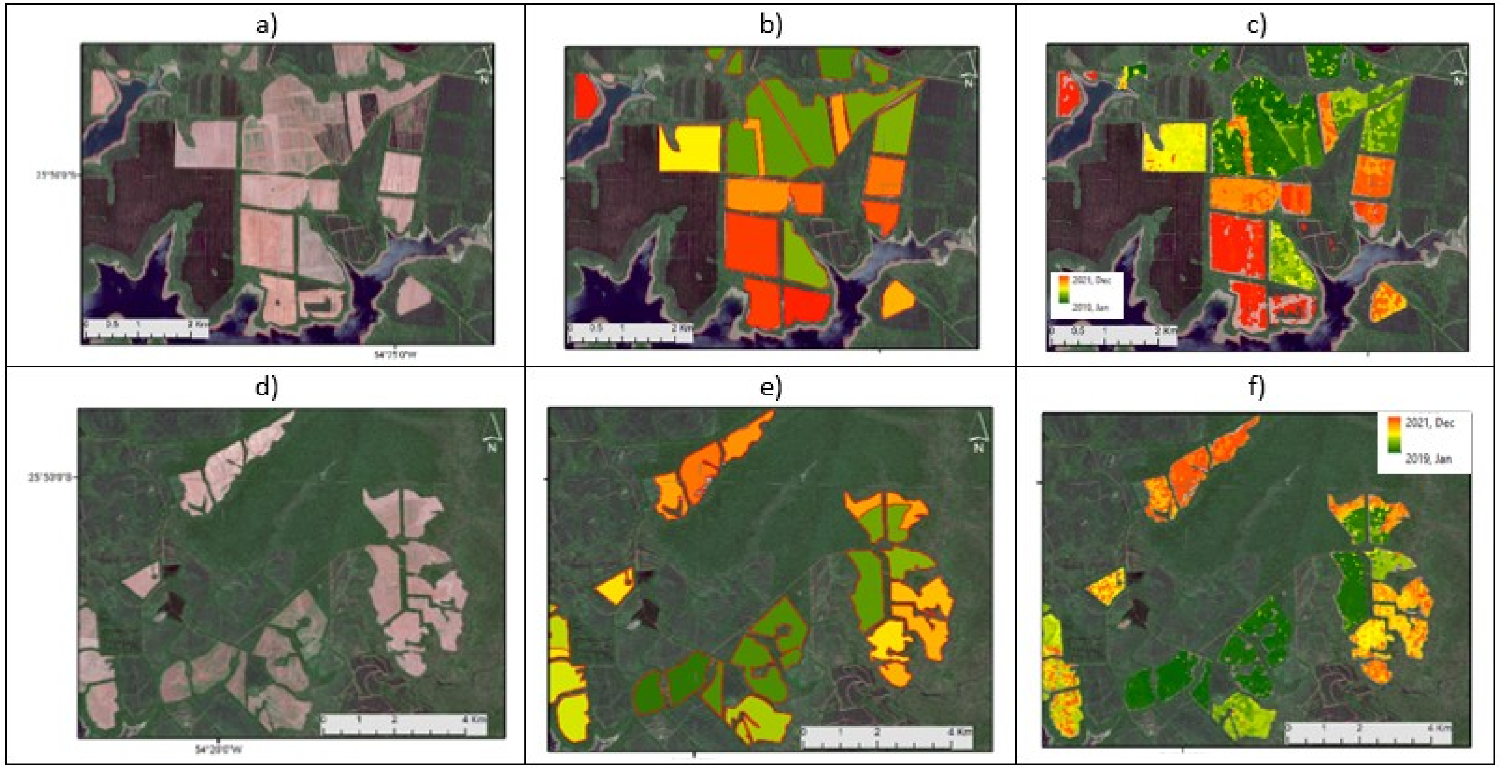

Figure 5. Reference data and colored pixels in function of the estimated date of deforestation for the two areas in Iguazu indicated with a red rectangle in figure 1. The first column (a) and d)) shows the multispectral Sentinel-2 image acquired at December 2022. The second column (b) and e)) shows the reference parcels colored with the reference date. The third column (c) and f)) shows the detected deforested pixels colored with the estimated date. The color scale is linear and ranges from January 2019 (dark green) to December 2021 (dark red).

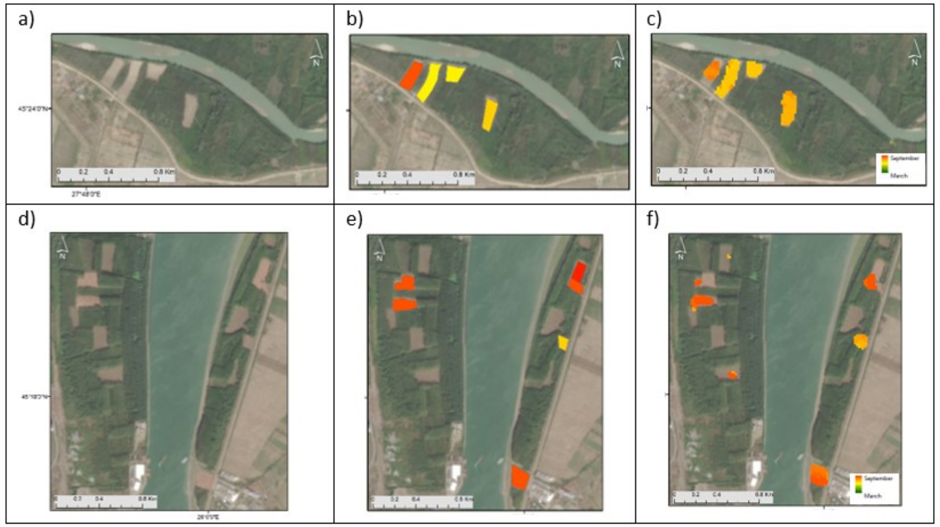

Figure 6. Reference data and colored pixels in function of the estimated date of deforestation for the two areas in Braila indicated with a red rectangle in figure 1. The first column (a) and d)) shows the multispectral Sentinel-2 image acquired at September 2021. The second column (b) and e)) shows the reference parcels colored with the reference date. The third column (c) and f)) shows the detected deforested pixels colored with the estimated date. The color scale is linear and ranges from January 2019 (dark green) to December 2021 (dark red).

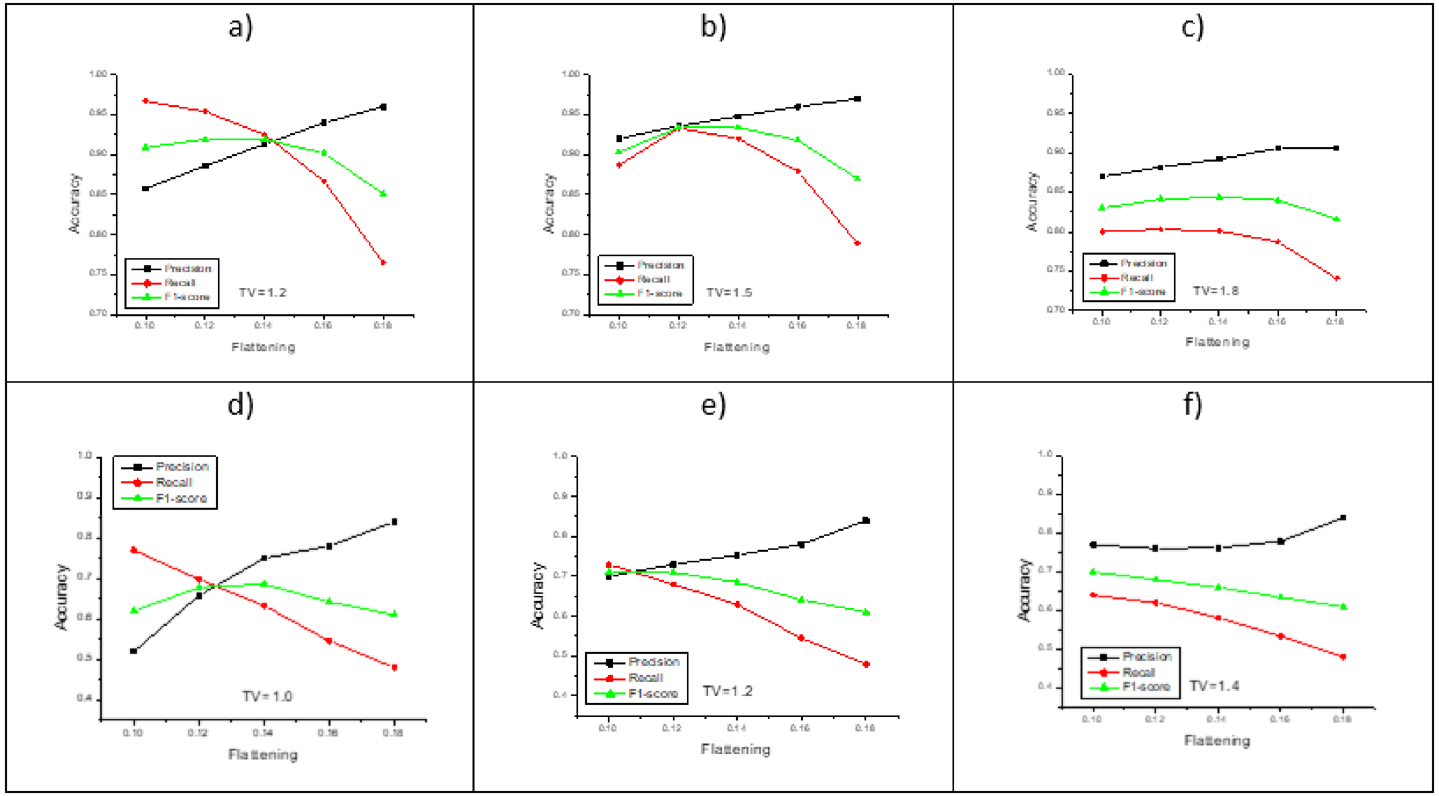

Figure 7. Deforestation detection accuracy as a function of the temporal variability and flattening. The first row shows the results for Iguazu for increasing temporal variability: a) 1.2; b) 1.5 and c) 1.8. The second row shows the results for Braila for increasing temporal variability: d) 1.0; e) 1.2 and f) 1.4.

IEEE TRANSACTIONS ON GEOSCIENCE AND REMOTE SENSING, VOL. 60, 2022 450560

Soil Moisture Estimation Using Atmospherically Corrected C-Band InSAR Data

Nuno Cirne Mira, João Catalão, *Member, IEEE*, Giovanni Nico, *Senior Member, IEEE*,

***Abstract*—A methodology to generate calibrated maps of soil moisture from C-band synthetic aperture radar (SAR) images processed by SAR interferometry (InSAR) technique is presented. The proposed methodology uses atmospheric phase delay (APD) maps obtained from a time series of Sentinel-1 interferograms, to disentangle the APD and soil moisture contributions to Sentinel-1 interferograms. We show how the high spatial resolution and short temporal baseline of Sentinel-1 image can help to estimate soil moisture using a daisy chain InSAR processing. The estimated soil moisture maps are compared with *in situ* data collected by five soil moisture sensors installed in an experimental field, characterized by bare soil, located close to Lisbon, Portugal. Results show that after removing the APD effects in SAR interferogram, there is a correction of the bias in the soil moisture estimation and an improvement in the correlation coefficient with the soil moisture measurements, from 0.38 to 0.78. Soil moisture changes were measured during a sequence of rain events in the winter season. A root-mean-square (rms) error less than 0.04 m^3/m^3 was found over a variety of meteorological conditions.**

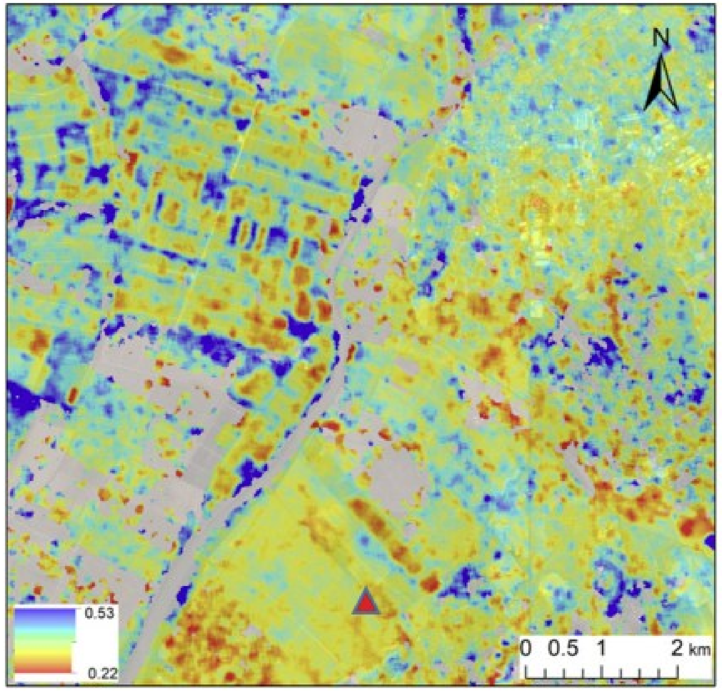

Fig. 8. Inverted soil moisture based on the residual phase from the interferogram 20190110–20190116. The location of the soil moisture sensor is marked with a red triangle.

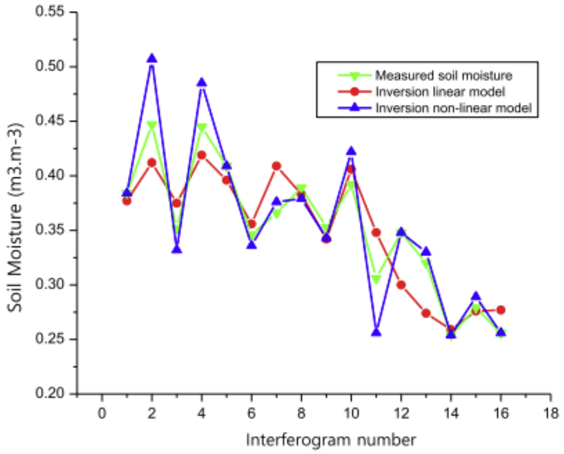

Fig. 7. Soil moisture predicted using the linear model (green) and nonlinear model (blue) and the *in situ* soil moisture measurement. Values in m^3·m^{-3}.

Missões ESA

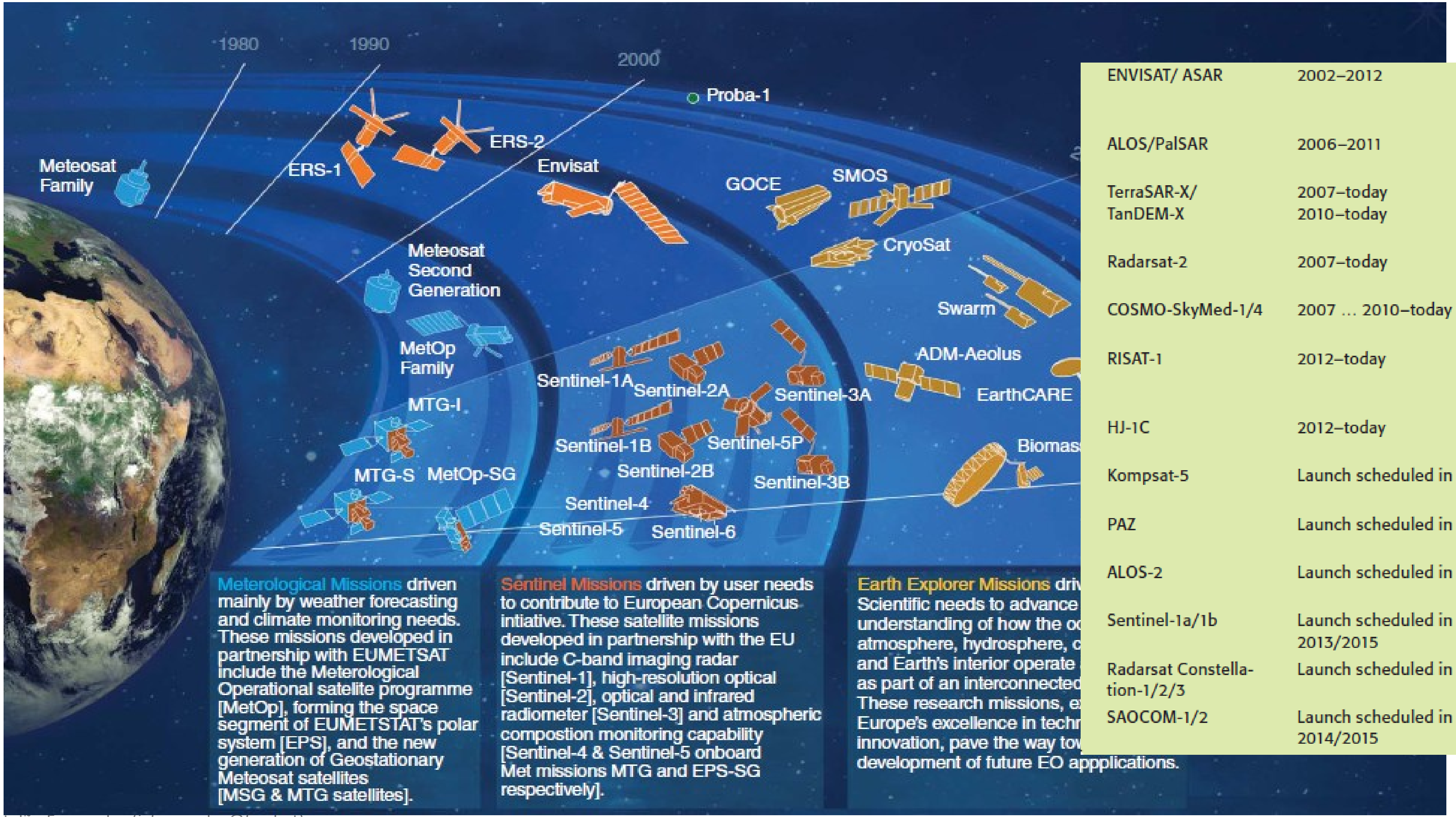

ENVISAT/ ASAR	2002–2012	C (dual)
ALOS/PalSAR	2006–2011	L (quad)
TerraSAR-X/ TanDEM-X	2007–today 2010–today	X (quad)
Radarsat-2	2007–today	C (quad)
COSMO-SkyMed-1/4	2007 … 2010–today	X (dual)
RISAT-1	2012–today	C (quad)
HJ-1C	2012–today	S (VV)
Kompsat-5	Launch scheduled in 2013	X (dual)
PAZ	Launch scheduled in 2013	X (quad)
ALOS-2	Launch scheduled in 2013	L (quad)
Sentinel-1a/1b	Launch scheduled in 2013/2015	C (dual)
Radarsat Constella-tion-1/2/3	Launch scheduled in 2017	C (quad)
SAOCOM-1/2	Launch scheduled in 2014/2015	L (quad)


Sent-1A/B
Sent-2A/B
Sent-3A/B
Sent-4A/B
Sent-5/5P
Sent-6A/B
▪ Copernicus is a European space flagship programme led by the European Union
▪ Copernicus provides the necessary data for operational monitoring of the environment and for civil security
▪ ESA coordinates the space component
Copernicus

Sentinel Scientific Toolboxes

esa

Sentinel-1 (A/B/C/D) – SAR Imaging
All weather, day/night applications, interferometry

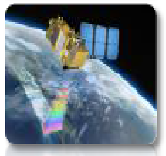

Sentinel-2 (A/B/C/D) – Multi-Spectral Imaging
Land applications: urban, forest, agriculture,...
Continuity of Landsat, SPOT

Sentinel-3 (A/B/C/D) – Ocean & Land Monitoring
Wide-swath ocean color, vegetation, sea/land surface temperature and altimetry

- The Toolboxes are based on sound heritage but also offer innovative technologies for analysing, processing and visualizing EO data.
- The Toolboxes are implemented incrementally in several releases with additional functionality to the public.
- Available free of charge, in line with the Sentinel free and open data policy.

SNAP SNAP 2.0-beta-07

S1A/B: Radar Mission	2014/ 2016
S2A/B: High Resolution Optical Mission	2015/2016
S3A/B: Medium Resolution Imaging and Altimetry Mission	2015/2017
S4A/B: Geostationary Atmospheric Chemistry Mission	2019/2027
S5P: Low Earth Orbit Atmospheric Chemistry Mission	2016
S5A/B/C: Low Earth Orbit Atmospheric Chemistry Mission	2020/2027
S6-(Jason-CS) **A/B:** Altimetry Mission	2019/2025

SAR

SAR Polarimetry

InSAR

SAR

InSAR

SAR InSAR

SAR Polarimetry

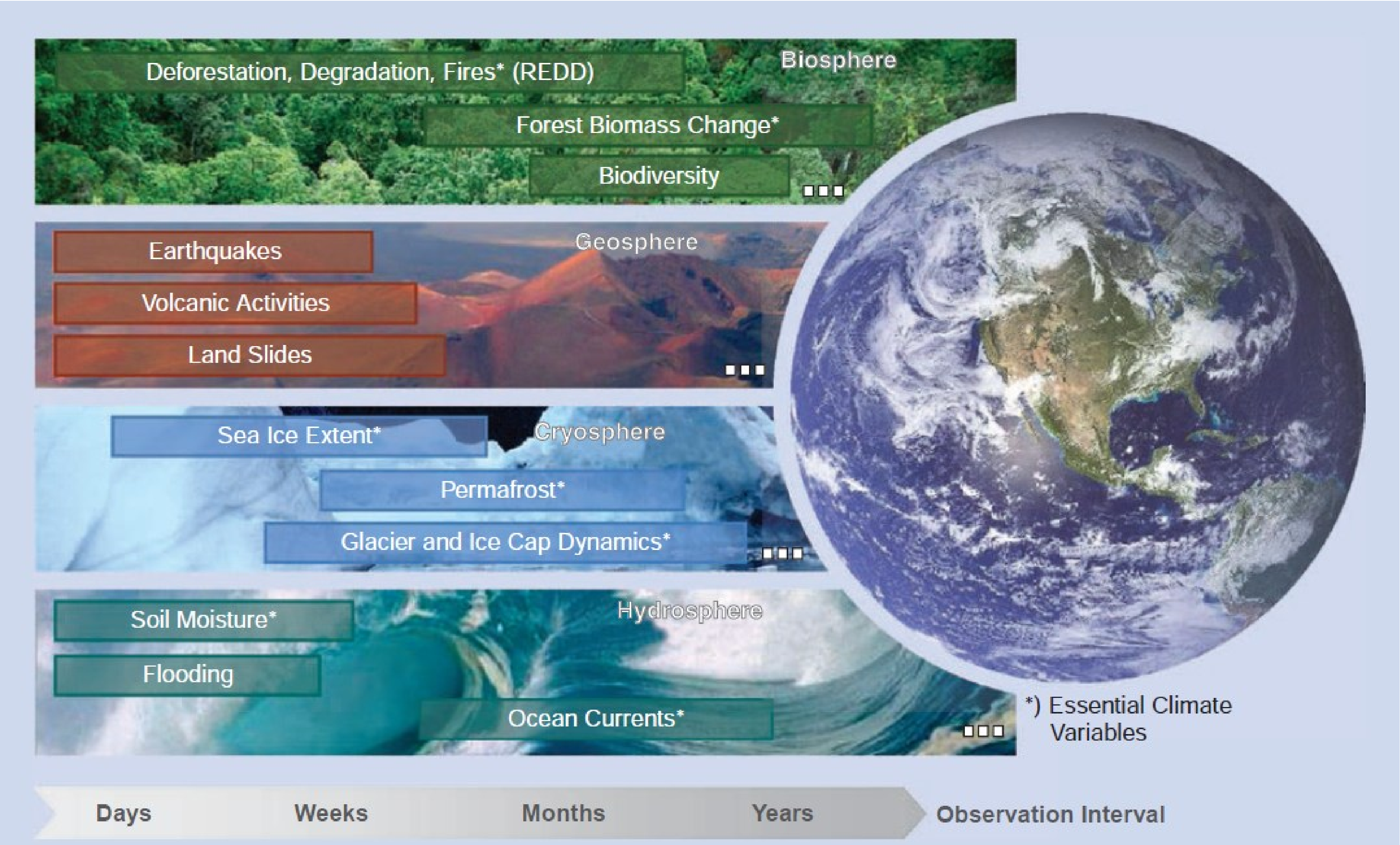

(Moreira et al, 2013)

Síntese

> Missões SAR + Programa Copernicus

> Formação imagem Radar

> Interação com a superfície

> Distorção das imagens SAR

> Mecanismos Scattering

> Polarização

> Interferometria SAR

> ESA / COPERNICUS, Global Monitoring for Environment and Security